2010

IN VIVO MEASUREMENT OF RAT SKELETAL MUSCLE OXYGEN CONSUMPTION FOLLOWING BRIEF PERIODS OF ISCHEMIA WITH REPERFUSION AS ASSESSED BY PHOSPHORESCENCE QUENCHING MICROSCOPY

William Nugent
Virginia Commonwealth University

IN VIVO MEASUREMENT OF RAT SKELETAL MUSCLE OXYGEN CONSUMPTION FOLLOWING BRIEF PERIODS OF ISCHEMIA WITH REPERFUSION AS ASSESSED BY PHOSPHORESCENCE QUENCHING MICROSCOPY

A thesis submitted in partial fulfillment of the requirements
for the degree of
Doctor of Philosophy
at the
Medical College of Virginia Campus, Virginia Commonwealth University

by

William H. Nugent
B.S. Virginia Commonwealth University, 2005

Director:
ROLAND N. PITTMAN, Ph.D.
PROFESSOR
DEPARTMENT OF PHYSIOLOGY AND BIOPHYSICS

Virginia Commonwealth University
Richmond, Virginia
August, 2010

Approval form for thesis/dissertation and final oral examination

Student name: Nugent (Last) William (First) H (Middle initial) **V number:** 00229210

Document type: (check one) ☐ Master's thesis ■ Doctoral dissertation

Department: Physiology and Biophysics

Thesis/dissertation title: IN VIVO MEASUREMENT OF RAT SKELETAL MUSCLE OXYGEN CONSUMPTION FOLLOWING BRIEF PERIODS OF ISCHEMIA WITH REPERFUSION AS ASSESSED BY PQM

Approval numbers

☐ IRB

☑ IACUC AM10114

☐ Exempt

☐ Not applicable

Thesis/dissertation and final oral defense

Date: 08-09-2010

Graduate Advisory Committee (type name and sign)

	Failed	Passed
Roland N. Pittman, Ph.D.		✓
Ivo P. Torres Filho, M.D., Ph.D.		✓
R. Wayne Barbee, Ph.D.		✓
Paul H. Ratz, Ph.D.		✓
Steven Price, Ph.D.		✓

Graduate program director/department chair: Dionysios Logothetis **Date:** 8/10/10

School/college dean: Jane F. Strauss gc **Date:** 8/10/10

Virginia Commonwealth University

TABLE OF CONTENTS

LIST OF FIGURES

LIST OF TABLES

Acknowledgement

We as humans have excelled as a species not by competition, but through cooperation. It is that enduring spirit that now compels me to list my debts to the many personalities who've provided insight, experience, training, and reassurance we pushed through to the completion of this work.

As my mentor and primary contributor to this work, it is appropriate that *Dr. Pittman* is recognized first. Without his patience in addressing my limited vocabulary and rampant usage of colloquialisms and sarcasm throughout my scientific writing, my thesis would be less a completion of a degree and more an admission's ticket to an asylum. In all seriousness, I could not have asked for a better mentor. His knowledge, experience, and seemingly effortless guidance of this project and my growth as a researcher was and is humbling. Thank you Dr. Pittman.

Dr. Aleksander Golub is possibly the best political officer with whom I've ever had the privilege of serving. His tireless efforts to input the administrative password to the local super computer have saved countless minutes of additional paperwork for me to get my own password. He is a fine gentleman whose knowledge and critical mind have generated solutions to daunting problems within heart beats. In addition to his expertise, his gracious, and joyful personality have made this project truly enjoyable. My only regret is that there will be no "Alex" to beg for assistance as I move on to the next phase.

Bjorn Song has been an invaluable asset and collaborator in surgical training and data collection for various parts of this work. He has been a great friend and purveyor of fine wisdom whenever called upon.

Dr. Helena Carvalho deserves special recognition for her technical assistance and training in lab technique. That and we stood shoulder to shoulder together in misery as the chemical detector of nitric oxide (DAF-2) failed to live up to expectations. Thank you for keeping me sane.

Drew and *Mike Connery* were not directly associated with the project, but their sharp minds and jovial personalities helped keep things in perspective. Drew in particular always seemed to have the right answer to seemingly off-the-wall questions. You're a well educated man sir, thank you. As for Mike: dude you submitted a late-breaking abstract. That's dedication.

Where would I be as an American without a committee? Drs. Ivo Torres, Wayne Barbee, Paul Ratz and Lou De Felice have all been very generous with their time and experience. Their thoughtful input greatly increased the scientific quality of the work done over the course of this project. *Dr. Steven Price* is also due special recognition for his tireless efforts to help raise this document to scientific standards.

On the more personal side, yet still quite professional has been the outstanding friendship of *Dr. Nicholas Pullen.* He has set the standard of what a true friend should be and never once been dismissive of my frustrations over the course of this doctoral program. His scientific perspective also greatly enhanced my own ability to step back and reevaluate my work and situation. Dude, if you're reading this it means you're probably late for our 5 o'clock consult.

My family has endured my continued schooling with all the patience and support I (or anyone else for that matter) could ever want. Thank you guys. I would also like to thank my precious wife *Elizabeth*. You believed in me and never doubted the worthiness of this goal. And wasn't it a wonderful surprise when you found out I really wasn't just typing "All work and no play makes Will a dull boy" over and over again? For your love, I am forever indebted.

Finally I would like to thank my *mother*. The timing of submission for this thesis could not be more appropriate. Happy birthday.

ABSTRACT

IN VIVO MEASUREMENT OF RAT SKELETAL MUSCLE OXYGEN CONSUMPTION FOLLOWING BRIEF PERIODS OF ISCHEMIA WITH REPERFUSION AS ASSESSED BY PHOSPHORESCENCE QUENCHING MICROSCOPY

By William H. Nugent

A thesis submitted in partial fulfillment of the requirements for the degree of Doctor of Philosophy at the Medical College of Virginia Campus, Virginia Commonwealth University

Brief periods of skeletal muscle ischemia (ischemic pre-conditioning) alter cellular metabolism in a way that confers protection over subsequent ischemic episodes. The mechanisms behind this effect have been studied indirectly through assays for the byproducts of ATP synthesis and in vitro studies of cellular signaling cascades and ROS generation. There have been no direct, in vivo assessments of the changes in respiration during reperfusion. We employed phosphorescence quenching microscopy in conjunction with a flow-arrest technique to assess the influences of external, pressure-induced 1- to 10-min focal ischemia on interstitial oxygenation ($P_{ISF}O_2$) and the consumption of oxygen (VO_2) in spinotrapezius muscles of Sprague-Dawley rats. During reperfusion following an ischemic period VO_2 was measured by the rate of $P_{ISF}O_2$ decline during brief, serial flow-arrest compressions. Our tests of this intermittent compression technique indicate that 5 s of flow-arrest followed by 15 s of flow restoration allow measurement of VO_2 without compromising baseline or reperfusion recovery of $P_{ISF}O_2$. There was a steady rise in VO_2 during early reperfusion which was correlated with increasing ischemic durations. Treatment with cyanide confirmed that at least some of this increase was due to an upregulation of cytochrome c oxidase activity. Nitric oxide (NO) suppressed VO_2 during rest and reperfusion,

while L-NAME did not influence respiration under normoxic conditions. L-NAME produced a significant rise in VO_2 under hypoxic conditions following 10 minutes of ischemia, indicating a greater role of NO in the regulation of respiration during low $P_{ISF}O_2$ conditions. We conclude that physiological levels of NO regulate mitochondrial respiration during hypoxia and confirm that pharmacological elevation of [NO] reduces VO_2 in a manner consistent with the ischemic pre-conditioning effect.

INTRODUCTION:

The Oxygen Supply

The microvasculature normally provides sufficient flow to meet the demands of perfused tissues and it readily adapts to local changes. The arterioles constitute the major resistance vessels to blood flow in the circulatory system. Their dilation and constriction maintain the O_2 supply to and metabolite washout from tissues. Thus, they are excellent indicators of local reactivity to both hypoxia and hyperoxia. Poiseuille's law relates blood flow through a vessel to the vessel's dimensions and blood's viscosity. It states that flow is proportional to the fourth power of vessel radius. Thus, the microvascular response to hypoxia is usually dilation, the opposite generally holding true for hyperoxia. This is achieved by relaxation or contraction of vascular smooth muscle in the arteriolar wall, but the specific direct or indirect sensing mechanism for this change in PO_2 is under debate (Buehler and Alayash, 2004).

The processes of blood flow regulation that tend to maintain the balance between oxygen supply and demand are typically grouped into three categories: the myogenic response, shear-stress, and metabolic mediated mechanisms (Carleson, et al. 2008). In considering the relation between regional changes in oxygen need and the corresponding flow-related response, this discussion will primarily focus on the feed and terminal arterioles; they are the chief regulators of functional capillary density in skeletal muscle (Segal, 2005).

The myogenic response is a vascular dilation or constriction following a decrease or increase, respectively, in transmural pressure (Bayliss, 1902). The mechanism of action is not fully understood, but it appears to maintain constant blood flow at some defined set point that can be altered by various hormones and signaling molecules (Schubert and Mulvany, 1999).

Sympathetic stimulation causes arteriolar constriction (Faber, 1988), resulting in a set-point that is more restrictive of flow. But this is the opposite of what would seem to be needed during exercise: increased flow to compensate for the increased metabolic activities of certain muscles. It has been reported that competing regulatory mechanisms override the myogenic response better as arteriolar diameter decreases (Folkow, et al. 1971). This permits better regional and local matching of O_2 supply to demand.

The shear-stress mediated mechanism allows the vasculature to react to and accommodate changes in the velocity and turbulence of blood flow (Kuo, et al, 1990). Increased or decreased levels of shear-stress are sensed by the vascular endothelium and it reacts by increasing or decreasing the release of nitric oxide (NO) and prostacyclin respectively (Kuo, 1991; Kaley, et al. 1989). NO is a potent vasodilator that is released by endothelial cells. It acts on vascular smooth muscle cell soluble guanylate cyclase receptors to initiate a cascade that inhibits smooth muscle contraction (Furchgott and Zawadzki, 1980; Ignarro et al, 1987). Although the specific role of this shear-dependent response is controversial (McGahren, et al. 1997), it is clear that it adds al layer of vascular regulation with its ability to override the myogenic response on a region by region basis (Carlson, et al. 2008). But the need for better precision in matching supply to tissue metabolic function involves another, more intimate mechanism.

The first two levels of flow regulation are largely mechanosensitive and relevant at regional and systemic levels. Thus, they are ill-equipped to precisely regulate capillary perfusion in local instances of poor O_2 supply-demand matching. The metabolic regulatory mechanisms can meet these demands in concert with the larger-scale activities of the first two. This third

mechanism of blood flow involves oxygen sensing and release of vasoactive metabolites (Segal S, 2005).

Changes in the partial pressure of oxygen (PO_2) can affect arteriolar diameter and, therefore, capillary perfusion (Klitzman, et al. 1982). This suggests that an O_2 sensor is a means of vascular regulation. Indeed, there are two compelling theories that focus on the red blood cells (RBC) as a vessel for O_2 sensors because they facilitate PO_2 dependent vascular relaxation (McMahon, et al. 2002). The first involves the storage and eventual release of NO's bioactivity through the production of s-nitrosyl-hemoglobin (SNO-Hb) (Jia, et al. 1996). NO readily binds to any of hemoglobin's four heme groups, forming an iron nitrosyl heme complex; this is the main reason RBCs are proposed to be NO scavengers. When hemoglobin is primarily in the T-state (deoxygenated) NO is better able to bind because O_2 does not have to be replaced (Pawloski, et al. 2001). In the R-state (reoxygenated), hemoglobin's Cys-93β becomes more susceptible to reaction and thus the resident iron nitrosyl heme can S-nitrosylate it, forming SNO-Hb (Jia, et al, 1996). SNO-Hb and other thionitrites are considered to be the most potent vasorelaxive compounds known with effectiveness much higher than that of NO (Singel and Stamler, 2005). This, coupled with the fact that they are more abundant in the blood and blood vessel walls than NO is, suggests a mechanism for hypoxic, vasodilatory mediation *in vivo* (Singel and Stamler, 2005). But it is unclear how SNO-Hb's vasodilatory signal is transduced through the RBC membrane to affect vascular dynamics. A second theory, which has gained substantial ground over the past decade, involves RBC adenosine triphosphate (ATP) release upon exposure to hypoxic conditions (Ellsworth, 1995). This is hypothesized to be mediated by deoxyhemoglobin's interaction with the N-terminal, cytoplasmic fragment of band 3 (a protein bound within the RBC membrane). Upon binding with deoxyhemoglobin under low PO_2

conditions, key regulatory glycolytic enzymes are displaced, resulting in glycolytic stimulation and an accumulation of ATP along the membrane that then triggers its release (reviewed by Jensen, 2009). Thus, as the RBC enters the hypoxic venules of respiring tissue, it releases ATP which then activates purinergic receptors on venular endothelial cells. This transduces a vasodilatory signal (NO) to nearby arterioles (Ellsworth, 2004). Which of these two mechanisms for RBC regulation of blood flow serves a greater role is unclear, but they most likely complement or augment each other under various conditions.

The preceding mechanisms are mostly reactive in nature, and the release of vasoactive metabolites by tissues could be considered a more proactive mechanism to match supply and demand during rapid changes in respiration. During periods of hypoxia, as seen in exercise and ischemia, skeletal muscle cells supplement oxidative phosphorylation with glycolytic ATP generation. A byproduct of this is lactate, which then diffuses to the local vasculature and acts as a vasodilator (Garhofer, et al. 2003). During active muscle contraction, the resulting potassium efflux induces vasodilation in skeletal muscles with mixed fiber-types (Hudlicka, 1985). As there is a rapid rise in interstitial potassium levels during skeletal muscle contraction (De Clerck, et al, 2003), this mechanism may function independently of hypoxia, allowing timelier perfusion matching to demand. Although these, in addition to other products of both resting and contracting skeletal muscle tissues, provide more precise control of the vasculature they cannot wholly account for vasodilation (Green, et al, 1996). For example, larger increases in flow are primarily dependent on the dilation of feed arterioles which are upstream from where the metabolite release occurs (Green, et al, 1996). The three major levels of regulation work in conjunction to provide rapid, precise and sustainable adjustments to blood flow, resulting in periods of hypoxia that are transient and less severe.

The Oxygen Demand

During exercise, the amount of oxygen needed varies proportionately with activity level. As energy needs rise, the mitochondria respond by increasing the generation of high energy phosphates through a proton gradient that is established by donating negative charges to oxygen. This activity is readily apparent in contracting skeletal muscle, and mitochondrial function can be translated directly to oxygen consumption. But what about resting muscle? Does high energy phosphate production account for all observed oxygen consumption (VO_2)? Certainly, at rest there is a need to maintain a consistent supply of cellular fuel that accounts for a great deal of oxygen utilization, but contributions from reactive oxygen species generation, extra-mitochondrial enzymatic processes, and variations in myoglobin PO_2 may account for a significant fraction.

Myocyte function depends on the availability of adenosine triphosphate (ATP), which is produced by both anaerobic and aerobic pathways. Anaerobic respiration occurs in the form of glycolysis and basically nets 2 molecules each of ATP and pyruvate from one molecule of glucose. Aerobic uses oxidative phosphorylation within the mitochondria to further reduce the 2 pyruvates from glycolysis to 30-32 molecules of ATP. Anaerobic respiration has the advantage of being able to generate ATP in an oxygen-free environment, but its low efficiency and waste products are limiting. Aerobic respiration is much more efficient and its byproducts are readily carried in the vasculature to the lungs, thus making it ideal for long-term energy production that is limited only by the diffusivity of oxygen (Wagner, 2000).

Oxygen is the terminal electron acceptor in the mitochondrial electron transport chain (see Figure 1), binding to the cytochrome c oxidase complex (complex IV), absorbing the

negative charge and leaving as H_2O. The rate of oxygen uptake is directly related to the maintenance of the cellular ATP/ADP ratio. During resting conditions, as ATP is converted to ADP, the mitochondria convert carbohydrates, fats, and proteins to NADH via oxidative phosphorylation. NADH is then oxidized and its electrons are passed into the mitochondrial matrix. These electrons are then carried along a series of complexes via intermediaries (see Figure 1) to power the transport of 10 protons per pair into the matrix. This leads to the development of the proton motive force necessary for the regeneration of ADP to ATP. Oxygen provides the driving force for the electrons and is easily removed as H_2O (Lodish, 2004). Under normal conditions, this system in skeletal muscle is capable of increasing ATP output by 100 fold during strenuous exercise limited only by the rate of oxygen diffusion to the mitochondria (Ortenblad, et al, 2009). Energy production is responsible for a majority of mitochondrial oxygen consumption. But since no system can be 100% efficient, there are other diversions of O_2.

In addition to energy production (released as ATP and heat), mitochondrial oxidative phosphorylation produces small quantities of reactive oxygen species (ROS). Complexes I (NADH coenzyme Q reductase) and III (ubiquinol cytochrome reductase) are two points that contribute to a loss of between 0.2 and 2% of the total O_2 consumed by mitochondria to the generation of ROS in myocytes under physiological conditions (Misra et al, 2009; Tahara, et al, 2009). Mitochondrial ROS generation occurs when O_2 is converted to superoxide ($O_2^{\bullet -}$) by single electron transfer during interaction with either of these two inner membrane complexes. Free radicals are generally considered to be harmful in their interactions with DNA, lipds, enzymes etc. and are usually kept in check by various enzymatic (catalases) and non-enzymatic (nitric oxide) processes. While ROS production accounts for only a small fraction of total

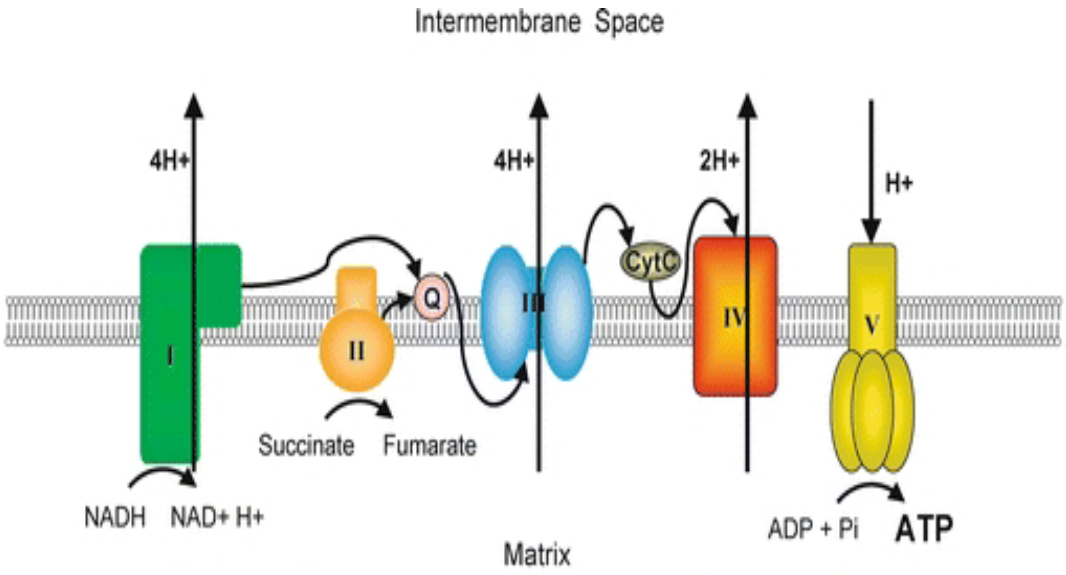

Figure 1: Diagram of mitochondrial electron transport chain. Electrons are passed through a series of complexes via electron carriers to facilitate proton (H+) loading of the intermembrane space. This H+ gradient is then used to convert ADP + Pi to ATP. Oxygen is the final electron acceptor as it receives the negative charges from cytochrome c oxidase (complex IV). Complex IV is also the site of respiratory inhibition for both cyanide and nitric oxide.

Figure adopted from:

Cuperus R, Leen R, Tytgat GAM, Caron HN, and Van Kuilenburg ABP. Fenretinide induces mitochondrial ROS and inhibits the mitochondrial respiratory chain in neuroblastoma. *Cell Mol Life Sci*. **67**(5): 807–816, 2010.

oxygen consumption, periods of oxidative stress do arise during altered mitochondrial function. When the ETC becomes highly reduced, for example, during a glut of NADH generated, in the mitochondrial matrix, from oxidative phosphorylation there is an increased likelihood that electrons will pass directly to O_2 from complexes I & III and form superoxide (Wallace and Fan, 2009). Though somewhat controversial (see Figure 2; Clanton TL, 2005), this situation has been observed during hypoxia, when low oxygen tensions inhibit aerobic respiration, causing the ETC to become reduced and mitochondrial ROS production to increase (Sato et al, 2005; Vanden Hoek, 1998). Mild hypoxia can deplete cellular ATP reserves. Oxidative phosphorylation's regulation is then shifted to cytochrome c, resulting in a PO_2-dependence on ETC activity (Lynn, et al, 2007), creating the reducing conditions for enhanced mitochondrial ROS production. Although ROS production has been reported to be proportional to mitochondrial oxygenation (Boveris, 1977), moderate hypoxia appears to provide enough oxygen to supply the newly converted ROS-producing ETC complexes I and III (Clanton, 2007). As one study has reported, ROS production had risen approximately 3 fold with total VO_2 suppressed from the normoxic state following the development of moderate hypoxia in isolated mitochondria from rabbit hearts (Korge, et al, 2008). This study also confirmed that ROS production was not elevated during periods of anoxia.

More severe disruptions in mitochondrial function, such as lengthy ischemia followed by reperfusion, can further disrupt the proton motive force across the mitochondrial inner membrane and thus divert an even greater percentage of oxygen utilization to ROS production (Chen et al, 2003; Thaveau et al, 2007). With severe perturbations to the mitochondria, ROS generation contributes to the eventual decline of cellular function. An ROS burst during early reperfusion can expand the existing size of the ischemia-derived infarct (Solaini and Harris, 2005; Yang, et

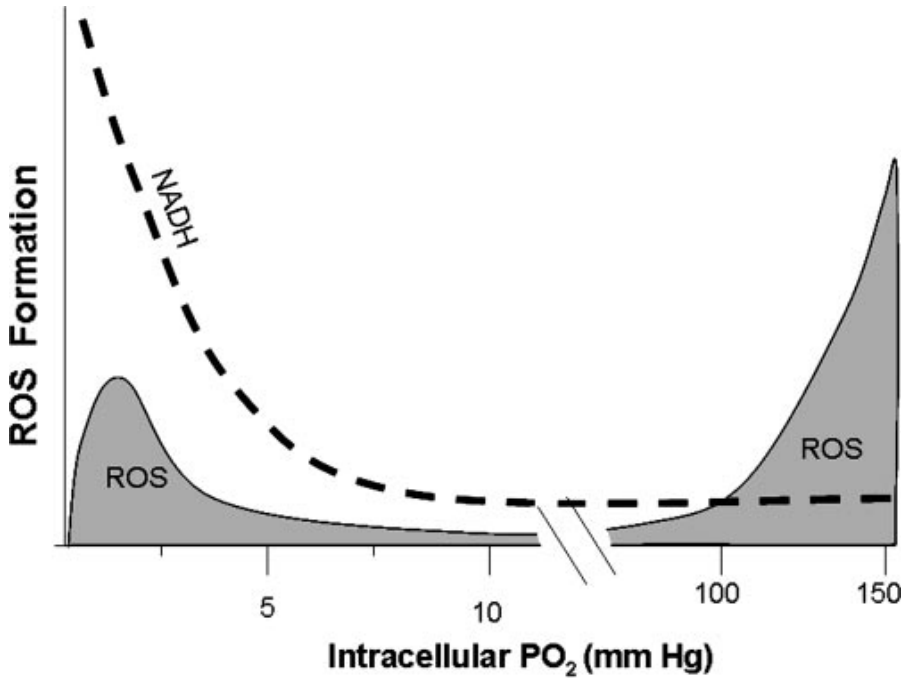

Figure 2: Model of the production of ROS and electron transport chain functionality over the physiological range of intracellular PO_2s. As oxidative phosphorylation becomes O_2-limted at ~8 mmHg, NADH levels begin to rise. Around 3 mmHg, ROS production becomes elevated and is slowed only when it becomes oxygen limited around 1 mmHg, long past the point where oxidative phosphorylation had become insufficient to reduce NADH to NAD+. This profile would likely be similar but shifted to the right for measurements of interstitial PO_2 ($P_{ISF}O_2$).

Figure adopted from:

Clanton TL. Hypoxia-induced reactive oxygen species formation in skeletal muscle. J Appl Physiol 102: 2379-2007, 2007

al., 2004). The time course of ischemia differentiating enhanced ROS production from the burst associated with reperfusion injury is difficult to determine, but one study has reported that superoxide production rose by 35% after 1 minute of ischemia and then by 95% following 20 minutes of ischemia in isolated guinea pig hearts (Kevin, et al, 2003). As this indicates a progressive rise in ROS production, it makes sense that measurements of oxygen consumption for the purposes of determining ETC function would be subject to greater error over time during hypoxia and become complicated by the confounding effects of reperfusion-associated mitochondrial dysfunction.

Accurately accounting for the ROS induced error when calculating tissue VO_2 is difficult because of numerous differences between the data derived from the in vitro and in vivo settings. Extra-mitochondrial sources of ROS, such as the metabolism of arachidonic acid by the lipoxygenase pathway and phospholipase A_2, exist under resting conditions, while NADPH oxidase and xanthine oxidase can contribute appreciably during muscle contraction (Mishra, 2009; Clanton, 2007). Extracellularly, when the cofactor tetrahydrobiopterin (H_4B) is absent or otherwise unavailable, nitric oxide synthase (prevalent in the endothelial cells of the intact vasculature) can uncouple and become an ROS generator (Moens and Kass, 2006). These additional sources may not be present in preparations of isolated mitochondria and *ex vivo* perfused tissues, nor might all forms of their counterparts—ROS scavengers. Antioxidants can be both enzymatic (catalase, super oxide dismutase etc) and non-enzymatic (NO, vitamin E, etc) and their availability may be compromised outside of the *in vivo* setting. Their presence may confound measuring ROS by consuming it. The *in vivo* setting is challenging as well because systematically inhibiting ROS production in living tissue to determine its share of oxygen

consumption would disrupt other cellular processes, thereby compromising the physiological situation.

Reactive oxygen species production can clearly be confounding when attempting to translate the measurement of oxygen consumption to mitochondrial energy production in states of long term ischemia followed by reperfusion. But, for situations where tissue oxygenation is either normal or moderately hypoxic, the contribution of ROS to VO_2 does not appear greater than 5%. Thus, VO_2 measurements probably do not have an appreciable error over the physiological range of PO_2, where hypoxia has not induced sufficient oxidative stress.

Measurements of VO_2:

In mammalian circulatory systems oxygenated blood flows into an organ and deoxygenated blood flows out, reoxygenation occurring at the interface with the atmosphere—the pulmonary system. As arteries and veins are separated by capillary beds, the O_2 extraction of an organ (VO_2) follows Fick's principle:

$$VO_2 = Q(Ca_{O2}-Cv_{O2}) \qquad \text{Equation 1}$$

where Q indicates blood flow and Ca_{O2}-Cv_{O2} indicates the difference in oxygen concentration between arterial inflow and venous outflow from the organ or tissue. During conditions of rest and exercise, VO_2 and energy production are proportional. Thus, VO_2 calculated from arterial/arteriolar oxygenation and venous/venular oxygenation is a metric of tissue/organ respiration. Using this approach, reported mean values for VO_2 in mammalian resting skeletal muscles range from 0.054 to 0.92 mlO_2/100g*min (Edmunds, et al, 2001; Hoy, et al, 2009). One

of the earliest reports assessing VO_2 in the resting human forearm gave a range of 0.09 to 0.52 mlO_2/100g*min, roughly consistent with subsequent findings (Mottram, 1955). Although it will determine the amount of O_2 consumed by a particular capillary bed, Fick's principle does not reveal the rate at which specific tissues are consuming oxygen or what the spatial relations are between VO_2 and the gradients of oxygen supply. Additionally, it has poor temporal resolution because the interstitium can act as a buffer between cellular respiration and changes in vascular oxygen levels.

Another approach to determining the rate of oxygen extraction in a particular region of tissue is to arrest blood flow and track the changes in local PO_2. A minimally invasive technique for region-specific sampling of vascular PO_2 is Near-Infrared Spectroscopy (NIRS). First developed for the simultaneous measurement of hemoglobin oxygenation and cytochrome c oxidase's redox state in the rat brain in 1987 (Masahide, et al, 1987), this method has been adapted to a number of tissues and extended to measurements of oxygen consumption (Schumacker and Samsel, 1990). Illuminating the target tissue with a pair of 700-805 and 830-805 nm wavelengths to assess hemoglobin oxygenation, blood volume dynamics (relative measurements of absorption at ~805 nm over time) and the mitochondrial cytochrome aa_3 oxygenation to simultaneously measure both vascular oxygen supply and tissue metabolic rate. During blood flow arrest, the rate of oxyhemoglobin conversion to deoxyhemoglobin gives the change in PO_2 over time and thus provides information on VO_2 kinetics. Values for resting VO_2 in human calf muscles have been reported to be ~0.20 mlO_2/100g*min using this technique (Cheatle, et al, 1991; De Blasi, et al, 2009). These values correspond to those found using the Fick principle, but have greater spatial and temporal resolution as well as an assessment of mitochondrial respiration by which to compare the measured oxygen disappearance rate. But a

significant temporal delay in oxygen uptake kinetics may exist because of the skeletal muscle interstitial space's buffering action.

Nitric Oxide

As reviewed by Lane and Gross (2002), nitric oxide (NO) is a gaseous free radical biomessenger with a diverse repertoire of *in vivo* functions including but not limited to: gastric emptying, long term potentiation in memory, neurotransmitter release, immunological defense, blood pressure regulation, etc. The observations that NO can alter both the supply and demand for oxygen differentially over a range of physiological and patho-physiological conditions that may persist in skeletal muscle seems relevant to discussions of VO_2. This molecule's ubiquity and near-universal involvement in biological functions is a result of two important properties—reactivity and hydrophobicity (Lane and Gross, 2002).

NO, as a free radical, possesses an unpaired valence electron that enables it to react with a number of biological components and constituents such as: itself, O_2, ROS, protein thiols, iron heme groups, and other free radicals. This reactivity is somewhat dampened compared to other free radicals, resulting in concentration-dependent regulation of both beneficial and harmful effects (Lane and Gross, 2002). The regulatory influences of NO on biochemical processes are typically associated with low concentrations (in the nM- μM range) with cytotoxicity coming into play at higher concentrations (in the higher μM range) (Chi, et al, 2006). Additionally, although many intercellular signaling molecules transduce their signals through the plasma membrane because of their inability to penetrate the lipid bilayer (Lodish et al, 2000), NO is lipid-soluble and mostly unaffected by this level of regulation. The current belief is that it is able to freely transverse these barriers—quite similar to O_2 (Lane and Gross, 2002). Therefore, NO's

involvement in various reactions is regulated both spatially and temporally by its sites of production or release in the tissues (Lane and Gross, 2002).

The vast majority of nitric oxide is enzymatically produced by nitric oxide synthases (NOS) expressed throughout the mammalian organism. At least three distinct isoforms of NOS have been identified with the designations neuronal (nNOS), inducible (iNOS), and endothelial (eNOS) by location of discovery, or, more recently, NOS1, NOS2, and NOS3 respectively by order of isolation (Michel ed, and Feron, 1997). The classical nomenclature has been deemed misleading as these NO producing enzymes are widely distributed. NOS1 has been detected in neuronal tissue, skeletal muscle (Michel ed, and Feron, 1997), mast cells and the vasculature (Kasiwagi, et al, 2002). NOS2, originally identified in immunoactivated macrophages, has been localized to cardiac myocytes, glial cells, and vascular smooth muscle (Michel ed, and Feron, 1997). Finally, NOS3, originally and still mostly identified with the endothelial cells of blood vessels has been detected in cardiac myocytes, blood platelets, extra-vascular regions of the brain (Michel ed and Feron, 1997), and red blood cells (Kleinbongard, et al, 2006).

NOS, in its functional dimeric state, catalyses a two-step reaction that converts L-arginine to the intermediate N^{ω}-hydroxy-L-arginine and finally to NO and L-citrulline (Li and Poulos, 2005). This process requires O_2 to bind to NOS's ferrous heme and nicotinamide adenine dinucleotide phosphate (NADPH) to act as an electron donor linked to the heme by a flavin mononucleotide/flavin adenine dinucleotide reductase (Li and Poulos, 2005). Additionally, there is a strict requirement for the cofactor tetrahydrobiopterin (H_4B), which serves as an electron donor to the heme-oxygen complex (Li and Poulos, 2005). Calmodulin (CAM), whose influence/binding is typically controlled by intracellular calcium (Ca_i^{2+}) levels, then regulates the NOS catalyzed oxidation of L-arginine to NO at the level of electron transfer between the

reductase and the heme domains (Li and Poulos, 2005). This reaction profile is essentially conserved amongst the three NOS isoforms, although kinetics and regulatory mechanisms are not.

Despite a >50% sequence homology between the three most verifiable NOS isoforms, with the active site being highly conserved, significant differentiation occurs in terms of their activities and expression (Li and Poulos, 2005). Both NOS1 and NOS3 are constitutively expressed enzymes whose activities are influenced by changes in Ca_i^{2+} (Li and Poulos, 2005). NOS2's expression, on the other hand, is transcriptionally regulated via cytokine signaling and is Ca_i^{2+} independent (Lopez- Figueroa MO, et al, 2000). The Ca_i^{2+} requirement arises from CAM. The constitutively expressed NOS's require Ca^{2+} to promote the CAM binding that enables the production of NO, while inducible NOS has a permanently bound CAM and is independent of Ca_i^{2+} levels (Li and Poulos, 2005). As a consequence, coupled with its high level of expression during transcriptional stimulation, NOS2 is capable of a high NO production rate for an extended period of time (4-24 h) compared to NOS's 1 & 3 whose rates are low and have durations on the order of seconds to minutes (Lopez-Figueroa, et al, 2000). Indeed, differences also exist between the two constitutive forms in terms of kinetics. Chen and Popel (2007) developed a computational mathematical model of vascular and perivascular NO release, (based on reported kinetic values of the biochemical pathways involved in NO synthesis) and determined that NOS1 has a steady state production rate (0.39-1.16 μM/s) much higher than that of NOS3 (~.017 μM/s). Additionally, their findings support indications of NOS1's high dependence of NO production on local $[O_2]$; as NOS1 production decreases with hypoxia, whereas NOS3 was much less sensitive (Chen and Popel, 2007; Li and Poulos, 2005). So, under normal physiological conditions, it is apparent that the distribution of NOS types 1 and 3 will determine which tissues/regions have the

greatest potential for regulation by NO, while actual concentrations are influenced by consumption.

Nitric oxide's longevity depends on the proximity of its production to its reactants (scavengers); unlike classical signaling molecules, there is no storage of its free radical form (Thippeswamy and Morris, 2001). Intravascular NO's half-life—endothelium derived—was measured, using microelectrodes, to be ~2 ms, which is less than what might be predicted (Thomas, et al, 2001). This is probably due to the presence of red blood cells, which contain high amounts of hemoglobin with a high binding affinity to NO. Extravascular measurements indicate a half-life of .09 to >2 s, as the interstitial space contains fewer NO scavengers (Thomas, et al, 2001). While the NO concentration gradients of skeletal and cardiac muscle have been found to extend over that of the vascular spaces (Rassaf, et al, 2007), consumers of NO such as intracellular myoglobin maintain a presence amongst the myocytes. Moreover, the changing conditions *in vivo* (i.e. hypoxia) may significantly affect the presence of scavengers.

ROS contributes to the disappearance of NO *in vivo*, as demonstrated by the ability of superoxide dismutase (SOD), an ROS scavenger, to induce aortic dilation by preventing NO consumption (Pohl and Busse, 1989). NO also undergoes auto-oxidation at a rate dependent on local [O_2] indicating a decrease in scavenging at low PO_2 (Liu, et al, 1998). Some workers, however, do not consider this reaction to be important to overall scavenging due to its slow rate under physiological concentrations of NO (Chen, et al, 2006). Others give it a much more significant role; it was found that within cellular membranes the reaction has a 300-fold acceleration (Liu, et al, 1998). This could be important due to the presence of membrane-bound NOS3 (Bachetti, et al, 2004), and may add validity to the idea of the membrane as an NO diffusion barrier under normoxic conditions (Lui, et al, 1998; Herrera, et al, 2006). It would

follow that a certain degree of hypoxia would result in a decrease in NO scavenging and a concomitant increase in regional [NO]. But the magnitude of influence events at the sarcolemma would have on the local mitochondrial NO concentration and ultimately respiratory kinetics is unclear.

NO and some of its derivatives have been implicated in facilitating a decrease in the proximal demand for oxygen (VO_2) via NO's direct and reversible competition with O_2 on mitochondrial cytochrome c oxidase (Brown, et al, 1994). For comparison, carbon monoxide, another diatomic, is a competitive inhibitor of O_2 in mitochondrial respiration and NO has been reported to be 1,000 to 2,000 times more effective (Mason, et al, 2006). Binding occurs on cytochrome c oxidase's reduced heme (referred to as heme a_3) site of action for the terminal electron acceptor (O_2) in the electron transport chain. As [NO] rises, there is a decrease in the ability of cytochrome oxidase c to utilize oxygen and thus a reduction in VO_2 (Schweizer and Richter, 1994). It should be noted that at rest under normoxic conditions the cytochrome oxidase c reserve capacity is large. It has been reported that endogenous mitochondrial respiration must be inhibited by over 50% before there is a noticeable difference in tissue oxygenation (Thomas, et al, 2005). This is most attributable to the fact that cytochrome c oxidase, collectively, does not typically operate at maximal capacity, so normoxic levels of NO do not interfere with VO_2 (Palacios-Callender, et al, 2007).

As NO is rather insidious, it is not surprising that a small percentage of interaction with mitochondrial respiration has been reported to involve alternative pathways. The competitive inhibition was first described as a single site model, in which binding of NO to the a_3 heme was completely reversible in both active and quiescent conditions of cytochrome c oxidase activities (Brookes, et al, 2003). This paradigm was supported by data indicating that VO_2 had a roughly

proportionate inverse relationship to [NO]. Brown, et al (1994) reported half inhibitions of cytochrome c oxidase at 250 nM NO when O_2 was 130 μM and 60 nM NO when O_2 was 30 μM—an indication that the percentages approximate closely. But Brookes et al, (2003) also reported that the single site model does not account for all of the data. They indicated a differential degree of NO inhibition between cytochrome c oxidase's active and quiescent states with greater potency during high enzymatic turnover. This prompted the development of a second model that involves the copper portion of cytochrome c oxidase's binuclear center (Mason, et al, 2006). Their data not only mimicked the original finding of greater inhibition during high enzymatic turnover, but also indicated that as activity decreased, the hill coefficient increased to above 1—an indication of a secondary binding of NO. Given NO's affinity for metallic centers, they focused on potential interactions with the local copper. It was found that during high enzymatic turnover, a_3 heme binding occurred as reported by the single site model, but NO began engage in lower affinity non-competitive interactions with the oxidized copper in an irreversible fashion as respiration dropped (Mason, et al, 2006). Presumably, NO's inhibitory effects during the quiescent state are reduced because a portion is oxidized to nitrite by reaction with the copper while this does not occur during high activity. This new, two site model was able to fit all of the data presented in the two studies described here for mitochondrial inhibition by NO (Buerk, 2007). Additionally, NO or its derivatives stimulate the production of both ROS and reactive nitrogen species (RNS) from the mitochondria (Brown and Borutaite, 2001), which then are capable of inhibiting the electron transport chain at multiple sites in addition to that of NO (Han, et al, 2007). These reactions tend to be more destructive and associated with a long-term elevation in [NO] that results in irreversible inhibition of mitochondrial respiration

(reviewed by Brown, 2001). The end result is that NO appears to have differential effects at various conditions of mitochondrial respiration and hence VO_2.

As hypoxia drives the regulation of VO_2 to the oxygen binding domain of cytochrome oxidase c, NO may be an important physiological regulator of VO_2 during this time. NO becomes more effective with diminished PO_2, supporting the potential relevance of this mechanism (Schweizer and Richter, 1994). This has been attributed to the similar conditions of high enzymatic turnover where PO_2 is the limiting reagent in both cases, which leads to the greater effective interaction of NO with the a_3 heme to facilitate competitive inhibition (Mason, et al, 2006). Thus, the same amount of NO has a much greater influence during times of hypoxia. The implication is that this mechanism results in a higher tissue PO_2 during low oxygen conditions than would occur if respiration was unaffected by NO (Chen, et al, 2006).

It is somewhat counterintuitive that NO might become more effective at regulating VO_2 during hypoxia because O_2 is one of the critical components to its production. As previously discussed, the kinetics of NOS production reveal that although NOS1&2's production has a strong dependence on O_2 over the physiological range, NOS3 is relatively insensitive to hypoxia (Chen and Popel, 2007; Li and Poulos, 2005). One consequence of this might be that endothelial-derived NO gradients would have a greater inhibitory effect on local myocyte mitochondria, but whether the continued production of NOS3 would be sufficient to compensate for the production drop-off from NOS1 is unclear.

Another mechanism may actually facilitate increased NO-bioavailability around the mitochondria of some skeletal muscle fiber-types during hypoxia. Myoglobin, an intracellular oxygen binding hemeprotein typically associated with temporary O_2 storage, possesses mechanisms similar to hemoglobin in the preservation and release of NO bioactivity via nitrite

reduction (Cosby, et al, 2003). This may be of critical importance to the overall scheme of O_2 regulation during muscle contraction since certain fiber types usually associated greater O_2 needs possess a larger mitochondrial population than others (Weibel, 1984). Similar to hemoglobin, myoglobin converts NO to nitrate under normoxic conditions and releases NO during hypoxia in cardiac muscle cells (Rassaf, et al, 2007). Additionally, as NO is released by deoxymyoglobin, it can escape immediate rescavenging because the reaction leaves behind the ferric form of myoglobin (met-myoglobin), which does not interact with NO (Rassaf, et al, 2007). This may facilitate a more substantial reduction in VO_2 than the limiting presence of O_2 alone but to what extent remains unknown as quantification of NO has yet to be conducted reliably in vivo.

The literature is rife with examples of increased [NO] leading to an elevation in tissue PO_2 (Chen, et al, 2005). Part of this may be explained by increased oxygen supply by NO-induced vasodilation, but the inhibitory effect on demand cannot be ignored. Studies have shown that supplementation with dietary nitrite, which is then converted to NO during raised metabolic demands, causes a decrease in VO_2 and an increase in gross skeletal muscle efficiency (Larsen, et al, 2007). NOS3 knockout mice have greater tissue oxygen consumption and a 40% decrease in their longitudinal oxygen gradients within microvessels (Cabrales, et al, 2005). It is clear that there is a physiological mechanism of VO_2 regulation and that it is important in pharmacological effects on hypoxic tissues.

Ischemia and Reperfusion:

Interruption of blood flow to the heart or brain, even for a few minutes can cause irreparable damage and may result in death. During a myocardial infarct, the damage done during a short period of ischemia may appear to be limited, but reperfusion with oxygen can

reveal irreversible effects. In fact, reoxygenation of an ischemic region can alter the ways mitochondria handle oxygen, adding to the damage. But ischemia/reperfusion injury is not a linear progression of effects; protective mechanisms involving the manipulation of VO_2 kinetics can provide some endurance to ischemia. Ironically, this mechanism of protection was identified by preconditioning the tissue with brief episodes of ischemia; this led to the search for its pharmacological reproduction to improve the clinical outcomes of heart attack and stroke. While much of the focus has been on the long-term influences of various protocols of preconditioning (with and without drug intervention) on infarct size and tissue survival, a description of VO_2 kinetics during brief ischemic preconditioning episodes may provide advance the understanding of these protective mechanisms. Overall despite the numerous regulatory mechanisms, no known chemical or mechanical intervention can protect the mitochondria (hence the tissue) from prolonged anoxia.

Ischemia:

For the purposes of this discussion, the state of ischemia in mammalian muscle tissue can be defined as dramatic reduction in blood flow due to occlusion of supply vessels that results in insufficient oxygen delivery to meet demand. The hypoxia or anoxia that occur in the ischemic tissue can then lead to damage. The time course of ischemic injury varies between tissues of different metabolic rates. Cardiac muscle tissue degrades rapidly, as exemplified by isolated neonatal rat cardiomyocytes showing morphological changes after ~30 minutes of anoxia (Musters, et al, 1991); human and mouse skeletal muscle tissue appears to remain viable for 2 to 2.5 hours (Eberlin, et al, 2008; Martou, et al, 2006). The principle mechanism of damage is suspected to be ischemia-induced alterations in mitochondrial structure and function (Veitch, et

al, 1992). As hypoxia is associated with increased ROS production by the electron transport chain, the oxidative stress of accumulating free radicals damages the respiratory chain complexes. Complexes I then III are affected first (Narabayashi, et al, 1982) and, being the primary mitochondrial generators of ROS during hypoxia, their dysfunction compounds the problem by further elevating ROS production (Chen, et al, 2003). While the precise length of time necessary to cause this is uncertain, there is one report that ischemic cardiac muscle ROS production is slightly elevated but stable for 25 minutes followed by a much higher rate of production (Kevin, et al, 2003). This self-feeding burst of ROS appears to be responsible for the poor outcomes associated with prolonged ischemia in skeletal and cardiac muscle tissues (Laskowski, et al, 2000).

Enhanced ROS production during prolonged ischemia in skeletal muscle is not solely due to functional changes in the mitochondrial ETC, but appears to come from other enzymatic sources as well. During ischemia, ATP is catabolized to hypoxanthine (ATP-ADP-AMP-adenosine-inosine-hypoxanthine-xanthine) with a rise in Ca_i^{2+} (McCord, 1987). Xanthine dehydrogenase is then converted to xanthine oxidase by a cytosolic protease whose activation is Ca_i^{2+} dependent (Korthuis, 1986). Xanthine oxidase a major source of ROS in both rat and human skeletal muscle (Smith, et al, 1989; Hellsten, et al. 1997), generates superoxide with any available O_2 during ischemia; more so if reoxygenation occurs (Singal, 1989).

Reperfusion:

Reoxygenation of ischemic tissues is necessary for their survival, but an unfortunate consequence of prolonged hypoxia and or anoxia is that normoxic oxygen levels become toxic and can cause further damage from mitochondrial dysfunction and necrosis (reviewed by

Halestrap et al, 2007). The stage for reperfusion injury is set during ischemia. As intracellular PO_2 falls below the critical point of VO_2 dependence on oxygen, oxidative phosphorylation slows down. The continued demand for ATP becomes reliant on anaerobic respiration, which is insufficient; the result is net conversion of ATP to ADP with a drop in intracellular pH due to the accumulation of lactic acid. The cell compensates for the increased acidity with the membrane-bound Na^+/H^+ antiporter. Because of the ATP deficiency, the extra sodium cannot be removed by Na^+/K^+ ATPase, and the Na^+/Ca^+ pump is activated. This results in intracellular calcium (Ca_i^{2+}) loading. The low pH_i exacerbates ROS production by the mitochondrial respiratory complexes, which then acts in combination with the elevated Ca_i^{2+} to break down the mitochondrial electrochemical gradient and hence, the ability to produce ATP upon reperfusion and the return to normal pH_i (Halestrap, et al, 2007; Griffiths and Halestrap, 1995; Kim, et al, 2006).

Reperfusion injury has been proposed to be mediated through the following two destructive events: 1) reoxygenation of mitochondria causes a burst in ROS production (Kevin et al, 2003); and 2) the high [Ca_i^{2+}] coupled with a return to normal intracellular pH increases the open-state probability of the mitochondrial permeability transition pore (MPTP) (Kerr, et al, 1999). While ROS is inherently destructive, and a burst of ROS even more so, one explanation of reperfusion injury may be that the opening of this MPTP that causes depolarization of the mitochondrial inner membrane, thus destroying the capacity for ATP synthesis, and eventual apoptosis (Halestrap, 2006). The MPTP has been described as a hole in the mitochondrial inner membrane that is permeable to anything <1.5 kDa. This causes obvious problems with maintaining the proton gradient needed to drive ATP synthesis and can reverse the proton-translocating ATPase so that it hydrolyses of any remaining ATP (Halestrap, 2007). While a

single MPTP opening will not doom an entire mitochondrion, the depolarization increases the chance of additional MPTPs opening (Scorrano, et al., 1997). ROS is not excluded from this model although it is also suspected to cause an increase in MPTP opening probability, thus contributing to both oxidative damage and energy starvation of the cell. The result of these reperfusion-induced mitochondrial dysfunctions is apoptosis and local inflammation, which can cause further degradation of surrounding tissues leading to increased infarct size (Schoen, 2006). It is reasonable to conclude that the usage and conditions of usage of oxygen by the mitochondria are tied to cellular fate. Thus, it should be no surprise that modulating the supply of oxygen to alter demand led to a key mechanism of protection against ischemic damage.

Preconditioning:

First described by Murry et al, in 1986, brief episodes of ischemia in dog myocardium prior to a typically destructive duration of ischemia and reperfusion, now referred to as ischemic preconditioning (IPC), reduces the infarct size (Murry, et al, 1986). The authors of this study theorized that the mechanism of protection was related to a reduction in the rate of ATP depletion conferred by IPC. This would improve endurance to a subsequently longer ischemic event. The IPC effect has been observed in human to rat cardiac and skeletal muscle (as discussed by Pang, et al, 1993; Veitch, et al, 1992), but despite the reproducible nature of the IPC response amongst various tissue types, the mechanism or mechanisms of action to confer this ischemic protection are not resolved.

A profile of 5 to 10 minutes of ischemia followed by 5 to 10 minutes of reperfusion for 1 to 3 cycles confers protection against prolonged ischemia in both cardiac and skeletal muscle (Martou, et al, 2006; Addison, et al, 2003). This time course for the induction of IPC protection

in skeletal muscle has been repeatedly confirmed over the past 20 years and is attributed to changes in mitochondrial potential that depress the rate of ATP depletion (Pang, et al, 1993; Pasupathy and Homer-Vanniasinkam, 2005). Although the exact mechanism of action remains controversial (as reviewed by Halestrap, 2007), there is a rise in ROS production upon reoxygenation following 5 to 10 minutes of severe hypoxia. Thus, brief episodes of ischemia induce this small ROS burst, which activates mitochondrial K_{ATP} channels, resulting in a reduced rate of ATP hydrolysis (Vurionen, et al, 1995; Vander Heide, et al, 1996; Santos, et al, 2002). This ROS burst upon reoxygenation has been consistently implicated as necessary for the protection conferred by the IPC protocol (Dost, et al, 2008), and there is considerable evidence that the subsequent opening of K_{ATP} channels leads to a reduction in both ATP hydrolysis and the probability of MPTP opening during a subsequent ischemic event with reperfusion (Moses MA, et al, 2005). An alternative mechanism in skeletal muscle is the necessary activation of protein kinase c (PKC) by ROS to elicit the effects of IPC (Ytrehus, et al, 1994; Pain, et al, 2000). Whether the two mechanisms are mutually exclusive or integrate to induce IPC protection is unclear, but they are downstream from the changes in mitochondrial function that have been identified as a burst in ROS, which is necessary for induction of IPC (Dost, et al, 2008).

The evidence indicates that the damaging and protective qualities of various durations of ischemia and reperfusion reflect changes in mitochondrial function during hypoxia and subsequent reoxygenation. As the O_2 consumption is tightly correlated to mitochondrial function, VO_2 may be a powerful indicator of changes in cellular respiration during the brief episodes of ischemia that are associated with preconditioning. The oxidative capacity of rat skeletal muscle following 5 hours of ischemia indicates a reduction of V_{max} by 43% (Brandao, et

al, 2003; Thaveau, et al, 2007), which is improved in groups exposed to IPC for the same time course and severity of ischemia (Thaveau, et al, 2007). This is consistent with the notion of progressive damage to mitochondria during severe ischemia. It is currently believed that IPC reduces the rates of ATP hydrolysis and oxidative phosphorylation. Therefore, a description of the VO_2 profile following these IPC regimens during this time is important as an assessment of mitochondrial function. Additionally, pharmacological modification of this profile may help resolve whether there is an earlier step to the ROS burst in mitochondrial adaptation to oxygen deprivation.

Pharmacological IPC:

Nitric oxide mimics IPC protection in heart, which is abolished by NO scavenging (Cohen, et al, 2006; Costa, et al, 2005; Jones and Bolli, 2006). This effect has also been noted in skeletal muscle sugesting that both tissues are protected by the same or similar mechanisms (Ozaki, et al, 2002). If preconditioning's primary mechanism of protection is to preserve mitochondrial function by a slowing down the kinetics of the ETC, then NO may function similarly to IPC in reducing the mitochondrial inner membrane potential and thus the probability of MPTP opening because it inhibits cytochrome oxidase c (Hausenloy, et al, 2004). Whether NO only functions during the IPC phase (Qui, et al, 1997), or continues to provide benefits during the subsequent phase of damaging ischemia and reperfusion is unclear, but following ischemia, a positive effect of "post-conditioning" is reduced by the NOS inhibitor L-NAME (Yang, et al, 2004). As post-conditioning involves brief periods of reperfusion following a damaging ischemic event (thus limiting the exposure of O_2 to dysfunctional mitochondria), NO

may act similarly to alter VO_2 kinetics and limit the destructive effect of full-scale reoxygenation.

Summary of Study:

A novel technique for multiple and continuous measurements of VO_2 dynamics in thin tissues is presented here, using the rat spinotrapezius muscle. The VO_2 sampling technique was adapted from a method that utilized externally transduced pressure to rapidly arrest flow while the resultant drop in interstitial oxygen tension ($P_{ISF}O_2$) was observed through phosphorescence quenching microscopy (PQM) (Golub, et al, in revision). The VO_2 sampling technique makes use of an automatic dual pressure system to toggle the pressurization of an objective-mounted air bag between high and low at regular intervals. With brief, periodic compressions, the initial component of the oxygen disappearance curve during complete blood flow arrest is reported by phosphorescence quenching microscopy and then translated into VO_2 without observable impact on subsequent measurements. The utility and sampling resolution of 3 per minute was extended to reperfusion following 1 minute durations of flow arrest (ischemia) via a sustained air bag pressurization. There was a slight indication of hyperemia for recovery profiles exposed to the VO_2 sampling technique, but the impact on VO_2 kinetics was presumed minimal when categorized to 3 different ranges of $P_{ISF}O_2$ immediately preceding compression. High compression pressure was also found to be optimal from 120-140 mmHg with minimal perturbation of the tissue for the 5x15 compression/recovery cycle.

Translation of the linear fall in $P_{ISF}O_2$ has 3 components: tissue VO_2, consumption by PQM (K), and refill (R). Using an in vitro analysis, K and R values were determined and a correction factor was developed to directly relate the initial part of the ODC to VO_2 with

minimal noise. This correction was universally applicable to measurements made with the R2 probe and under the conditions of topical application described in Methods and Materials.

Resting skeletal muscle VO_2 was assessed and plotted against $P_{ISF}O_2$ to determine the point at which cytochrome c oxidase became a limiting factor for respiration as measured by PQM's assessment of $P_{ISF}O_2$. VO_2 data was then divided into three categories: hypoxic, intermediate, and normoxic by the $P_{ISF}O_2$ immediately prior to compression (P_0), allowing those groups to be compared. Data from the Normoxic and Intermediate groups were statistically similar and slightly higher than other reported VO_2 measurements in skeletal muscle tissue. The resting state VO_2 of the rat spinotrapezius muscle was then pharmacologically altered with cyanide, nitroglycerin, and L-NAME and compared to control values.

The VO_2 profiles for 5 through 85 seconds of reperfusion following ischemic durations of 1, 5, and 10 minutes were assessed with the VO_2 sampling technique and compared in the categories of hypoxia, intermediate, and normoxia. Ischemia clearly produced a rise in VO_2 over baseline proportional to the duration. This effect was attenuated, but not abolished, by cyanide, attributing at least some of the effect to cytochrome c oxidase activity. Treatment with the nitric oxide donor nitroglycerin produced a similar reduction in VO_2 and a corresponding enhancement in $P_{ISF}O_2$. L-NAME, an inhibitor of nitric oxide synthase, reduced tissue PO_2 through a reduction in vascular delivery by constriction of arterioles, but did not appear to stimulate respiration in the normoxic $P_{ISF}O_2$ range. It produced a significant rise in VO_2 during hypoxia, which indicates that NO has a greater influence during hypoxia. Since NO is protective during ischemia/reperfusion injury and a down-regulation in ATP production is consistent with the induction of this protection during preconditioning, the data in this study support the hypothesis that that treatment with NO prior to the induction of ischemia results in a reduction in VO_2

consistent with the mitochondrial inhibition needed to confer protection during ischemia/reperfusion.

MATERIALS AND METHODS

Animals

The following non-aseptic, non-survival animal protocols were approved by the Virginia Commonwealth University Institutional Animal Care and Use Committee and are consistent with both the National Institutes of Health guidelines for the humane treatment of laboratory animals as well as the American Physiological Society's Guiding Principles in the Care and Use of Animals. By following these standards of humane animal research, both animal duress and the appearance of confounding data from the effects of undo surgical and experimental stress on the physiological situation were minimized.

Seventy-four male Sprague-Dawley rats (Harlan, Indianapolis, IN), chosen due to their ease of handling, calm disposition, and wide usage throughout medical research, were used. Males with an average weight of 286.30 grams (SE: 4.60) were used exclusively in order to reduce the influence of hormonal cycling on systemic parameters that might have complicated analysis of the microcirculation. These animals, segregated by pairs, were housed in plastic isolation containers in the facilities maintained by the Virginia Commonwealth University Division of Animal Resources. The animal housing provided continual ventilation in a climate-controlled room kept at 20-23 ^{o}C on a 12 hr: 12 hr light-dark cycle. Laboratory chow and water were provided *ad libitum* along with sanitation under the supervision of a certified animal care technician.

In accordance with standard non-aseptic, non-survival surgery protocols, all animals were euthanized under anesthesia via intravascular injection of 0.1 ml Euthasol (Pentobarbital 390

mg/ml and Phenytoin 50 mg/ml Delmora Laboratories, Inc., Midlothian, VA) following the conclusion of experimentation.

Surgical Practices

Pre-op

The animals were weighed on a triple-beam balance and given an intraperitoneal injection of Ketastet/Acepromazine (75 mg/kg and 2.5 mg/kg respectively) as an initial anesthetic in the lower left quadrant of the abdomen. Ketastet (Ketamine HCI, Fort Dodge Animal Health, Fort Dodge, IA) is commonly used to provide a sufficient depth of anesthesia for major surgical procedures before venular access is available for the use of a continually infused anesthetic. Acepromazine Maleate (Boehringer Ingelheim Vetmedica Inc., St. Joseph, MO) was used to reduce anxiety and stress and mitigate some of the sympathetic stimulation caused by the use of Ketastet.

Once an animal was verified to have entered a sufficiently deep anesthetic plane by inspection of reflexes such as toe and heel "pinch", it was transported to a mat, thermally-stabilized at ~37 ^{o}C via circulating, heated water, and made ready for "shave and prep." Three areas were cleared by use of electric clippers and a depilatory (Nair, Church and Dwight Co. Inc., Princeton, NJ): (1) the left, dorsal region that extended from the shoulder blades to the lower lumbar area for exteriorization of the spinotrapezius; (2) the skin above the ventral clavicle for the tracheotomy and any necessary jugular vein and carotid artery canulations; and (3) the ventral, inner right thigh for access to the femoral vein and artery.

With all surgical areas cleared and wiped clean with isopropyl alcohol swabs (Curad, Medline Industries Inc., Mundelein, IL), the animal was moved to the pre-heated,

homoeothermic surgical mat for immediate femoral vein cannulation and tracheotomy to ensure the continued maintenance of the anesthetic plane and health.

Femoral Vein Cannulation:

The right hind leg was taped to the bench top and a 1 cm incision was made into the integument along the limb/abdomen boarder. Next, the blunt dissection scissors were used to tease apart the skin from the deeper fascia, revealing the cleft between the leg and abdominal muscles. Probing the cleft and teasing away the deeper layers of fascia exposed the femoral vein, artery, and nerve bundle. At this point, the region was placed under a stereomicroscope (Nikon SMZ660, Melville, NY) and the bundle was dissected from the surrounding tissue with micro-dissecting forceps.

The isolated femoral vein was lifted superficially onto a thin, hand carved metal platform (sometimes referred to as the "lift") for cannulation. Taking care to maintain vessel moisture with the application of phosphate buffered saline (PBS), a tie (Ethicon surgical silk size: 00, San Angello, TX) was placed approximately 0.5 cm distal of the intended cannulation site to arrest flow and a second tie (not tightened) was positioned approximately 0.5 cm proximal to the intended cannulation site. Micro-dissecting (3mm straight) scissors, with careful direction beneath the stereomicroscope, were then used to cut an incision just large enough to accommodate the cannula (Polyethylene Tubing (PE)-50, Clay Adams, Parsippany, NJ) into the femoral vein. The cannula, having been checked to ensure that it was free of air bubbles, was then fed into the vein ~2 cm deep and then the proximal tie was tightened to secure it in place. The integument was then closed with superglue (Loctite® Super Glue Gel, Henkel Consumer Adhesives Inc., Avon, OH).

Gaining prompt access to the femoral vein allowed for a seamless transition in terms of anesthetic depth between the initial use of Ketastet and the onset of the continuously infused Alphaxan (Vetoquinol Uk Limited, Buckingham, MK18 1PA). In the rare occasion of indications of animal arousal prior to femoral vein access, an additional injection of 0.1-0.2 ml Ketastet was given as described above and surgery was delayed until the animal returned to the appropriate plane of anesthesia. Alphaxan was administered continuously at an average rate of 0.38 ml/h (SE: 0.01) using an electronic infusion pump (Sp120P Syringe Pump, WPI, Sarasota, FL) with adjustments to the flow rate by diligent monitoring of the animal via toe and heel pinch in addition to other appropriate metrics of anesthetic depth.

Tracheotomy:

Taking into consideration animal well-being and sensitivity of systemic oxygen levels on proper ventilation, the maintenance of a patent airway was essential. The ability to rapidly clear aspirating fluids that might otherwise confound measurement or bring about animal death was achieved via the insertion of a flexible tube (PE-240) into the trachea immediately following femoral vein cannulation.

To start, a 1 cm lateral incision was made into the skin perpendicular to the body axis (across the throat), approximately 1.5 cm below the mouth and separated from the underlying connective tissue revealing a thick tissue layer bracketed by two mandibular glands. The fascia between the glands was then teased apart to expose the underlying sternohyoid muscle. Next, using the microdissection forceps, the natural separation running down the center of the muscle was spread apart revealing the deeper tracheal tube. The trachea was then carefully freed from its surroundings and elevated by the passage of one of the curved micro-dissecting forceps

beneath it. Ensuring that the airway was not constricted by this action, any bleeding that might have occurred during tracheal exposure was then staunched using a low temperature cautery (Gemini RS-300, Roboz Surgical Instrument Co., Rockville MD).

A piece of 3-0 non-sterile, braided silk suture (Ethicon, San Antonio, TX) was threaded under the trachea and positioned caudal to the intended site of tracheal insertion. Then, using the microdissecting scissors, a cut just large enough to accommodate the PE-240 tube was made between the bands of cartilage lining the trachea and the tracheal tube was inserted. Once positioned to a sufficient depth to prevent expulsion, but not deep enough to obstruct the branching bronchioles, the suture was tied to fix the tube in place and the integument was closed around it with super glue. Subsequent observances of fluid in the trach-tube were dealt with by suction from an inserted PE-90 tube attached to a 10 ml syringe.

Spinotrapezius Preparation:

The protocol for the exteriorization of the rat spinotrapezius muscle for intravital microscopy was first described by Gray (1973) and has since been adapted to suit our needs for continuous sampling of tissue VO_2 on our thermostatic animal platform (Golub and Pittman 2003; see Figure 3).

To begin, a region of hair approximately 8 x 5 cm starting at the shoulder blades on the rat's dorsal side and proceeding caudally to the rat's lower lumbar area was trimmed with hair clippers and subjected to a depilatory (Nair, Church and Dwight Co. Inc.) to allow access to the skin. Next, having completed all canulations, tracheotomy, and assured the continued maintenance of a proper plane of anesthesia, a dorsal midline incision was made in the lower lumbar region of the hairless patch to expose the underlying fascia. Care was taken to cut only

the thick layer of skin and not penetrate the fascia as this can cause damage to the deeper spinotrapezius muscle. Using the curved blunt dissecting scissors (pointed up and away from the spinotrapezius), the skin was carefully teased apart from the underlying fascia proceeding rostrally towards the shoulder blades. As the skin was freed, the incision was continued along the midline until reaching the shoulder blades. Excess bleeding from the cut dermal layer was staunched with the low temperature cautery and a few drops of PBS were occasionally applied to the exposed, deeper tissues to prevent desiccation.

Using the same technique of teasing, cutting, and cauterizing, the incision was continued at both endpoints turning 90 degrees left and proceeding laterally for approximately 3 cm (longer for larger rats). This produced a flap of skin that was pulled away, exposing the underlying fascia covering the left spinotrapezius muscle. Some additional teasing and cauterization was occasionally required to fully separate the skin flap from the deeper layers.

Grasping the superficial layer of fascia around the lumbar region with the micro-dissecting forceps, a pinched section was lifted away from the underlying tissue. Next, a hole was made in the pinched fascia and the curved blunt dissecting scissors, faced upwards, were inserted to begin teasing the fascia apart from the deeper layer. As some of the deeper layer was the actual spinotrapezius muscle, care was taken to prevent damage. The fascia pulled away along its lateral boarder, allowing it to be folded up and over the dorsal midline. In the event that it did not pull free, use of the cautery to cut the remaining connections was appropriate. Teasing was then continued rostrally until the left, lateral feed vessels to the spinotrapezius were revealed and then progressed medially along the entire flap of fascia until reaching the midline. This exposed the entire exteriorizable portion of the spinotrapezius along with its attached “strap” muscle along the lateral boarder. Continued dripping of PBS prevented drying.

With the superficial fascia cleared, the thin "strap" muscle (lateral to the spinotrapezius) was gripped and cut away from the connective tissue along its lateral boarder. This separation was coupled with the careful teasing apart of both the strap and attached spinotrapezius from deeper muscle layers. This technique required the insertion of closed, curved blunt dissecting scissors beneath the spinotrapezius followed by their slow opening and withdrawal. It was important to keep the curved end pointed away from the spinotrapezius (downward in this case) at all times to minimize tissue damage. Separation of the spinotrapezius began at the lateral grouping of feed vessels and proceeded distally to the "tip." Upon reaching the tip, a low temperature cautery was occasionally necessary to prevent bleeding from cut distal feed vessels. At this point, two equidistant sutures (Surgik 4-0, Broken Arrow, OK) were placed along the strap muscle at the lateral boarder of the spinotrapezius with a third being fixed to the muscle's tip. This allowed the spinotrapezius muscle to adopt a more natural form when it was placed on the pedestal. Separation then continued proximally along the medial boarder with careful use of the cautery to staunch bleeding until such a point was reached where the medial and lateral separations were of equal length. At this time, two final sutures were placed along the medial boarder mirroring the work on the lateral boarder.

Note: Surgik 4-0 monofilament nylon suture was ideal for use in this situation as it minimizes tissue damage and stretching. The needles came pre-attached to the suture, which allowed for a smooth transition from the metal to line. This prevented damage from trying to yank knots through the tissue. Additionally, the needles were disposable after a few experiments and thus never reached the point of dulling under normal use.

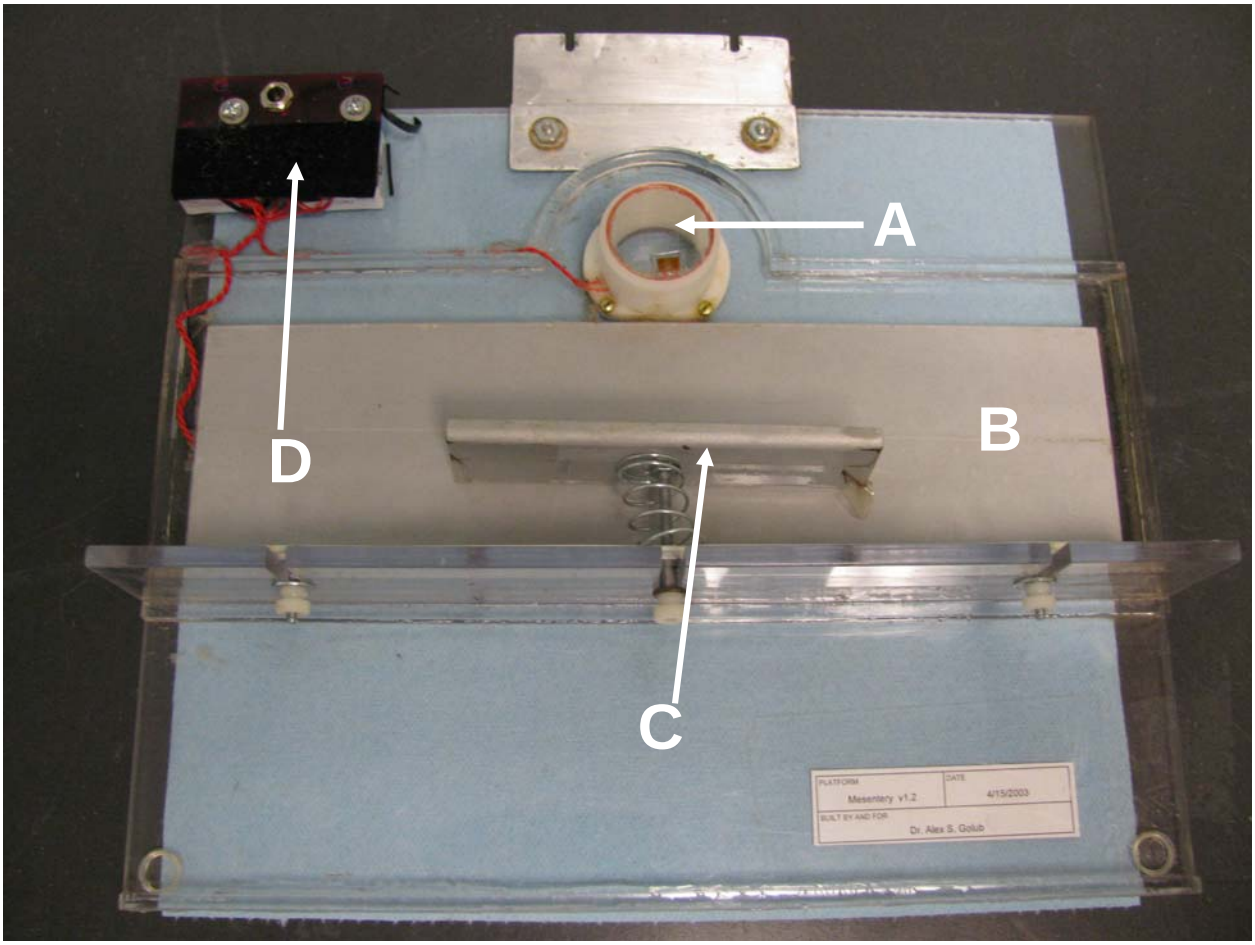

Figure 3: Thermostatic animal platform adapted for use with the PQM setup. A: The transparent, heated pedestal that allows for isolation and measurement of the exteriorized spinotrapezius preparation. B: A thermal plate that maintains the animal's core body temperature during anesthesia. C: An adjustable spacer that can accommodate animals of varying body size. D: This is the thermo regulator that controls platform heating.

Animal Mounting on Thermostatic Platform:

To meet the demands of microscopy and animal well-being during experimentation, the rat was placed on a platform that was specially adapted for use with PQM. Prior to animal mounting, the stage was prepared by covering the spinotrapezius observation pedestal with a single layer of oxygen impermeable Krehalon (Krehalon CB-100) and then securing it in place with a neoprene pedestal ring. This prevented the R2 probe from contaminating the pedestal surface as well as allowing for easy cleanup. Additionally, the stage was preheated to minimize the amount of time both the rat and tissue might spend below normal body temperature.

To mount, the rat was first laid down on the stage's core heating platform and the spinotrapezius was placed flat on the pedestal so that the deeper side was faced upwards. The sutures were then gently pulled and anchored to the neoprene pedestal ring with hot glue so that the spinotrapezius was held flat against the platform, yet still retained a close approximation to its natural size and shape. Some mild stretching of the tissue was necessary to prevent it from bunching up during experimentation (see Figure 4). An ideal mounting of the muscle showed a clear image under trans-illumination and had no discernable shift (movement/compression artifact) in PO_2 when switching between high and low compression. Additionally, when shifting locations under trans-illumination and low pressure, the tissue remained in focus.

Note: in general, proper exteriorization has not been found to significantly alter blood flow in the rat spinotrapezius muscle (Bailey, et al 2000). Thus, inconsistent and improper technique was the greatest enemy to consistency. Along with gentle handing of the muscle during exteriorization, it was important to maintain muscle hydration at all times or else the microcirculation would reflect that of an undesirable dehydrated state. A few drops of PBS whenever the surface of the muscle seemed to have lost the sheen of wetness took care of this

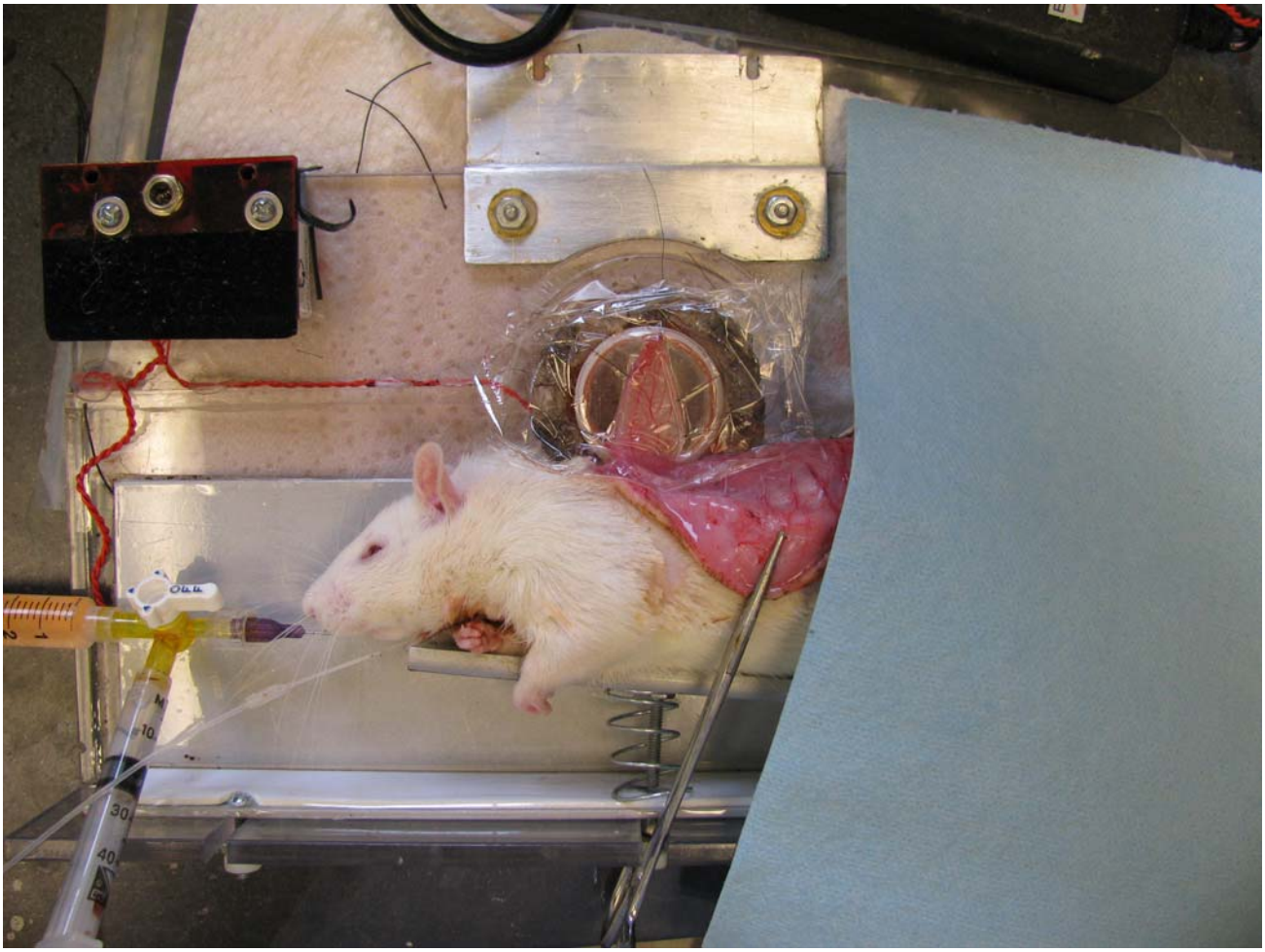

Figure 4: An exteriorized spinotrapezius preparation. The muscle has been secured to the observation pedestal and covered temporarily with a sheet of saran to prevent drying. This image was taken immediately prior to the application of the R2 probe.

problem and allowed for consistently strong flow along with proper phosphorescent probe loading and reporting.

R2 Probe Application:

The R2 phosphorescence probe was necessary for measurements of $I_{SFP}O_2$ using PQM. It was bound to 5% human serum albumin (HSA), as described later, to maximize the uniformity of signal and allow for efficient loading into the interstitium To apply, approximately 100 to 150 µl of R2 probe was first dripped on to the surface of the muscle—already properly hydrated and mounted on the observation pedestal—until completely covered. Next, a few drops of PBS were placed around the pedestal's perimeter, but not in contact with the tissue, and a single sheet (~10x8 cm) of Krehalon was laid gently atop the prep. Where air bubbles remained along the boarder of the tissue, they were pushed out with a cotton swab taking care not to disturb the layer of probe that sat atop the tissue. Once bubble-free contact had been made with the Krehalon flush against the pedestal, pushpins were used to anchor the Krehalon to the neoprene ring.

R2 Loading:

The platform, complete with animal, was relocated to its relevant PQM setup (see Figure 5) and the onboard heating was reengaged immediately. Anesthesia tends to disable hypothalamic control over thermoregulation, causing a rapid decline in body temperature (McKay and Clement, 1977) and thus the platform's thermal plates were needed to supplement heat for both the animal's core and the exteriorized spinotrapezius on the pedestal. Although normal core temperature was maintained during surgery via the heating pad, the spinotrapezius probably underwent some cooling during exteriorization and mounting. Thus, in addition to

satisfying the need for a sufficient probe loading time, a 30 minute period before beginning the measurements allowed the microvasculature to stabilize and return to its best approximation of the physiological condition. No pressure or other experimental intervention was made during this period in order to prevent regional variations in final probe concentration.

Upon completion of the rest/incubation phase, a cotton swab was used to apply a thin layer of silicone lubricant (Touch Massage: KY Brand) to the surface of the Krehalon, which reduced the friction at the bag interface. The gentle brushing action also served to ensure that the Krehalon was in good, solid contact with the tissue. Finally, the objective was lowered into place so that the Krehalon compression bag (Figure 10), pressurized at 5 mmHg, was in contact with the Krehalon above the tissue. The low pressure minimized the fluid layer above the tissue and therefore allowed the majority of the phosphorescent signal to originate from the dye-saturated tissue interstitium.

Intravital Microscopy:

Observation and measurement of exteriorized spinotrapezius preparations—mounted on the thermostatic animal platform—were conducted via an intravital microscope (Axioimager2m, Carl Zeiss, Germany; see Figure 5) configured for both epi and trans-illumination through a 20X/0.8 objective (Plan-APOCHROMATE, Zeiss, Germany). To ensure exclusive measurement of the tissue and for purposes of blood flow interruption, the objective was affixed with a transparent saran bag that maintained physical contact at low (5 mmHg) and high (120-140 mmHg) pressures with the Krehalon-covered preparation throughout experimentation. Friction between the two layers of Krehalon was minimized with a layer of KY lubricant.

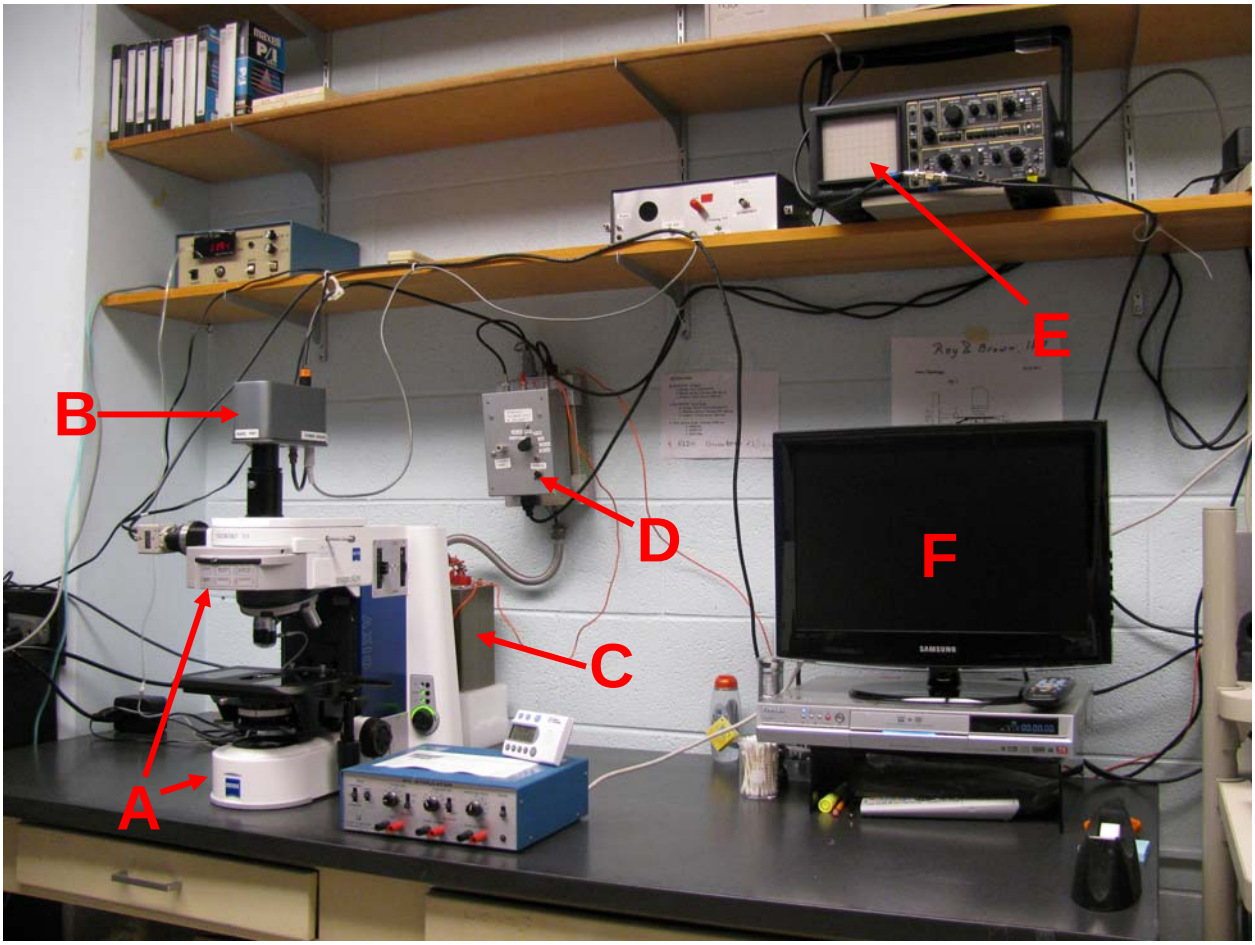

Figure 5: Intravital Microscopy Setup. **A**: The optical components and base of the Axioimager2m light microscope. **B**: The photomultiplier tube which provided signal enhancement of the phosphorescence emissions. **C**: The xenon flash lamp delivered uniform pulses of light to the 300 μm diameter octagonal excitation region to induce phosphorescence. **D**: This device controlled pulse frequency. **E**: The oscilloscope provided a visual representation of the phosphorescence lifetime during experimentation. This enabled real-time feed back for tissue oxygenation under various conditions. **F**: Images could be viewed during transillumination on this LCD monitor. The TV's high resolution was essential for site selection, flow assessment and measurements of arteriolar diameter.

Epi-illumination:

Excitation of the R2 phosphorescent probe, distributed in the interstitium of the spinotrapezius preparation, was achieved via a xenon flash lamp (Model FX249, EG&G Electro-optics Co., Salem, MA) epi-illumination, which delivered 0.5 J/Flash for a duration of 4 μs (full width at one third maximum pulse height) to an octagonal region of tissue 300 μm in diameter at a frequency of 10 Hz. Light from the flashtube was directed through a filter cube into the objective lens and delivered to the desired point of focus within the tissue's microvasculature. The filter cube consisted of a narrow-band filter (INTOR 525/70/75%, Intor Inc. Socorro, NM), specifically designed to excite the probe at the 525 nm wavelength of light (the Q-band), a dichroic mirror (Chroma 565 DCLP, Chroma Technology Corp. Bellows Falls, VT) and a wide-band filter (Oriel Cut-on >650nm, Newport Corp, Stratford, CT) for selective collection of phosphorescence emissions. The subsequent phosphorescence emission was collected through the 20X objective and detected by a photomultiplier tube (PMT). The signal from the PMT then traveled to a modified amplifier (OP37EP, Analog Devices, Norwood, MA) which functioned as a current-to-voltage converter outfitted with a precision analog switch (ADG419BN, Norwood, MA) allowing for a gating time of 12μs. The 12 μs delay between pulse initiation and data collection covered the 5 μs propagation delay from the plasma arc to the flash, the 4 μs light pulse, and 4-5 μs of any residual thermal tail from the flash lamp and lingering fluorescence signal from tissue or probe. Thus, the data collected were optimized to contain the highest contribution from phosphorescence with the time resolution to acquire the earliest components of the lifetime for reliable measurements of high PO_2. These signals were visually monitored in real-time with an oscilloscope (72-3060, Tenma, Springboro, OH) before they were passed to a 12-bit analog-to-digital converter (PC-MIO-16E-4, National Instruments, Austin, TX), and saved

digitally on a Dell Optiplex PC (Round Rock, TX). See Figures 5 and 6 for pictorial and diagrammatical views of this setup.

Data Acquisition and Analysis:

Data acquisition was controlled by the "ASGARD" program, written by Dr. Aleksander Golub using the software LabVIEW (National Instruments, TX) for this specific application. This allowed sampling at 500 kHz with 500 data points per curve. Curve collection number per measurement varied from 600 to 3000 depending on the time course. "RECTSINHFixFOff," another program written in LabVIEW by Dr. Golub, was used to automatically calculate the phosphorescence decay curves and translate them into measurements of PO_2 (see Figure 8), while Origin 6.1 and Origin 7.0 (OriginLab, Northampton, MA) were used to further analyze measurements of oxygen disappearance, interstitial PO_2 averages. An Origin 6.1 non-linear fit program (CONS&REFILL, written by Dr. Golub) was used to additionally calculate the rate of oxygen consumption occurring as a result of phosphorescence quenching.

Transillumination:

The tissue's microvasculature was visualized under transillumination with white light from a light emitting diode (Luxeon V Star white, Quadica Developments Inc., Brantford, Ontario) that was fed up through the microscope's condenser (Model LN19A450C1D, Samsung, Seoul, Korea. The image, under 20X magnification, was captured in real-time by a color CCD camera (KP-D20BU, Hitachi, Tokyo, Japan) and displayed on a flat-screen color TV (Model LN19A450C1D, Samsung, Japan). Transillumination was used during the measurement site selection process, establishment of the appropriate focal plane and verification of flow

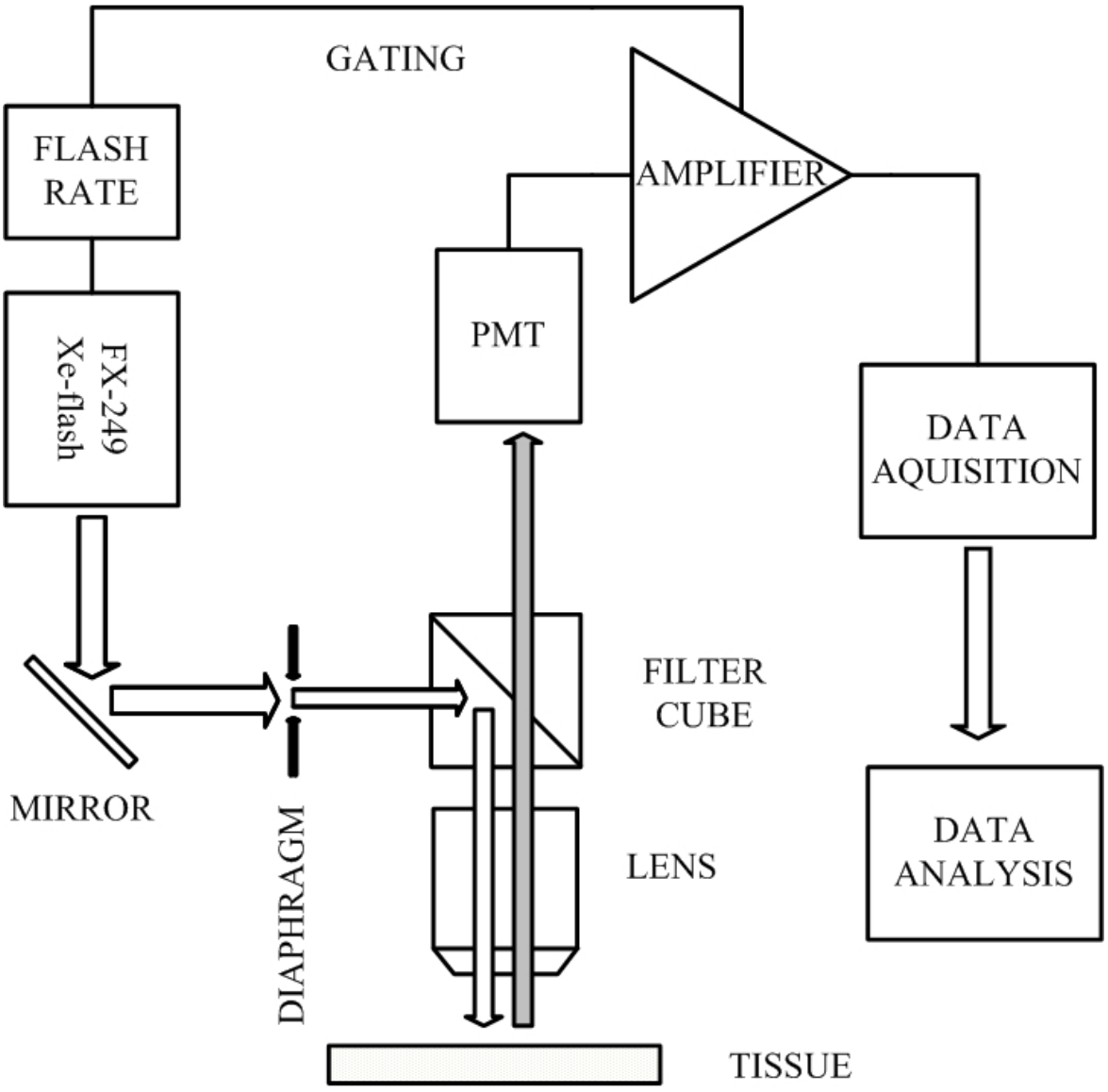

Figure 6: Schematic of the intravital microscope and data acquisition equipment as adapted for phosphorescence quenching microscopy.

conditions. For phosphorescence excitation and measurement, it was blocked along with other sources of stray light in order to minimize their influence.

Phosphorescence Quenching Microscopy

Partial pressures of oxygen were measured using phosphorescence quenching microscopy (PQM), a non-invasive method with high selectivity and spatial and temporal resolution. Phosphorescence occurs when molecules absorb an appropriate wavelength of light and transition from the ground to the singlet state. While many quickly return to ground state via fluorescent emission, some undergo intersystem crossing into the triplet state before returning to ground state with a phosphorescence emission. The conversion to the triplet state separates the rapid burst of fluorescence from the lingering phosphorescence, which decays with lifetimes from microseconds to milliseconds (Wilson, et al. 1987). In addition to emitting a photon (phosphorescence) to return to the ground state, molecules in the triplet state can transfer their energy to other molecules, a process known as quenching. Quenching has the effect of reducing phosphorescence lifetimes in inverse proportion to the concentration of the quencher. As O_2 is the principle quenching agent in biological tissues and is only limited by diffusion, a relationship between phosphorescence lifetime and tissue PO_2 can be readily established. The oxygen dependence of the phosphorescence decay is described by the Stern-Volmer equation:

$$1/\tau=1/\tau_0+k_qPO_2 \qquad \text{(Equation 2)}$$

where τ is the lifetime at the measured PO_2, τ_0 is the phosphorescence lifetime in the absence of oxygen, and k_q is the quenching coefficient. While this simple equation is sufficient for samples

with homogenous PO_2, the interstitium of skeletal muscle exists as a dynamic gradient between vascular supply and tissue respiration—most noticeably during changes in metabolic demand. This heterogeneity can cause underestimates of PO_2 when calculations are made with a mono-exponential function. In response, Golub et al (1999) proposed a rectangular distribution model that minimizes the systematic error by accounting for regional variability in PO_2 levels within the measurement area (see Figure 8). All interstitial PO_2 values were therefore calculated using the following equation:

$$y_1 = a*\exp[-(k_0+k_qM)\tau]*\sinh(k_q\delta\tau+y_0 \qquad \text{(Equation 3)}$$

where a is the phosphorescence signal amplitude in volts, k_0 is the phosphorescence lifetime in the absence of oxygen, k_q is the coefficient of quenching, M is the mean PO_2, δ is the half-width of the PO_2 distribution, and y_0 is the baseline offset. The values for constants k_0 and k_q, $1.53*10^{-3}$ μs^{-1} and $0.43*10^{-3}$ $\mu s^{-1}mmHg^{-1}$ respectively, were determined by systematically accounting for conditions of temperature and pH in living tissue (Dunphy I, et al. 2002), and confirmed with micro slides containing various known PO_2s.

Description of Phosphorescence Probe:

Pd-meso-tetra-(4-carboxyphenyl)porphyrin (Oxyphor R2) was solubilized in phosphate buffered saline and bound to human serum albumin as described later. The R2/Albumin-bound probe was topically applied to the spinotrapezius muscle at a concentration of 10 mg/ml and, following 30 minutes of incubation, reached a level within the interstitium that allowed for a

strong phosphorescence signal that did not appreciably diminish over 3-4 hours of experimentation and followup post mortem analysis. The average interstitial probe concentration was 19.5μg/ml (SE: 2.3) and this value was used as an in vitro reference for quantifying the oxygen consumption by the method. Additionally, the skeletal muscle tissues were not uniform in terms of structure and density, which resulted in some minor heterogeneity in the distribution of the probe. These differences were not noticeable or were excluded from measurement. It has also been established that the probe concentration does not affect the phosphorescence lifetime, thus, all measured sites could be accurately converted to measurements of PO_2 regardless of minor variations in signal amplitude (Vanderkooi, et al. 1987).

R2 has two absorption peaks (415 and 524 nm, the soret and Q bands respectively) and an emission peak of 690 (see Figure 7; Dunphy et al, 2002). A filter cube set the excitation wavelength at 525 nm in order to take advantage of the deeper tissue penetrance of a longer wavelength of light with maximum and specific excitation at the Q-band. The resulting emissions signal, collected through the 20x objective, was passed through a >650 nm cut-on filter that allowed for the exclusive collection of the wide R2 phosphorescence 690 nm emission peak before reaching the photomultiplier tube. This, in conjunction with signal gating, helped ensure the best possible collection of a pure phosphorescence signal. Additionally, all measurements were performed under dark conditions with the microscope shielded from stray light. When necessary, an amber light source that did not alter the R2 probe's disposition was used to illuminate the setup for adjustments and maintenance of rat health.

The binding of the phosphorescence probe Pd-MTCPP to albumin not only penetrates the entire depth of the spinotrapezius muscle during topical application, but occupies only the

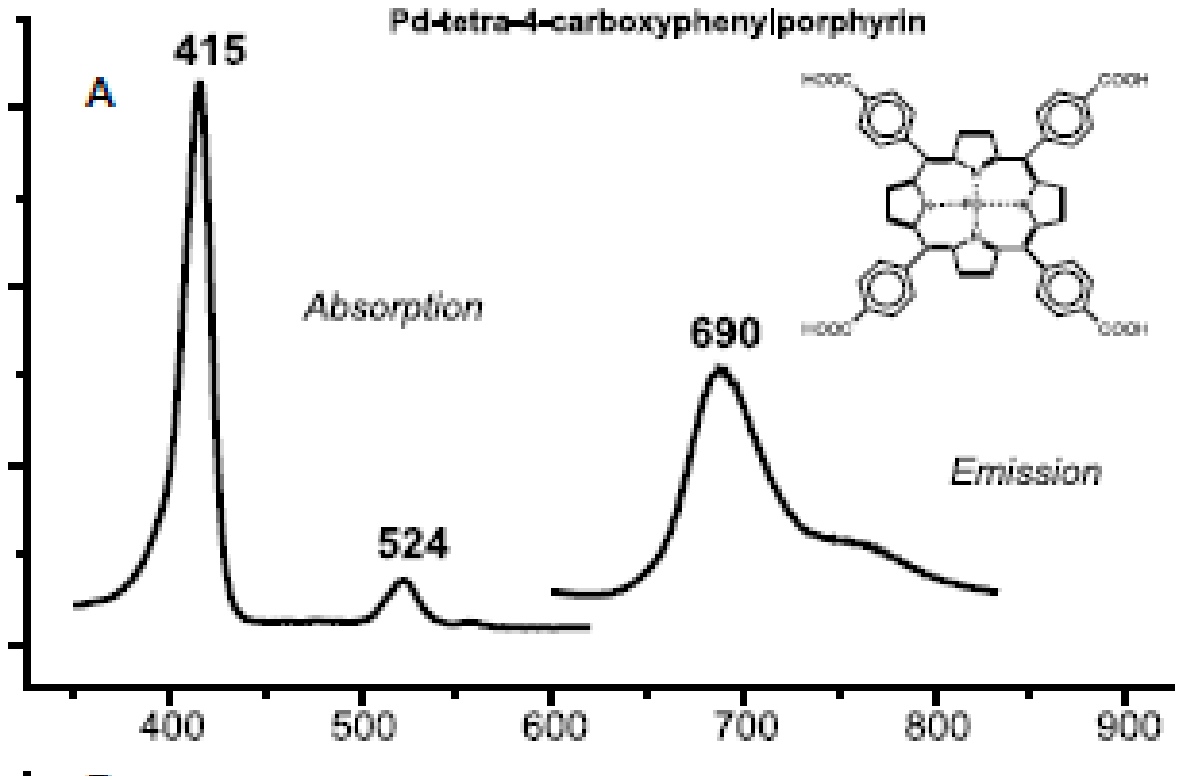

Figure 7: Diagram of the R2 phosphorescent probe's absorption and emission peaks. This study made use of the "Q-band" at 524 nm for excitation.

Figure adopted from:

Dunphy I, Vinogradov SA, and Wilson DF. Oxyphor R2 and G2: phosphors for measuring oxygen by oxygen-dependent quenching of phosphorescence. *Anal Biochem* **310**: 191-198, 2002.

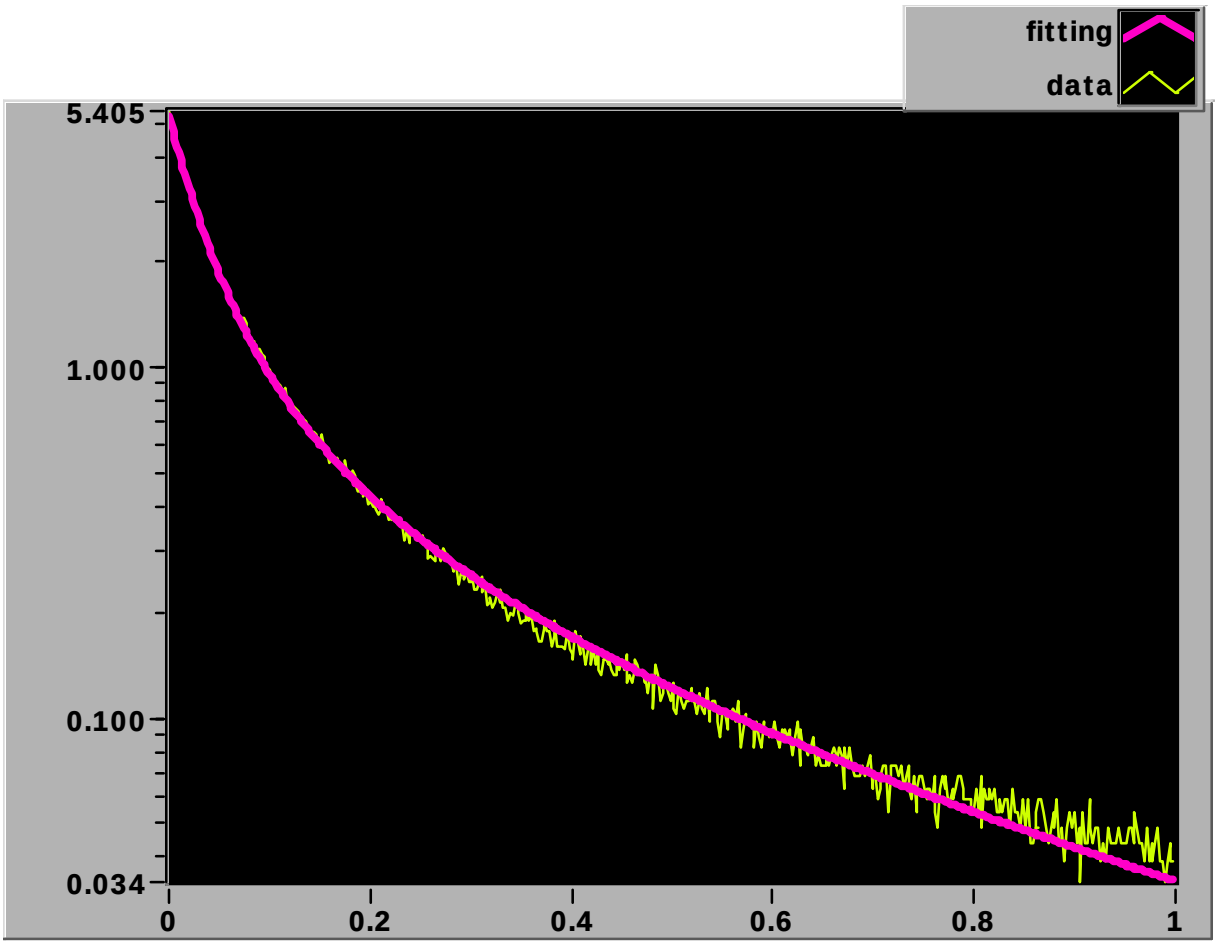

Figure 8: Mathematical fitting of an R2 phosphorescence decay curve. The fitting (pink line) of raw decay curve (yellow line) was done using the RECTSINHFixOFF software developed by Dr. Golub based on equation [2], this calculation gave a PO_2 value of 75.4.

interstitial space (Tevald, 2006). R2 was similarly bound to albumin, and therefore had a similar diffusivity to Pd-MTCPP. Any proliferation into the vascular lumen would have resulted in immediate clearance and the sarcolemma were impermeable to albumin. Thus, all measurements are from probe that is exclusively within the interstitium of the spinotrapezius muscle.

Energy Density

The excitation energy impacting the tissue was measured using a commercially available sensor (Lasercheck, Coherent, Auburn, CA). Using a flash rate of 20 Hz, the energy per flash was measured to be 5.366 (SE: 0.0078) μW. With an octagonal excitation area of 74,600 μm^2, the energy density per flash was $3.59*10^{-12}$ $J*\mu m^{-2}$.

Oxygen Consumption by the Method

Excitation and intersystem crossing of a phosphorescent molecule produces a triplet state that is capable of interacting with O_2 to yield singlet oxygen and superoxide (Vanderkooi, et al., 1987). Although reactive oxygen species generation does not appear to cause damage during lengthy excitation of phosphorescence probes (Vanderkooi, et al., 1987), their production consumes oxygen. This could lead to measurement error with repeated measurement of a stationary volume of tissue. Prior PQM measurements have taken advantage of a relatively low level of oxygen consumption per flash compared to the large and continual influx of oxygen in well perfused tissues, so the method did not significantly alter interstitial PO_2 (Tevald, 2006). Since the most recent setup was designed to make use of 140 mmHg air bag compression to completely arrest blood flow, and thus the primary source of oxygen influx, consumption by the method became an important component when accounting for the PO_2 disappearance rate.

Determination of Probe Concentration in Tissue:

After the experiment, the spinotrapezius muscle was cut at its proximal connection and pressed to a thickness of 500 μm between two glass microscope slides. The assembly was then placed on the heated pedestal of the thermostatic animal platform and allowed to equilibrate to ~38 ^{o} C for 10 minutes. Simultaneously, three 100 μm thick micro capillary tubes (Vitrotubes 0.1X1.0 mm I.D. Fiber Optic Center Inc., New Bedford, MA) were loaded with 25, 50, and 100 μg/ml solutions of R2 probe bound to 5% albumin in PBS. This range of probe concentrations were chosen based on the projected level in the interstitium upon topical loading with 10mg/ml R2 bound to 5% albumin in PBS. The tubes were sealed with Critoseal (Krackeler Scientific Inc., Albany, NY) to prevent contamination by atmospheric O_2 and placed on the heated pedestal alongside the muscle prep for equilibration to 38 ^{o} C.

The amplitude of the phosphorescence signal was a function of both probe and oxygen concentrations. Thus, for a given PO_2, the concentration of R2 in a particular measurement area could be expressed in terms of the signal voltage. It was determined that measurement of the signal amplitude was most accurate when conducted at the lowest PO_2 possible. This then allowed a reliable comparison between the tissue sample and known concentrations. A high intensity green LED was shone on both the tissue preparation and the micro capillary tubes following the 10 minute equilibration period to stimulate photoconsumption and reduce the PO_2 to the practical zero. The tissue was then measured with PQM at multiple sites in order to obtain the average signal amplitude, with a gating time of 50 μs. Without altering the signal gain, the tissue was removed and replaced with the known samples. The average amplitudes from each sample were compared to that of the tissue average and known concentration with the same

signal strength as that of the tissue was divided by 5, accounting for the 5 fold difference in thickness between the micro capillary tube and the muscle preparation, to achieve an approximate value for the concentration of R2 probe bound to albumin in the interstitial fluid of skeletal muscle.

In Vitro Consumption Microcapillary Tubes:

A solution of R2 bound to 5% albumin in PBS at a concentration of 19.5 μg/ml (based on previous measurements of tissue concentration) was oxygenated by simple agitation during atmospheric exposure under dark conditions. The probe concentration was not scaled to account for the difference in excitation volume since the consumption rate at a particular probe concentration should be independent of volume. It was then loaded into micro capillary tubes, sealed with Critoseal to prevent further contamination by atmospheric oxygen, and placed on the heated pedestal of the thermostatic animal platform for 10 minutes to equilibrate to 38 ^{o} C. Next, using a short series of 1 hz pulses, the solution PO_2 was approximated. A green LED was then shone on the micro capillary tubes for brief periods until the PO_2 had decreased to ~100 mmHg. Our reasoning was that the analysis would be complicated in both consumption and refill by having unrealistically high PO_2s inside and outside the excitation region. Finally, various sites were exposed to 3000 flashes at 1, 10, and 100 hz excitation to obtain both the rate of PQM consumption and the refill from passive diffusion at the periphery of the measurement site.

In Vitro Consumption by Alginate Gel

Three 2% alginate gels were prepared and loaded with the R2 probe for assessment of PQM oxygen consumption. First, a 2% alginate solution was prepared by producing a 5 ml

solution of 5% HSA in deionized H_2O, and R2 probe at 19.5 µg/ml and combining it with 100 mg sodium alginate (Sigma Aldrich, St. Louis, MO) under vigorous stirring. The solution was then allowed to sit undisturbed for 30 minutes to eliminate any bubbles. Next under dark conditions, 600 µl of the solution was pipetted into plastic molds 39 cm in diameter to give an eventual thickness of 0.5 mm. Finally, a solution of 0.2 M calcium chloride was misted onto the molds and the alginate was covered and left alone for 1 hour to gel.

Once hardened, the alginate gels were carefully removed from their molds and placed on glass microscope slides. A sheet of Krehalon was then laid on top of the gel, in the same fashion as done with the spinotrapezius muscle preparation, to act as a barrier against atmospheric oxygen. Two 0.5 mm spacers were then placed alongside the gel and a second glass microscope slide was used to press the gel to the 0.5 mm thickness. Clips were attached to ensure stability and the assembly was then placed on the heated animal platform pedestal for a 10 minute equilibration period to achieve ~38 ^{o}C temperature. Sites nearest to the center of each gel were then selected and exposed to 10 Hz excitation for 3000 curves (5 minutes). The volume of gel was sufficient so that reoxygenation was not necessary between measurements. Data were truncated to begin at 100 mmHg since the PQM setup was optimized to function over the PO_2 range of 100 to ~0 mmHg.

VO_2 Sampling Technique

Interstitial fluid PO_2 is a function of oxygen supply and demand. Under resting conditions in skeletal muscle, supply and demand are sufficiently balanced by regulatory mechanisms so that the value of $P_{ISF}O_2$ lies between the PO_2 at the nearest vascular source of oxygen to the lower value at the neighboring respiring cells. For the most part, these PO_2

gradients can be averaged over a 300 μm diameter region of measurement without apparent heterogeneities in the phosphorescence lifetime due to dramatic differences in $P_{ISF}O_2$. As this average is a balance between vascular inflow of oxygen and tissue respiration, alterations in one or the other will result in a shift to a new average $P_{ISF}O_2$. Thus, when temporarily eliminating the vascular supply of oxygen by both flow-arrest and the extrusion of red blood cells in the localized region of interest, the rate of decline in $P_{ISF}O_2$ becomes a function of tissue respiration and consumption of oxygen by the method. Measuring the rate of $P_{ISF}O_2$ decline immediately following cessation of the vascular supply, with correction for PQM oxygen consumption yields the rate of tissue oxygen consumption by the tissue (VO_2).

Air-Bag Design and Assembly

Flow-arrest and blood extrusion for the purpose of VO_2 measurements in the rat spinotrapezius muscle were facilitated by a focused compression of the PQM excitation region using a transparent air-bag mounted to the objective lens. The use of a compressive force to alter vascular dynamics for purposes of microscopic observation was first described by Roy and Brown in 1880, and recently adapted towards the goal of VO_2 measurements in a variety of thin tissues (Golub et al, 2007). What follows is a further modification of this approach to accommodate serial VO_2 measurements as part of a local ischemia/reperfusion protocol (see Figures 9 and 10).

First, the interior a rubber grommet (The Hillman Group, Cincinnati, OH) was bored out until a snug fit was obtained to the 20X objective of the Axioimager2m microscope. The grommet was then punctured with a syringe tip to provide a means of airflow into the air-bag that would be placed over the objective lens. Next, a 10 cm x 10 cm sheet of transparent

Krehalon was cut and placed flat on a clean surface. Since the objective used is wider than previous models, an additional piece of restraint plastic was needed to focus the force of the bag's pressure on the site of measurement. Thus, a piece of thicker plastic was cut and folded so that a ~3 cm diameter hole could be precisely cut in the center. It was then placed atop the Krehalon. Both sheets together were then flipped over and placed over the mouth of an open cylinder—sized with a gauge slightly wider than the 20X objective—centered on the opening in the restraint-plastic. While maintaining the alignment of the opening in the restraint-plastic within the mouth of the cylinder, the Krehalon+restraint-plastic sheet was depressed ~1cm and then overlaid with the objective so that the grommet made contact with the edges of the mouth and the optics now fitting within the sheet's 1 cm depression. Next, the objective, sheet, and tube were carefully flipped and an O-ring (Danco #30 O-ring: Irving, TX) was slipped downwards and snapped over the grommet so that the Krehalon+restraint-plastic sheet was now affixed to the objective, thereby encasing the optics in an air-tight bag. A brief inflation was then conducted to test the bag's form. It was determined that a pressure of 5 mmHg should inflate the bag so that its lower border was between 1 and 2 mm from the objective lens. If the lower border of the air-bag were any closer to the objective lens, the bag would not make sufficient contact with the preparation to extrude the fluid layer and furthermore would cause insufficient flow-arrest during high pressure. Finally, all excess plastic was trimmed around the edges and the bag was sealed with tight wrappings of black electrical tape. Once tested for form and integrity at extreme pressure (200 mmHg), the air bag was assessed for its ability to stop flow in tissue before operational use.

Figure 9: Materials involved in mounting air-bag to the 20X objective. **A**: A 20X objective provided a mount for the air-bag as well as optics for both intravital microscopy and PQM. **B**: This sheet of plastic is heavier than Krehalon and was used as an elastic restraint to control the size of the air-bag's compression area. **C**: The Krehalon sheet provided the substance of the air-bag and was the only component to make physical contact with the Krehalon-covered spinotrapezius muscle preparation. **D**: When forming the air-bag around the objective's tip, this open-ended cylinder was used for correct positioning. **E**: An O-ring was used to secure the Krehalon air-bag to the grommet forming an air-tight seal. **F**: The grommet was fit snugly to the objective to provide a mounting for the air-bag. **G**: This needle acted as the pressure input into the air-bag. It was threaded through the grommet and secured in place by hot glue.

A

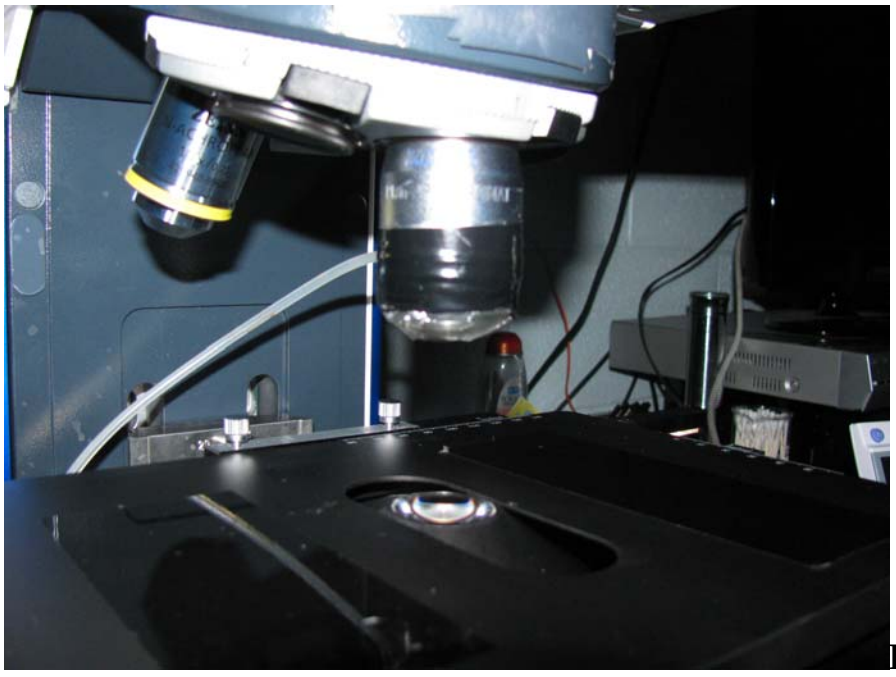

B

Figure 10: Air-bag mounted to 20X objective. **A:** The objective as it appears with the mounted air-bag. Black electrical tape helps to seal any minor air-leaks. **B:** The 20X objective with mounted air-bag as it appears during operation. The pressure is set to 5 mmHg.

Flow Arrest

Assessment of VO_2 in the intact, perfused rat spinotrapezius muscle preparation with PQM required an immediate and complete cessation of flow and extrusion of blood from the measurement area. To achieve this, an objective-mounted air-bag (see Figures 7 and 8) was inflated to topically deliver a focal compression that accomplished both aims of flow-arrest and blood extrusion.

Initially, the air-bag was pressurized to 5 mmHg to make soft contact with the preparation while providing sufficient force to press the Krehalon layer against the tissue. This functioned to extrude any surface accumulation of fluid that might report erroneous phosphorescent lifetimes. By observing the microvasculature in the focal plane during low pressure contact, it was determined that 5 mmHg did not visably alter blood flow. Typically, exclusion of the surface fluid layer via 5 mmHg pressurization of the air-bag was necessary for accurate PO_2 measurements even when flow-arrest was excluded from the protocol. Next, the bag was pressurized to 120-140 mmHg (depending on the tissue thickness), which immediately (<1s) stopped flow. Flow-arrest and red blood cell extrusion was visualized via transillumination for quality assurance. Additionally, transillumination was used during tissue compression to observe whether compression caused any shifting of the measurement area within the horizontal plane. Unintended tissue movement could typically be corrected by relocating to a different site, or in the most extreme cases, preparing a new air-bag. Following sufficient compression duration, the pressure in the air-bag was released back to 5 mmHg and flow was restored. Flow restoration was best assessed using PO_2 measurement by PQM, as visual inspection through transillumination was in some cases subjective.

Quasi-Continuous VO_2 Sampling

It was systematically determined, as described later, that a 5 second blood flow arrest brought on by pressurizing the air-bag at 120-140 mmHg followed by 15 seconds at 5 mmHg allowed for a sufficient temporal resolution of VO_2 without compromising either VO_2 or the recovery back to baseline PO_2. This rate of measurement provided a VO_2 sampling resolution of 3 per minute for as long as necessary. To precisely deliver the compressions of the appropriate duration and pressure, an automatic dual stage pressure cycling device was designed and constructed by Dr. Golub (Figure 9). Its function allowed for appropriately timed oscillation between two pressure levels, high and low, accommodating the 5 seconds of compression and 15 seconds of recovery in the measurement sequence. A digital display reported the current pressure inside the air-bag and a toggle switch allowed for the selection of manual pressure delivery for longer durations of both high and low pressure.

VO_2 sampling in vivo was conducted in the following manner: First the low (~5 mmHg) and high (~120-140 mmHg) pressures were selected and the device was set to manual control. This pressurized the air-bag to 5 mmHg for soft contact with the spinotrapezius muscle preparation—necessary for extrusion of any accumulated fluid layer that might interfere with the measurement. Next, PQM was used to record a baseline PO_2 at the typical 10 Hz excitation frequency. Finally, the device was switched to automatic mode for the prescribed duration and switched back to manual until the next measurement (see Figure 10 for typical VO_2 sampling profile).

Figure 11: Automatic Dual Stage Pressure Cycler. This device allowed for both manual toggling of low/high pressure and an automatic cycling of 5 seconds high pressure followed by 15 seconds of low pressure. High and low pressures could be adjusted to fit the individual needs of each measurement.

Arteriolar Diameter

Measurements of vessel diameter in the spinotrapezius preparation were made by visual inspection under transillumination at either 10X or 20X objective magnifications. The microscope was focused in the microvascular plane and the image projected to a TV screen. Vessel widths were then measured in millimeters as they appeared on the screen and then converted to actual values using the following equation:

$$d = (x*0.9) \qquad \text{Equation 4}$$

where x is the value measured from the image in millimeters and d is the actual arteriolar diameter in μm. This conversion appropriately adjusts the image size to the actual size.

Chemical Preparation

R2 Probe

For the purposes of measuring the interstitial PO_2 of the rat spinotrapezius muscle, the phosphorescent probe Oxyphor R2 (a palladium porphyrin dendrimer) was bound to human serum albumin (HSA) as follows:

First, 100 μl of 25% HSA by wt. (ZLB Behring AG, Berne, Switzerland) was removed from the stock container via a sterile syringe wiped with alcohol swabs before and after insertion. It was then mixed via gentle pipette action with 400 μl PBS in a 1 ml microcentrifuge tube to yield 500 μl of 5% HSA by wt. in PBS. Next, 5 mg of dry R2 grains were placed into a weigh boat and measured on a Sartorius CP64 digital scale (Balance People Inc., Newport News, VA).

Then, the solution of 5 % HSA was poured into the weigh boat and swirled until the R2 grains were completely dissolved. Finally, the R2 probe solution was poured back into the microcentrifuge tube, encased in photoprotective aluminum foil, and refrigerated until needed. Prior to each use, the probe solution was checked for signs of bacterial contamination and each preparation was discarded at the end of its 3-5 day shelf-life.

Phosphate Buffered Saline

In addition to the requisite maintenance of ionic balance during fluid intervention, many of the chemicals used in these studies were pH-sensitive and, thus all solutions were buffered to the physiological pH of 7.4 with isotonic Phosphate Buffered Saline (PBS). This solution was prepared by mixing 1 packet of powdered PBS (Sigma Aldrich, St. Louis, MO) with 1000 ml of deionized H_2O to obtain a concentration of 0.01 M.

Cyanide

Cyanide (NaCN) has a molecular weight of 49.01 and is water-soluble. It was used as an inhibitor of mitochondrial respiration in the rat spinotrapezius muscle preparation. 49.01 mg of powdered NaCN (Sigma Aldrich, St. Louis, MO) was added to 100 ml of room temperature PBS to produce a 10 mM stock solution. A dilution of 1:10 was then conducted by taking 100 µl of stock and adding to 900 µl PBS to obtain 1 mM NaCN. Further dilutions followed the same procedure with the exception that the 100 µl of NaCN were taken from the newly diluted concentration rather than the stock solution.

L-NAME

N_{ω}-Nitro-L-arginine methyl ester hydrochloride (L-NAME) was used as a non-specific inhibitor of the enzymatic production of nitric oxide (through nitric oxide synthase, NOS) in the rat spinotrapezius muscle. A 1.48 mM stock solution was made by adding 100 mg of powdered L-NAME (Sigma Aldrich, St. Louis, MO) to 250 ml PBS. This volume was refrigerated when not in use and serially diluted for application by factors of 10 to obtain the additional concentrations of 0.148, 0.0148, and 0.00148 mM in PBS.

Nitroglycerin

Nitroglycerin (NTG) was used as a nitric oxide donor that was topically applied to the rat spinotrapezius muscle preparation. To prepare as a solution, 1 tablet consisting of 0.4 mg NTG was allowed to dissolve in 1 ml PBS for 5 minutes. This mixture was then shaken vigorously until homogenized and then passed through a syringe filter (size: 0.45 μm type: HA, Millipore Corp, Bedford, MA) to remove any undissolved particulate matter. The resulting 1.76 mM NTG stock solution was then wrapped in aluminum foil to protect against photo-damage and serially diluted by factors of 10 in PBS as needed.

Specific Protocols

Determination of Stop-Flow Pressure

Microvascular flow-arrest was induced by the downward projection of force onto the rat spinotrapezius muscle via a pressurized airbag. Since these protocols required multiple compressions of both short and long durations at a single site, it was necessary not only to stop flow completely, but to allow for rapid and total reperfusion. This meant providing enough

pressure to overcome intravascular pressure, but not so much as to cause damage and prevent return of normal flow.

The baseline mean arterial pressures (95.2 ± 2.5 mmHg) of 13 Sprague Dawley (SD) rats under anesthesia for our non-survival surgery protocol were determined and used as an indicator of the pressure needed for the collection of preliminary data. Further investigation revealed that in normotensive SD rats, feed arterioles with diameters of ~60 μm had an average intravascular pressure of ~60 mmHg (Boegehold, 1991). As these vessels were at least 4-fold greater in diameter than what was generally included in the area of compression, a lower pressure was sought for use. With decreasing pressure, complete flow-arrest became more difficult to obtain and it was decided that a systematic approach was needed to determine an ideal pressure range.

The spinotrapezius muscle was prepared and mounted as previously described. Following a 30-minute adaptation period, a site was selected that contained well perfused vessels with diameters < 15 μm. Based on preliminary and concurrent measurements, a compression recovery profile of 5 seconds high pressure and 15 seconds low pressure was selected to assess the influence of increasing pressure on both $-dPO_2/dt$ and the PO_2 recovery time course back to baseline. After a brief baseline measurement using PQM at low pressure (~5 mmHg) the sequence of high and low pressures was initiated. The first compression was set to 40 mmHg and each one was subsequently increased by 10 mmHg to a maximum of 180 mmHg. Upon completion of a single round, another site was selected and the process repeated.

Determination of VO_2 Sampling Resolution

Optimization of the quasi-continuous VO_2 sampling technique was necessary to maximize the number of measurements per unit time, while minimizing method-induced alterations to the microvasculature.

A 5-second compression at 120-140 mmHg was determined to provide an adequate rendition of $-dPO_2/dt$ upon inspection of the oxygen disappearance curve and measurements at various stop-flow pressures. At the 10 Hz excitation rate, this meant 50 points could be collected during the entire time course of compression. The first second of the resulting curve was ignored during data analysis to reduce any noise arising from a compression artifact. The remaining 4 seconds yielded 40 points and a robust fit of the linear decline in $P_{ISF}O_2$.

With the compression duration fixed at 5 s, the next step was to assess the appropriate recovery time needed to restore PO_2 to baseline. The rat spinotrapezius muscle was prepared and mounted as previously described and allowed to accommodate for 30 minutes prior to experimentation. The microvasculature was visualized though a transilluminated 10X objective to locate measurement sites within 200 μm of 70-100 μm arterioles with robust capillary perfusion. Next, the site was observed through the airbag-mounted 20X objective pressurized at 5 mmHg and the totality of flow-arrest was assessed during a quick compression (<2 s) for purposes of quality control. After a subsequent 5-minute rest period, quasi-continuous VO_2 sampling was conducted over multiple sites with 5-, 10-, 15-, 20- and 30-second recovery durations. Each measurement lasted 100 s and was preceded by a 10 s baseline recording by which to compare the $P_{ISF}O_2$ during each recovery period. To reduce the influence of any sort of sequence artifact, multiple recordings at the same site were performed in random order. The data obtained following high pressure compression were then compared in terms of recovery to baseline PO_2 and any systematic changes in VO_2.

Determination of Stop-Flow Influence for the 1-Minute I/R Protocol

To assess the potential sensitivity of the reperfusion period following various ischemic durations, 8 animals were exposed to ischemia and reperfusion protocols with and without quasi-continuous VO_2 sampling where applicable.

Following site selection, a 20-second baseline at low (~5 mmHg) bag pressure was obtained and then blood flow was arrested via high (120-140 mmHg) bag pressure for a duration of one minute. Next, the bag was switched to low pressure and flow was restored. The $P_{ISF}O_2$ was measured during this period of reperfusion for 100 seconds with and without the 5 s x 15 s high/low pressure cycle described above. Measurements were conducted in a random order at the same site and different sites and compared in terms of the $P_{ISF}O_2$ time course.

Determination of PO_2-Dependence of VO_2

VO_2 measurements were made in the spinotrapezius muscle preparation as described above over the entire physiological range of $P_{ISF}O_2$. This was accomplished by selectively targeting regions proximal to venules for lower $P_{ISF}O_2$ and arterioles for higher $P_{ISF}O_2$. Poorly perfused regions also contributed information for the analysis in VO_2 for hypoxic regions. The data were then plotted as VO_2 versus $P_{ISF}O_2$ to define the point where VO_2 became dependent on $P_{ISF}O_2$.

Quasi-Continuous VO_2 Sampling to Determine VO_2 of Resting Muscle

The spinotrapezius muscle was prepared and mounted as described above. Following a 30 minute stabilization period, sites proximal to arterioles 40-100 μm in diameter that were well-

perfused were selected and visualized under 20X magnification with air-bag contact at low pressure. A brief compression (<2 seconds) was observed under transillumination to confirm that the selected pressure was sufficient to cause immediate and complete flow arrest. Then, upon determination that the site was acceptable, quasi-continuous VO_2 sampling of varying duration (1-10 minutes) was performed using the 5 s x 15 s high/low pressure cycle with a preceding 20-second baseline at low pressure. All measurements were made at 10 Hz excitation frequency.

I/R Protocols

Ischemic durations of 1, 5, and 10 minutes were assessed in terms of PO_2 recovery and changes in VO_2 during early reperfusion. To begin, the spinotrapezius muscle preparation was mounted, as previously described, and allowed to stabilize for 30 minutes. Next, well-perfused sites within approximately 200 μm of large arterioles (40-100 μm in diameter) were located using the 10X objective under transillumination. The sites were then assessed at 20X objective magnification with low pressure contact from the air-bag both in terms of vessel perfusion and relative $P_{ISF}O_2$ via a rapid sequence of 1 Hz PQM pulses. Sites having relatively low PO_2 (as assessed by the phosphorescence decay tracing on the oscilloscope) and/or poor perfusion were rejected.

The protocols for ischemia/reperfusion (see Figure 13) were separated into 1-, 5- and 10-minute durations. The period of ischemia was defined as the moment of high pressure tissue compression onset until the moment reperfusion began with low pressure in the air-bag. For the 1-minute ischemia protocol, a 20-second baseline measurement of $P_{ISF}O_2$ at low air-bag pressure preceded the high pressure induction of flow arrest. After 1 minute, the air-bag was switched

back to low pressure to permit reperfusion and the automatic regulation of quasi-continuous VO_2 sampling was engaged via the Automatic Dual Pressure Cycler. VO_2 measurements were taken at 5, 25, 45, 65 and 85 seconds after reperfusion onset. The same protocol was observed for the 5- and 10-minute durations of ischemia except a 10-second baseline preceded ischemia and $P_{ISF}O_2$ was only recorded for the first 50 seconds following bag compression and 10 seconds prior to reperfusion to establish the totality of ischemia and reduce the excessive time that would have been required to process these redundant low $P_{ISF}O_2$ values. Since the 1-minute ischemic period was relatively short, PQM measurements at 10 Hz were continuously made for the entire 3 minutes.

Drug Intervention in the I/R Protocol

To better understand the mechanisms regulating VO_2 over the time course of the above-described I/R protocol, cyanide, nitroglycerin, and L-NAME were used to alter mitochondrial metabolism. These agents were topically applied prior to measurement in a similar fashion to the application of the R2 probe. Dose-response pilot experiments derived from concentration values found in the literature helped establish the most effective concentrations for generating an appreciable change in VO_2.

The pilot dose-response experiments were conducted as follows: First, I/R controls of 1, 5, and 10 minutes were recorded prior to chemical intervention as previously described. Then, using 10X objective magnification, baseline arteriolar diameters were measured. Next, the Krehalon layer covering the spinotrapezius muscle preparation was removed and 100 µl of the lowest dose of an agent was applied to the tissue. Two minutes later a second application of 100 µl of the lowest dose was made. The Krehalon coversheet was reapplied, but before being

pressed against the tissue, arteriolar diameters were measured (except in the case of cyanide) as an assessment of chemical action. Sites were then selected based on their proximity to arterioles and observed rate of capillary perfusion. The 20X objective with attached air-bag, making low pressure contact with the preparation, was then used and measurements of 1-, 5- and 10-minute I/R were performed in random order as done previously during the control measurements. Next, the objective was switched back to 10X and follow-up measurements of arteriolar diameter were made as an indicator of persisting chemical activity over the ~20 minutes needed to perform a single series of all I/R durations. For agents with short half-lives, I/R durations of 1 and 5 minutes were measured and then an additional application of the same dose was made in the fashion of one 100 µl topical application followed 2 minutes later with another 100 µl dose as described above prior to the 10-minute ischemia protocol. This process of agent application, arteriolar measurements, and I/R PQM measurements was then duplicated for each subsequent dose. Agent concentration was raised by a factor of 10 in each succeeding step.

Once an appropriate dose was identified, it was used to assess its effect on VO_2 during the conditions of rest and reperfusion following ischemic durations of 1, 5 and 10 minutes. The spinotrapezius muscle was mounted and allowed to stabilize for 30 minutes before experimentation as previously described. Sites were selected with 10X transillumination and PQM was used to measure both $P_{ISF}O_2$ and VO_2 (as reported by $-dPO_{2ISF}/dt$) for 1-, 5- and 10-minute ischemia/reperfusion time courses. Following 1-3 randomized series of all control (no chemical intervention) ischemic time courses, baseline diameter measurements were made under 10X objective magnification immediately prior to agent administration. The dose was then administered in the fashion of the pilot experiments where 100 µl was topically applied with an additional 100 µl two minutes later. Arteriolar diameters were then measured again to assess the

effectiveness of the treatment and then measurements using the 1-, 5- and 10-minute I/R protocols were conducted in random order for 1-3 rounds. Additional treatments were administered if there was a noticeable attenuation of their effects.

Data Analysis

VO_2

The interstitial space of skeletal muscle tissue contains gradients of oxygen from the vasculature to the respiring myocytes, which are reported as an average over an octagonal area of 74,619 μm^2 using PQM. Although the average PO_2 over this size region tends to be stable under resting conditions, alterations in oxygen supply/demand matching are readily reported by changes in $P_{ISF}O_2$. During conditions where the oxygen supply is completely eliminated (e.g., flow-arrest), $P_{ISF}O_2$ will shift to a new steady-state that is reflective of the sole action of oxygen efflux from the system through various activities of consumption. When the oxygen supply is halted abruptly and totally, the rate of change of $P_{ISF}O_2$ can be described by Equation 5:

$$dP_n/dn = -V_n - KP_n + Z(p_n - P_n) \qquad \text{Equation 5}$$

where dP_n/dn is the initial slope of the oxygen disappearance curve, P_n is the average $P_{ISF}O_2$ within the 300 μm diameter measurement area after flash n, V_n is the amount of oxygen consumed by respiring tissue per flash, K is the coefficient of oxygen consumption by the PQM method, and Z (also referred to as R in this text) is the coefficient of oxygen inflow by passive diffusion at the periphery of the measurement area. The contribution of oxygen inflow decreases as the illuminated measurement area's radius increases and, with an excitation area of 74,619

μm^2, the coefficient of refill was determined to be $2.08x10^{-4}\pm1.4x10^{-4}$ per flash. The driving force behind *Z* is the difference in $P_{ISF}O_2$ that is generated within the area of PQM illumination over n flashes. Thus, over time, a high consumption by the method (KP_n) might generate a sufficient driving force for oxygen to make $Z(p_n - P_n)$significant. But as *K* was found to be $7.16x10^{-4}\pm1.9x10^{-4}$ per flash, and the measurement of dP_n/dn did not exceed n=50, then with *Z* being small and the $P_{ISF}O_2$ difference between outside and inside the excitation area also being small (see Figure 15), then refill can be practically ignored for the early part of the oxygen disappearance curve and Equation 5 can be simplified as follows:

$$dP_n/dn = -V_0 - KP_0 \qquad \text{Equation 6}$$

The rate of oxygen disappearance now consists of consumption by the tissue and the method. After subtracting the consumption by PQM, V_0 can be converted to VO_2 by accounting for both flash rate (F) and the solubility of oxygen in skeletal muscle tissue (α):

$$VO_2 = V_0F\alpha \qquad \text{Equation 7}$$

Thus the complete formula for the transformation of dP_n/dn into a measurement of tissue oxygen consumption is as follows:

$$VO_2 = (-dP_n/dn - KP_0)F\alpha \qquad \text{Equation 8}$$

PO_2

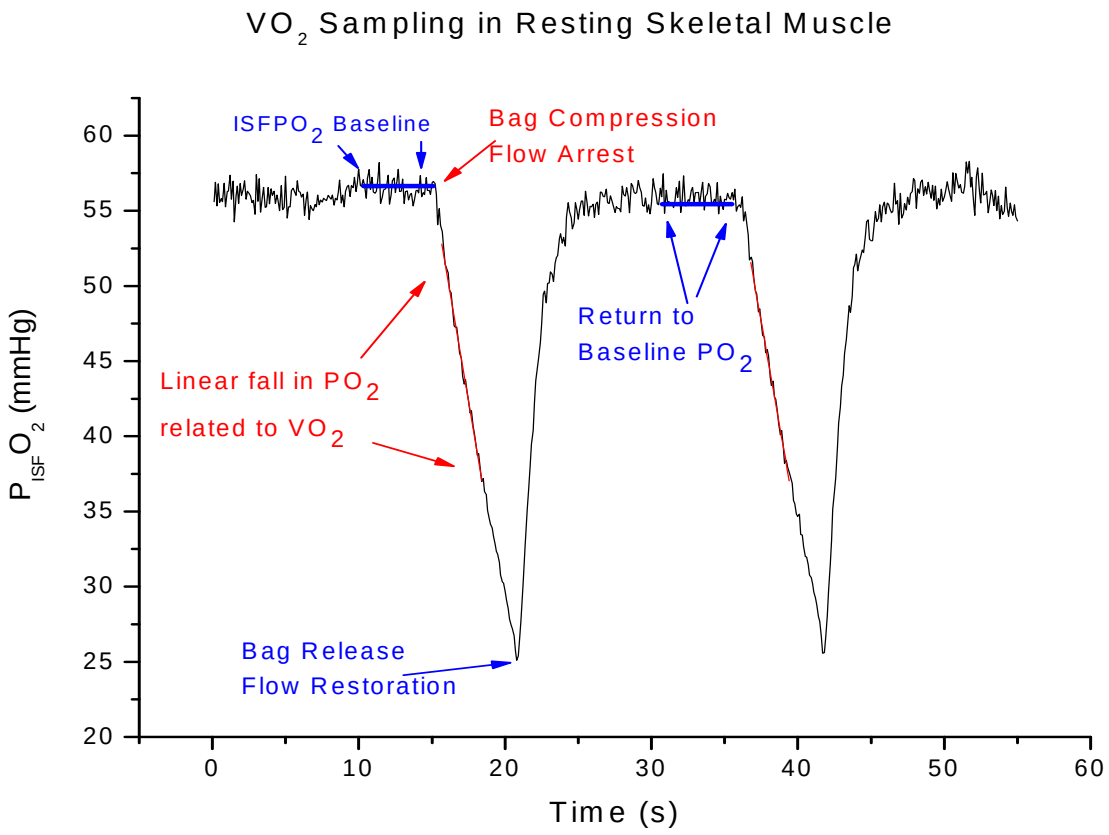

Figure 12: Representative plot of the 5 s x 15 s VO_2 sampling profile. A 20-second baseline measurement at 10 Hz was taken at low pressure to observe $P_{ISF}O_2$ as an assessment of the integrity of the preparation and to create a baseline measurement against which to compare the $P_{ISF}O_2$ following compression recovery. Baseline and recovery $P_{ISF}O_2$'s were recorded as the 5-second averages prior to each compression as indicated by the blue lines above. The linear fall in $P_{ISF}O_2$ was measured, as shown by the red lines, during compression, and was then related to VO_2 (see Equation 8). Blue and red coloring indicates measurements during low and high pressure, respectively.

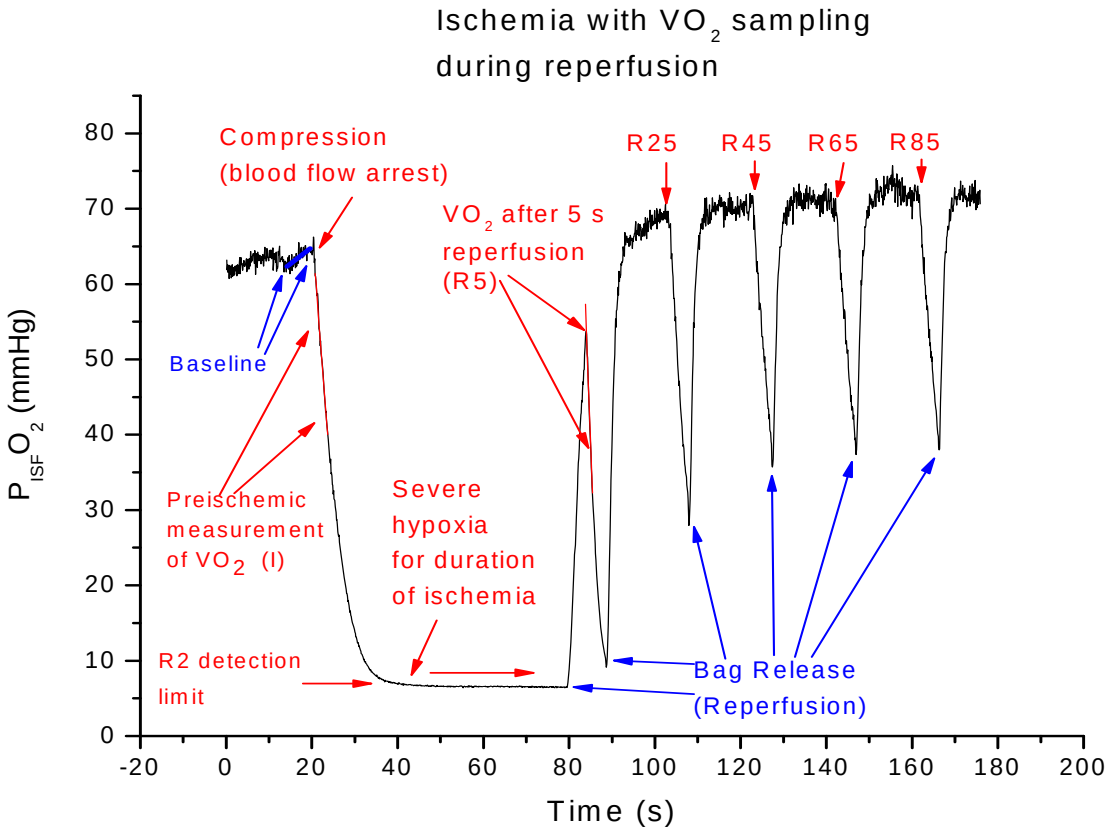

Figure 13: Representative plot of a 1-minute ischemia/reperfusion protocol with VO_2 sampling. Baseline and recovery $P_{ISF}O_2$'s were measured as the 5-second average prior to the induction of high pressure with the exception of the R5 measurement being the 2-second average prior to compression due to the limited amount of reperfusion time. The initial induction of ischemia (I) was considered the baseline VO_2 against which reperfusion VO_2 measurements could be assessed. Due to a dependence of VO_2 on tissue oxygenation at low $P_{ISF}O_2$'s, the data for measurements of $-dPO_2/dt$ where the pre-compression $P_{ISF}O_2$ (P_0) was <40 mmHg were grouped into P_0 ranges of Hypoxic ($P_0 < 22$ mmHg), Intermediate ($22 < P_0 < 40$ mmHg), and Normoxic ($P_0 > 40$ mmHg).

$P_{ISF}O_2$ values were calculated as a 5-second average (50 measurements) immediately prior to the time point of interest. For assessment of the PO_2 recovery during the 5 s x 15 s VO_2 sampling profile, this meant that following 10 seconds of low-pressure reperfusion, the final 5 seconds before compression were averaged to obtain $P_{ISF}O_2$ for the VO_2 (P_0) measurement immediately following (see Figure 12).

$P_{ISF}O_2$-Dependence and Independence of VO_2

Values for dPO_2/dt were calculated as shown in Figure 12. The linear portion of the fall in PO_2 during compression was selected and fit to a linear function and then converted to VO_2 using Equation 8. Only values with a P_0 greater than 40 mmHg were found to be reliably independent of $P_{ISF}O_2$ and grouped together for comparison in the category of Normoxia. P_0 values less than 40 but greater than 22 mmHg appeared to have both PO_2-dependent and independent components and were thus grouped into the Intermediate category. P_0 values lower than 22 mmHg were considered Hypoxic.

Interpretation of I/R Plots

The ischemia/reperfusion protocol consisted of a low-pressure measurement of baseline $P_{ISF}O_2$ that preceded an ischemic duration of 1, 5 or 10 minutes, followed by a period of reperfusion that was assessed by quasi-continuous VO_2 sampling. The initial baseline PO_2 was compared to subsequent measurements (5-second average immediately prior to each compression) as an indicator of recovery. The initial drop in $P_{ISF}O_2$ at the onset of ischemia (referred to as "I" or "BL") was used as a baseline VO_2 to which the reperfusion VO_2 measurements R5, R25, R45, R65 and R85 could be compared. "R" stands for reperfusion and

the numerical value indicates the seconds after the start of reperfusion that the measurement was taken as shown in Figure 13. As it was determined that the oxygen consumption of the tissue becomes oxygen-dependent at low $P_{ISF}O_2$'s, VO_2 measurements where the pre-compression PO_2 was less than 40 mmHg were found not to be directly comparable with compression measurements where the PO_2 was higher than 40 mmHg and thus the data were grouped into the P_0 ranges of Hypoxic (P_0 < 22 mmHg), Intermediate (22 mmHg <P_0 < 40 mmHg), and Normoxic (P_0 > 40 mmHg).

Measurements of Oxygen Consumption by the Method

The data derived from the microcapillary and gel measurements were analyzed in terms of how $P_{ISF}O_2$ in the excitation cylinder was altered by the PQM method in the absence of tissue perfusion and oxygen consumption. The oxygen disappearance curve was fit (see Figure 14) using Origin 6.1 (OriginLab, Northampton, MA) to the following equation:

$$P = P_0*R*(1+(K/R)*exp(-K+R)*x))/(K+R) \qquad \text{Equation 9}$$

where P_0 is the initial $P_{ISF}O_2$, K is the coefficient of consumption by the method, and R is the component of oxygen refill from outside of the excitation area. The PQM setup was optimized for phosphorescence lifetimes in situations where the PO_2 was in the physiological range of 100 to ~0 mmHg and, as such, these consumption data were truncated to begin at 100 mmHg. K was determined by the rate of decline in PO_2 per flash in the absence of other oxygen consumers. The refill component was determined by the asymptotic approach of $-dPO_2/dt$ to a low PO_2. As discussed above and shown in Figure 15, the coefficient of refill and the difference in $P_{ISF}O_2$

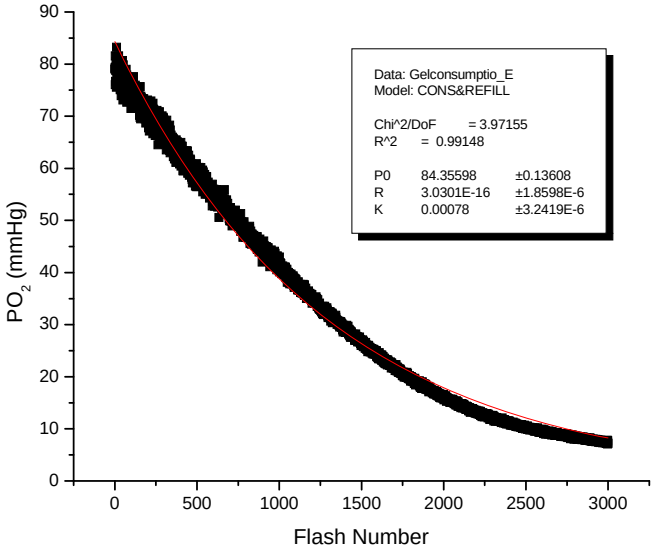

Figure 14: Example of Consumption by PQM Analysis. The excitation region was flashed at 100 Hz and fitted with the CONSREFILL function to show the rates of oxygen consumption by PQM with the R2 probe and refill.

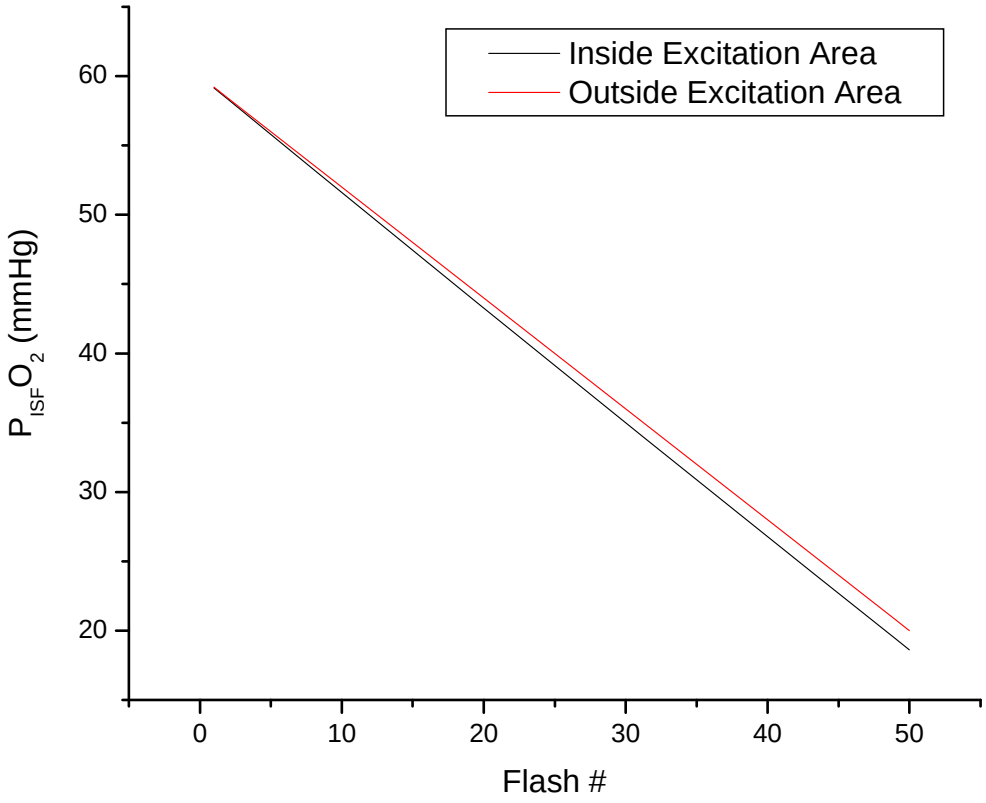

Figure 15: Simulation of the development of oxygen gradient at measurement periphery in respiring muscle. The refill coefficient (*R*) is multiplied against the $P_{ISF}O_2$ gradient at the periphery of the measurement area to determine the influence of refill. As that difference is only ~1.5 mmHg following 50 flashes with an average resting $-dPO_2/dt$ of 0.8 mmHg/flash and the reported *K* value of 7.16×10^{-4} per flash, refill's ability to confound the measurement of $-dPO_2/dt$ is well below 0.01% per flash at the maximum difference between outside and inside, which is negligible for the early part of the ODC.

between inside and outside the excitation area were both sufficiently small to be ignored when fitting the early part of the ODC for VO_2 measurements.

Statistical Methods

Data within these experiments are shown as mean ± standard error (SE) unless otherwise noted in figures and tables. ANOVA was conducted using JMP software version 8.0 (SAS Institute Inc., Cary NC) to assess statistical significance for the means of each experimental condition. Tukey's multiple comparison test used to identify significant differences between groups for I/R protocols and measurements of arteriolar diameter. Dunnet's test was used to delineate differences between control (or baseline) measurements and various time points during reperfusion. Statistical significance was taken to be $p < 0.05$.

RESULTS

VO_2 Sampling Technique

Determination of Compression Duration:

Early observations of air-bag compression on the spinotrapezius muscle preparation indicated that a 5-second duration would be sufficient to obtain a reliable assessment of the linear decline in oxygen tension of the interstitial fluid ($P_{ISF}O_2$). This rate of decrease could then be related to tissue oxygen consumption (VO_2) as described on page 76 of the Methods section and elsewhere (Golub et al, in revision). The rapid pressurization of the air-bag was revealed through both direct visualization of the microvasculature under transillumination and phosphorescence quenching microscopy (PQM) to result in a timecourse of flow-arrest to be <1 second as shown in Figure 16. At each compression onset, there was a sudden and sharp drop in $P_{ISF}O_2$ that followed a linear decline before deviating from linearity and presumably indicating onset of cellular hypoxia. Given a 10 Hz excitation rate, it was then determined that 5 seconds would provide an adequate representation of the linear decline in $P_{ISF}O_2$ with 50 data points. This large number of points in the linear region would also allow for some dropping of any data points that might skew the linear trend, which might occasionally occur due to the intrinsic variability of the measurement the measurement process.

Determination of Compression Interval for Intermittent VO_2 Sampling

Measurement, by its very nature, disrupts the environment of study. Whether the magnitude of this disruption is significant enough to generate a false image of reality is important to understand. As the VO_2 sampling technique necessitates a temporary reduction in $P_{ISF}O_2$, it is possible that any mild alterations in the microvasculature could be cumulative. Thus, several different values of recovery time interval between the 5-second compressions were assessed for changes in both the return of $P_{ISF}O_2$ and VO_2 toward baseline.

Figure 16 shows the averaged, raw $P_{ISF}O_2$ curves from 5-, 10-, 15- and 20-second recovery durations following 5 seconds of compression of the spinotrapezius muscle. Some sites were excluded from this analysis because the baseline $P_{ISF}O_2$ values were below 40 mmHg and therefore would result in skewed VO_2 data. It is clear from these measurements that 5 seconds of recovery was insufficient, since over time there was a cumulative reduction of $P_{ISF}O_2$. As shown in Figure 17, there is a statistically significant drop of 23.2 (SE of Difference 6.7; $p<0.05$) mmHg between baseline and the first measurement of recovery that shows a negative trend in subsequent measurements. For intermittent VO_2 sampling profiles using 10 seconds of recovery, Figure 16 shows an overall return of $P_{ISF}O_2$ to baseline following each 5 second compression. Neither measurements of $P_{ISF}O_2$ nor VO_2 following compression and 10 seconds of recovery showed a statistically significant difference from baseline. However, there appeared to be a slightly negative trend for the return of $P_{ISF}O_2$ (see Figure 18). The 15- and 20-second profiles of recovery showed no significant differences between baseline and VO_2 sampling measurements in terms of $P_{ISF}O_2$ and VO_2 (see Figures 19 and 20, respectively).

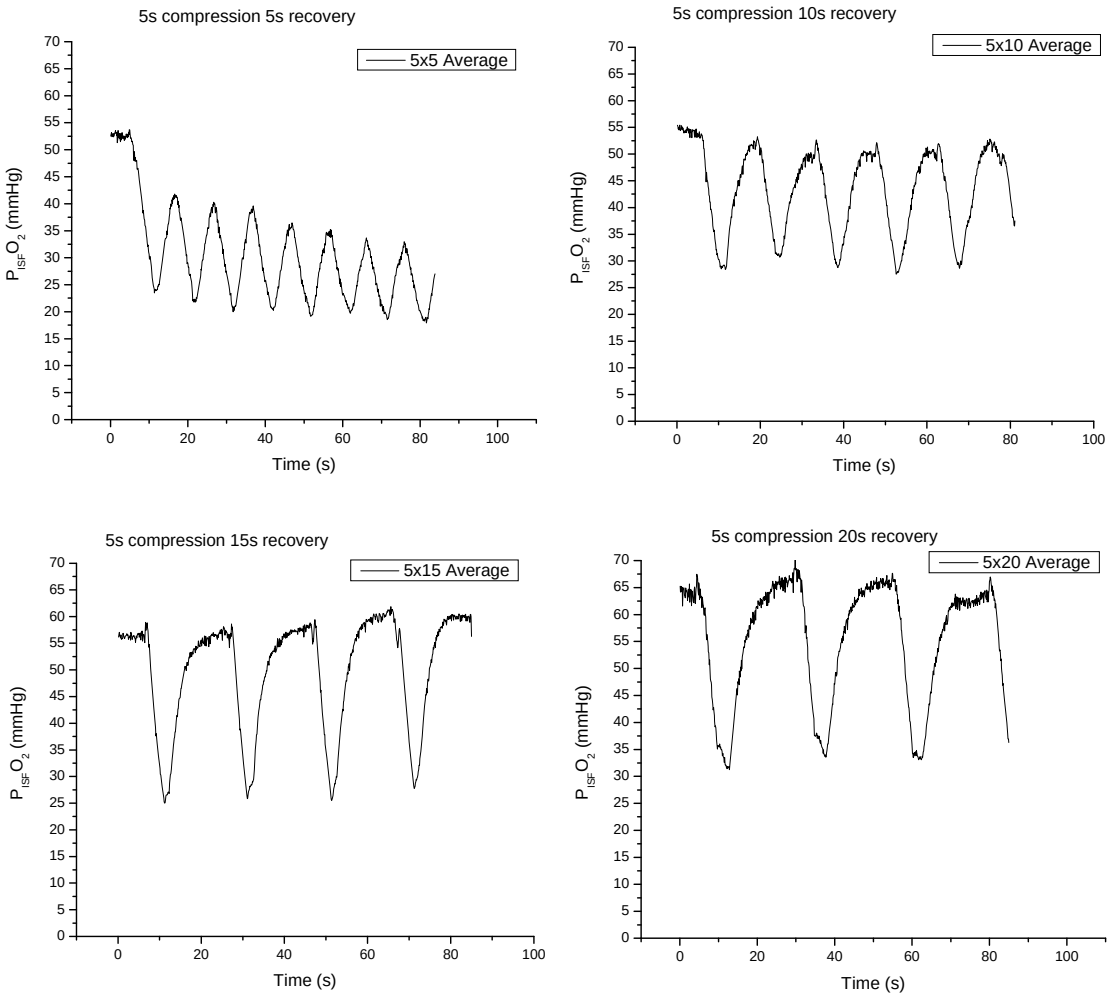

Figure 16: $P_{ISF}O_2$ tracings for 5, 10, 15, and 20 seconds of recovery between 5-second compressions. Each plot represents the combined average of multiple tracings (5x5, n=9; 5x10, n=8; 5x15, n=8; 5x20, n=9). Following a baseline assessment, the air-bag was pressurized to arrest blood flow for 5 seconds and then depressurized to allow reperfusion for varying durations. 15 seconds of recovery was chosen to accommodate the 5 seconds of compression and thus a sampling rate of 3 per minute. These data were collected using a low air-bag pressure of 5 mmHg to squeeze out any interfering fluid accumulation and a high pressure of 140 mmHg to ensure flow-arrest.

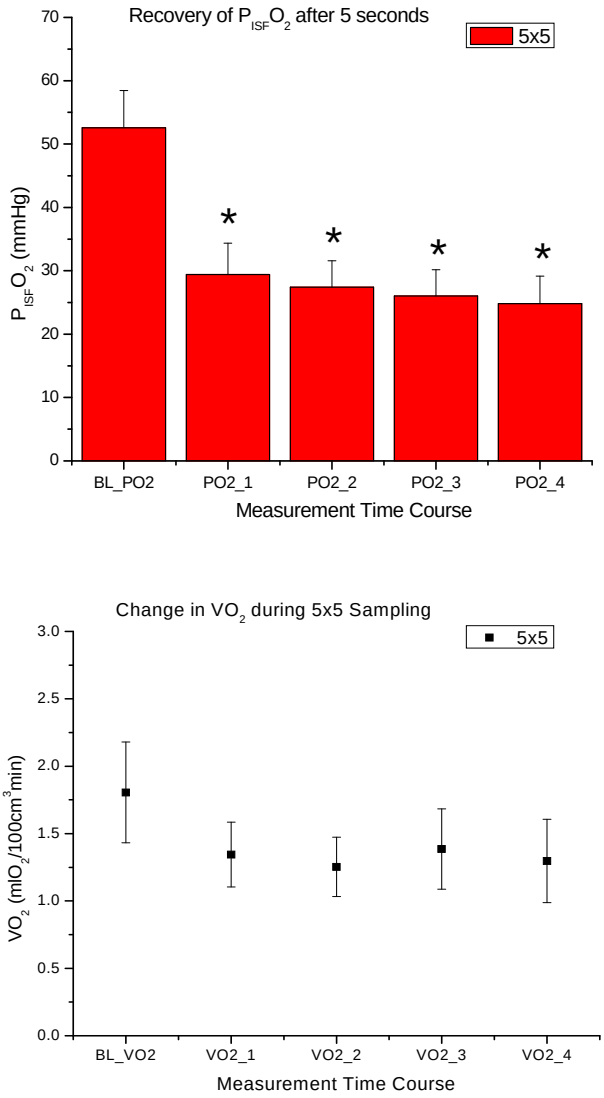

Figure 17: Changes in $P_{ISF}O_2$ and VO_2 for 5 seconds of recovery following 5 seconds of compression. **Top:** Recovery $P_{ISF}O_2$ values for 5 seconds of flow restoration after each 5 second compression. The first measurement, BL_PO2, is the baseline $P_{ISF}O_2$ prior to initiation of the compression/recovery cycle. Values for PO2_1, 2, 3, and 4 were found to be significantly different from baseline, but not each other, with p values of 0.012, 0.005, 0.003, and 0.002, respectively. **Bottom:** Measurements of VO_2 taken during each compression for the 5x5 sampling profile. BL_VO2 corresponds to the initial compression, or baseline. There are no statistical differences between baseline and subsequent measurements.

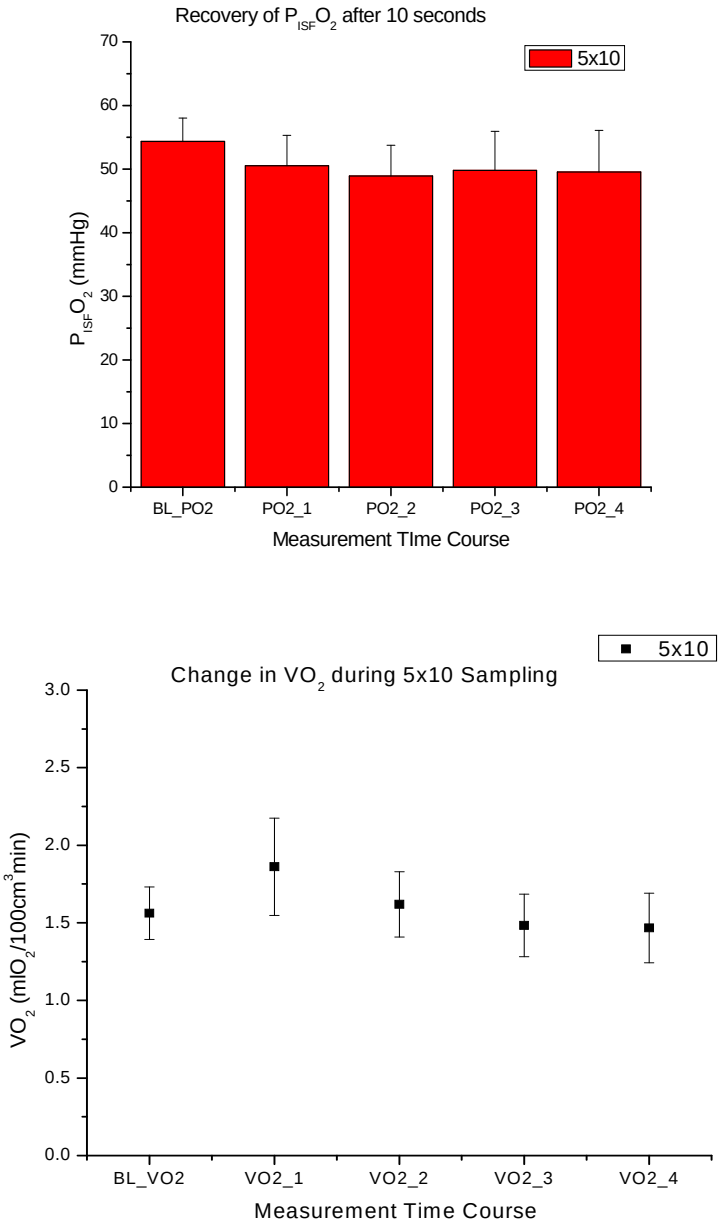

Figure 18: Changes in $P_{ISF}O_2$ and VO_2 for 10 seconds of recovery following 5 seconds of compression. **Top:** Influence of 10 seconds recovery on return to baseline $P_{ISF}O_2$. There are no statistical differences between baseline (BL_PO2) and measurements following compression (PO2_n). **Bottom:** Influence of the 5x10 compression/recovery cycle on VO_2. There are no statistical differences between baseline (BL_VO2) and subsequent measurements (VO2_n).

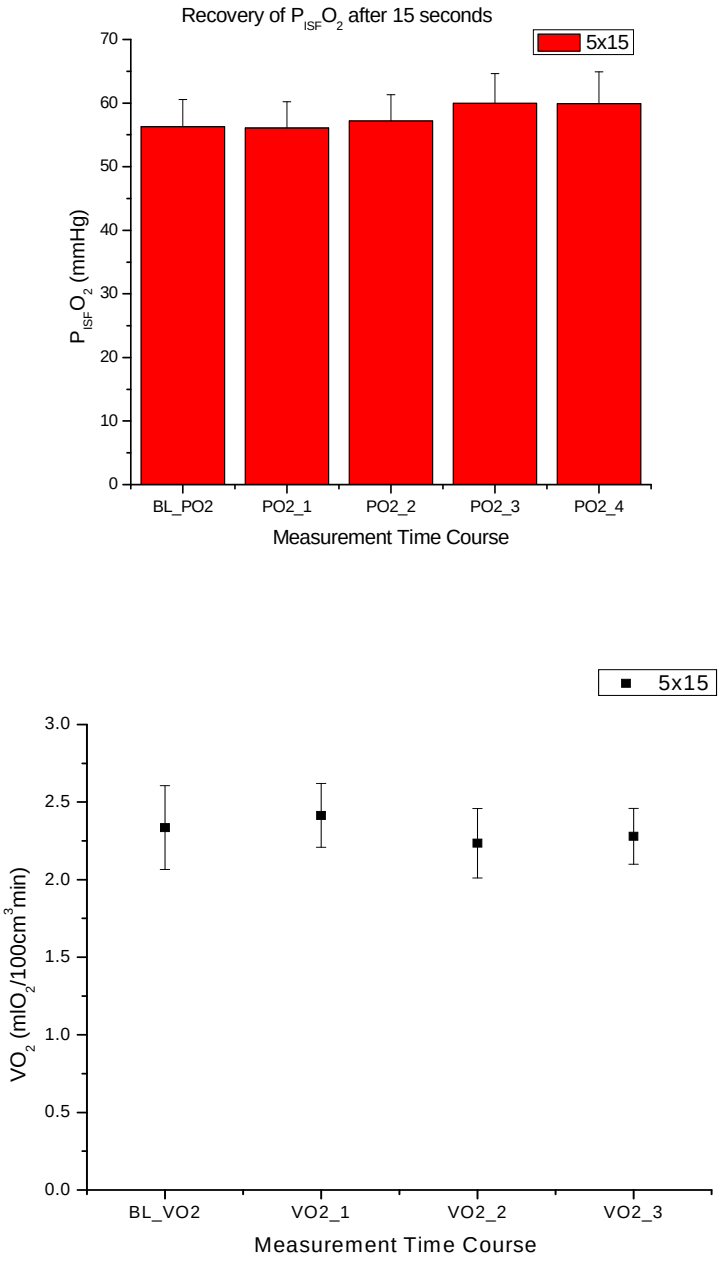

Figure 19: Changes in $P_{ISF}O_2$ and VO_2 for 15 seconds of recovery following 5 seconds of compression. **Top:** Influence of 15 seconds of recovery on return to baseline $P_{ISF}O_2$. There are no statistical differences between baseline (BL_PO2) and measurements following compression (PO2_n). **Bottom:** Influence of the 5x15 compression/recovery cycle on VO_2. There are no statistical differences between baseline (BL_VO2) and subsequent measurements (VO2_n).

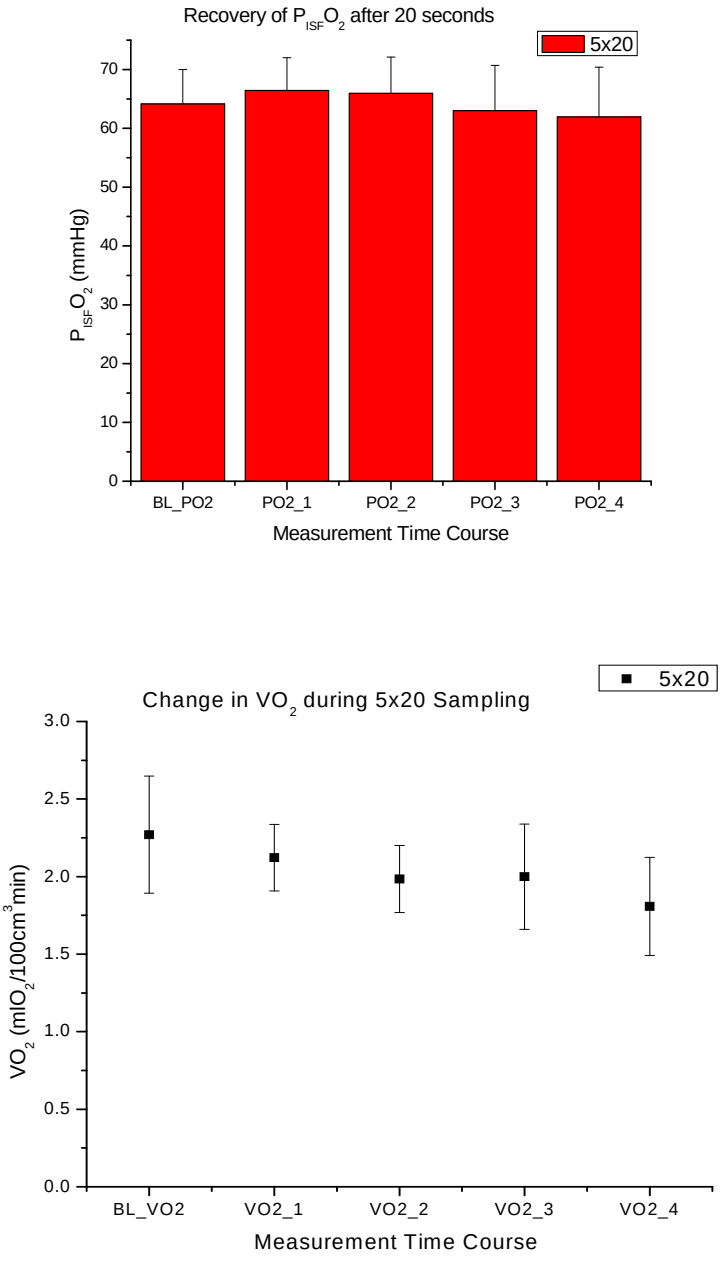

Figure 20: Changes in $P_{ISF}O_2$ and VO_2 for 20 seconds of recovery following 5 seconds of compression. **Top:** Influence of 20 seconds of recovery on return to baseline $P_{ISF}O_2$. There are no statistical differences between baseline (BL_PO2) and measurements following compression (PO2_n). **Bottom:** Influence of the 5x20 compression/recovery cycle on VO_2. There are no statistical differences between baseline (BL_VO2) and subsequent measurements (VO2_n).

Influence of 5x15 VO_2 Sampling on Reperfusion

Although 5-second compressions spaced 15 seconds apart did not appear to negatively impact tissue oxygenation, this profile of VO_2 sampling required testing in the more demanding situation of reperfusion where both $P_{ISF}O_2$ and VO_2 had been significantly affected by an ischemic event. VO_2 could not be assessed independently of the 5x15 VO_2 sampling technique, but it was possible to compare the recovery of $P_{ISF}O_2$ following a 1-minute arrest of blood flow with and without the 5x15 compression/recovery cycle (see Figure 21).

Following the establishment of a baseline $P_{ISF}O_2$ by which to compare the eventual recovery during reperfusion, the air-bag was switched to high pressure and blood flow arrested. After 1 minute of ischemia, the pressure was returned to minimum (i.e., 5 mmHg) and blood flow was immediately restored. For the control group, the $P_{ISF}O_2$ timecourse was observed without further air-bag compressions (n=17), while the experimental group was subjected to the 5x15 compression/recovery cycle beginning 5 seconds after the onset of reperfusion (n=11). Both groups showed a rapid rise in $P_{ISF}O_2$ during early reperfusion ending in a small increase over the original baseline. This overshoot was more pronounced in the group exposed to intermittent compression/recovery cycles, but did not exceed 5% over control at its highest point. After 100 seconds of reperfusion, both control and 5x15 VO_2 sampling groups had similar $P_{ISF}O_2$ levels.

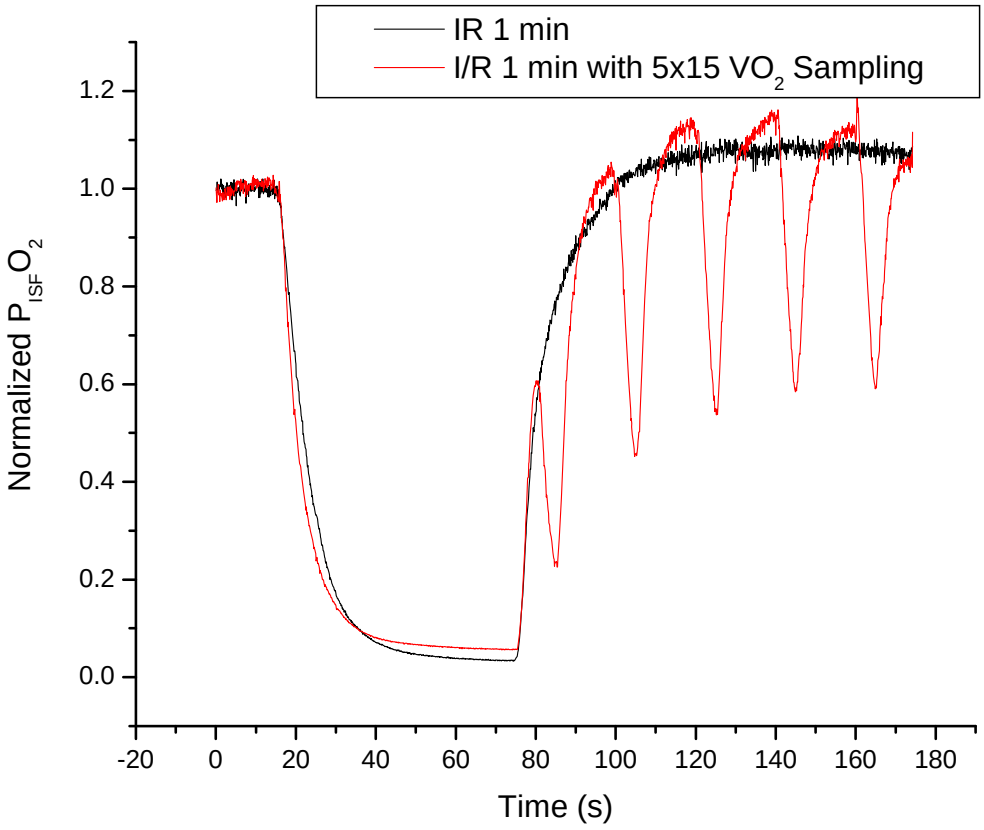

Figure 21: Normalized comparison of a 1-minute ischemia/reperfusion (I/R) tracing of $P_{ISF}O_2$ with and without intermittent 5x15 VO_2 sampling. These plots represent the combined averages of their respective groups and have been normalized to their baselines (measurement before initial induction of flow-arrest). The rise over baseline during reperfusion is consistent with other data collected from I/R protocols and VO_2 sampling appears to slightly enhance this phenomenon. These data were collected using a low air-bag pressure of 5 mmHg to squeeze out any interfering fluid accumulation and a high pressure of 140 mmHg for flow-arrest.

Air Bag Pressure

Early tests of intermittent air bag compression/recovery cycles used a high compression of 140 mmHg to arrest blood flow for the measurement of the Oxygen Disappearance Curve (ODC), which provided a sufficient pressure to overcome the rat mean arterial pressure (MAP recorded for 13 animals was 95.2±2.5 mmHg; Song and Nugent, unpublished results). To minimize damage done by compression, however, it was deemed necessary to find the minimal reliable pressure required to arrest blood flow in the microcirculation where arteriolar pressures are much lower than arterial.

Seven spinotrapezius muscles were subjected to a stepwise increase in air bag pressurization from 40 to 140 mmHg and assessed for changes in the rate of oxygen disappearance ($-dPO_2/dt$) (see Figure 23) and the restoration of $P_{ISF}O_2$ (see Figure 22) during the 5x15 compression/recovery protocol. A baseline measurement of $P_{ISF}O_2$ at the standard low pressure of 5 mmHg preceded initiation of the 5x15 VO_2 sampling protocol. $P_{ISF}O_2$ was not significantly different ($p = 0.1$) over the range of increasing compression pressures when compared against each other and baseline. There is a positive trend in recovery $P_{ISF}O_2$ beginning with 50 mmHg compression and leveling off at 80 mmHg, which is consistent with the previously observed overshoot of baseline when employing the 5x15 compression/recovery cycle, but it was not statistically different from baseline. The linear drop in $P_{ISF}O_2$ ($-dPO_2/dt$) that occurred with each progressive compression by the air bag was also reported as an absolute value in terms of mmHg/sec as shown in Figure 23. There was a progressive rise in $-dPO_2/dt$ from 1.6 mmHg/sec at 40 mmHg air bag pressurization to 5.2 mmHg/sec at 80 mmHg, above which $-dPO_2/dt$ leveled off. There was no statistical difference in terms of the rate in $P_{ISF}O_2$ decline between groups from 80 mmHg to 140 mmHg. There was a slight, but insignificant,

elevation in $-dPO_2/dt$ for 90 to 100 mmHg which may be indicative of some physiological interplay between blood extrusion and the tissue respiratory rate. To accommodate the highest number of tissues and ensure that both blood flow-arrest and red blood cell extrusion took place rapidly and effectively, 120 mmHg was chosen as the minimum pressure for the 5x15 VO_2 sampling protocol.

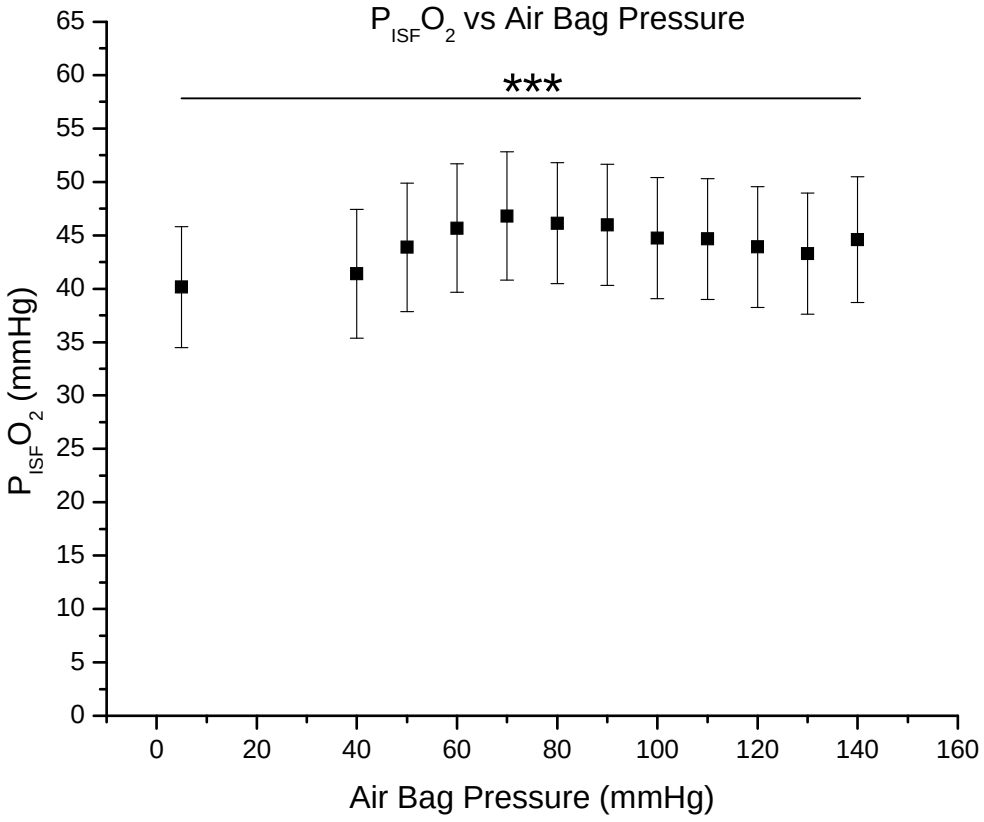

Figure 22: $P_{ISF}O_2$ restoration during 5x15 compression/recovery cycle vs air bag pressure in the spinotrapezius muscle. Measurements were made using the 5x15 VO_2 sampling profile with each compression receiving a 10 mmHg increment above the previous one from 40 to 140 mmHg. After an initial baseline reading at 5 mmHg (minimum pressure), each $P_{ISF}O_2$ was related to the recovery following the compression pressure for which it was listed. Thus, a PO_2 reading at 40 indicates that the PO_2 returned to that level following the 5 second compression of 40 mmHg. The *** indicates that no significant difference was found between the measurements it covers (n=26 for measurements at 5, and 80-130 mmHg; n=23 for measurements at 40-70 mmHg; n=24 for measurement at 140 mmHg.) These data represent measurements from 26 sites over 7 animals.

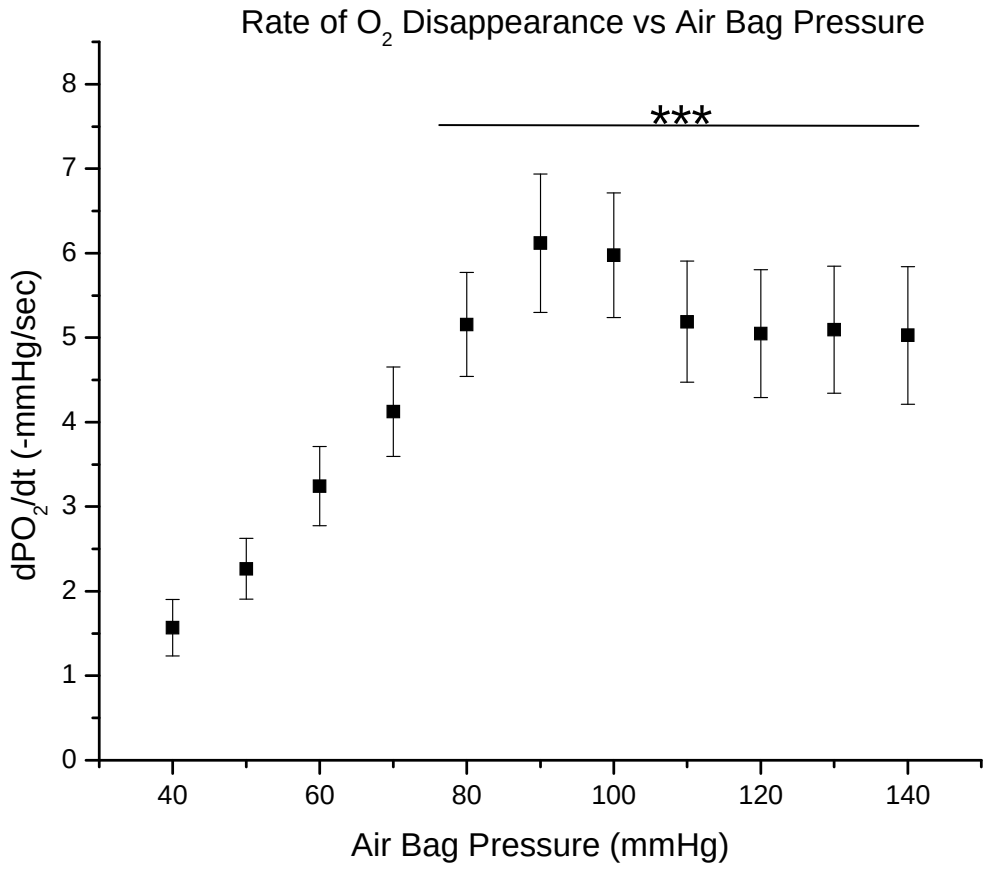

Figure 23: O_2 disappearance rate vs. air bag pressurization during the 5x15 VO_2 sampling profile in the spinotrapezius muscle. Each measurement represents the linear portion of O_2 disappearance time course observed during a 5-s compression at the pressure indicated. Data were not converted to VO_2 because in the cases of lower pressure, flow did not appear to be fully arrested and therefore no valid comparison of VO_2 could be made. The *** indicates that there are no statistical differences between the measurements beneath it (n=23 for measurements at 40-80 mmHg; n=26 for measurements at 90-140 mmHg.) These data represent measurements from 26 sites over 7 animals.

Oxygen Consumption by PQM

Development of a correction for the observed O_2 consumption caused by the conversion of O_2 to singlet oxygen during interaction with the R2 probe in its triplet state required a system that offered an exclusive observation of the probe-dependent depletion of oxygen during excitation. Initially, the idea of performing measurements on dead tissue harvested after experimentation was pursued, since these tissues had already been loaded with the probe and retained a similar matrix to the original living tissue. However, complications related to necrotic tissue pH and lingering sources of oxygen utilization would have confounded measurements of PQM oxygen consumption. Instead, the in vitro microslide and gel models were considered superior for their lack of endogenous oxygen consumers and their ability to closely mimic the concentration of the R2 probe as it is averaged in tissue for direct measurement of PQM's oxygen consumption.

The microslide model, loaded with 20 μg/ml of R2 probe bound to 5% human serum albumin (HSA), was exposed to full intensity 10 Hz excitation for 3000 flashes and the coefficient of PQM oxygen consumption (K) was found to have a mean value of 8.08 ± 2.98 (SE) x 10^{-4} mmHg/flash (n=9). The 2% alginate gel experiments, which matched tissue thickness and were also loaded with the measured R2 concentration in tissue of 20 μg/ml bound to 5% human serum albumin, produced a mean K value of 7.16 ± 1.87 (SE) x 10^{-4} mmHg/flash (n=10) for 3000 flashes at 10 Hz (see Table 1). These two PQM coefficients were not found to be statistically different (P = 0.05), thus lending utility to both approaches. For the purpose of correcting VO_2 sampling technique measurements, the coefficients from gel were used due to the similarity in molecular distribution of the phosphor to that of the tissue. Using the gel's K coefficient and an initial PO_2 of 60 mmHg in a solution loaded with the R2 probe at 20 μg/ml

bound to a physiological concentration of albumin, PQM's share of oxygen consumption is 0.1 mlO_2/cm^3min or 5.1% of resting skeletal muscle oxygen consumption (as measured to be 1.97 ± 0.11 mlO_2/cm^3min by the VO_2 sampling technique). This allowed for a relatively simple correction to be applied to measurements of the rate of oxygen disappearance in the spinotrapezius muscle during flow arrest.

The component of oxygen refill (R) into the 300 μm diameter excitation area was determined from the ODC of both microslide and gel measurements as the approach of the measured PO_2 to the asymptotic equilibrium between PQM depletion within the excitation region and oxygen diffusion from outside it (see Eq. 9). Both the gel and microslide models produced similar mean values for R of 2.08 ± 1.39 (SE) x 10^{-4} mmHg/flash (n=10) and 2.80 ± 0.56 (SE) x 10^{-4} mmHg/flash (n=9), which showed no significant difference (P=0.05). This factor R, which is the coefficient by which the PO_2 difference between inside and outside of the measurement area is multiplied to determine the rate of refill, is of greater importance to measurements of consumption by PQM with R2 in the absence of other oxygen consumers so that the only decline in PO_2 occurs within the excitation area—leading to a larger gradient between inside and outside over time. In tissue, however, the consumption of oxygen is large and the region of blood flow arrest is several times larger than that of the excitation area. This means that there is a concomitant decrease in PO_2 both inside and outside the excitation area, which results in a smaller driving force—basically the cumulative consumption per flash by the PQM method—for oxygen refill into the measurement window. This indicates that refill is unlikely to skew measurements taken at the early part of the ODC, which are the ones used to calculate VO_2.

Medium	**P_0± SE** (mmHg)	**R± SE mmHg/flash**	**K± SE mmHg/flash**	**N**
Microslide	78.3±9.7	$2.80\pm0.56\times10^{-4}$	$8.08\pm2.98\times10^{-4}$	9
Gel	84.7±5.4	$2.08\pm1.39\times10^{-4}$	$7.16\pm1.87\times10^{-4}$	10

Table 1: In vitro measurement of O_2 consumption by PQM and refill. The coefficient of the PQM consumption rate (K) of 20 μg/ml R2 bound to 5% human serum albumin was determined in both microslide and 2% alginate gel vehicles at 10 Hz excitation frequency. From the PO_2 ODC, the component of oxygen refill (R) into the 300 μm in diameter excitation area was also calculated. P_0 was the initial $P_{ISF}O_2$. Measurements in both media were calculated per flash and were not significantly different from each other for all variables.

In Vivo Resting VO_2 of the Rat Spinotrapezius Muscle

Once the parameters of the VO_2 Sampling Technique had been optimized, its utility was tested in the exteriorized rat spinotrapezius muscle preparation for the measurement of VO_2 during resting conditions. Early data analysis of randomized sites indicated that for various levels of perfusion, as indicated by the $P_{ISF}O_2$ prior to the rapid onset of compression (P_0), there existed a range of $P_{ISF}O_2$-dependence for VO_2. Further study (see Figure 24) showed a negative trend in VO_2 as P_0 fell below 40 mmHg, whereas VO_2 remained steady for values of P_0 above 40 mmHg—even into what might be considered the range of hyperoxia (>75 mmHg data not shown) for some measurements of PO_2 that had clearly received some degree of atmospheric contamination. Given the detection of PO_2 gradients both longitudinally along the microvasculature and in the interstitial fluid of skeletal muscle tissue (Tsai AG, et al. 2003), the hypoxic situation is likely a variable physiological occurrence at rest. But, in order to determine the resting VO_2 for the well-perfused state where it is not limited by the activity of cytochrome c oxidase, the data were divided into three different ranges for analysis: hypoxic ($P_0 < 22$ mmHg); intermediate (22 mmHg < P_0 < 40 mmHg); and normoxic ($P_0 > 40$ mmHg and therefore PO_2 insensitive).

The assessment of VO_2 in the range of hypoxia revealed a mean value of 0.59 ± 0.10 (SE) x 10^{-2} mlO_2/cm^3min (n= 33) for an average $P_{ISF}O_2$ of 13.5 ± 0.4 (SE) mmHg (n= 33). Due to practical limitations of the VO_2 Sampling Technique when employed with the R2 probe, assessment of the linear fall in $P_{ISF}O_2$ was restricted to P_0 values above 9 mmHg. A further reduction in the oxygen tension could be and was achieved, but those measurements were associated with a reduction in the signal-to-noise ratio. The mean value of P_0 in the intermediate range, where some normoxic data likely mixed with the hypoxic situation, was 30.3 ± 0.9 (SE)

mmHg (n= 50) and produced a VO_2 of 1.71 ± 0.10 (SE) x 10^{-2} mlO_2/cm^3min (n= 50). For the range of P_0 values above 40 mmHg (mean P_0= 59.6 ± 1.2 (SE) mmHg, n= 74) where the VO_2 Sampling Technique data could be reliably considered insensitive to $P_{ISF}O_2$, the mean VO_2 was measured to be 1.97 ± 0.08 (SE) x 10^{-2} mlO_2/cm^3min (n= 74). As indicated in Figure 24, the VO_2 values for the $P_{ISF}O_2$-insensitive and intermediate ranges were not significantly different ($p = 0.11$). However, the VO_2 values in the hypoxic range were significantly different from both the intermediate and the $P_{ISF}O_2$-insensitive groups ($p<0.0001$ for both groups).

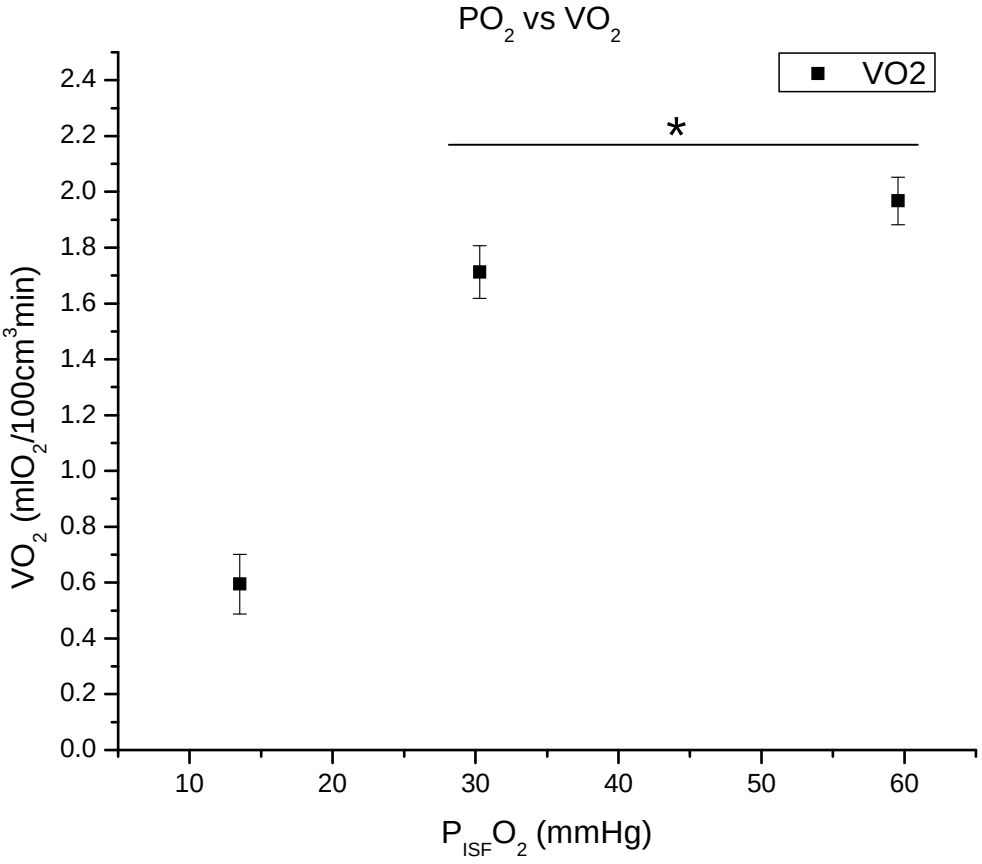

Figure 24: $P_{ISF}O_2$ vs resting VO_2 in the rat spinotrapezius muscle. Measurements were divided by initial $P_{ISF}O_2$ values immediately prior to compression (P_0) into hypoxic (P_0= 13.5 ± 0.4; VO_2= 0.59 ± 0.10, n=33), intermediate (P_0= 30.3±0.9; VO_2= 1.71±0.10; n= 50), and $P_{ISF}O_2$-insensitive ranges (P_0= 59.6±1.2; VO_2= 1.97±0.08; n= 74). The * indicates a lack of significant difference between groups at p=0.05. The hypoxic measurement of VO_2 is significantly different from both the intermediate and $P_{ISF}O_2$-insensitive ranges ($p < 0.0001$ in both cases).

Ischemia/Reperfusion

VO_2 was assessed prior to and after longer durations of blood flow arrest to develop an understanding of the metabolic changes that can occur during ischemia. Following a baseline assessment of $P_{ISF}O_2$, blood flow to the measurement area was arrested and red blood cells extruded by a rapid and continued pressurization of the air-bag at 140 mmHg. $P_{ISF}O_2$ declined to the point of hypoxia within ~20 seconds and the early part of this initial oxygen disappearance curve (ODC) was used as a baseline VO_2 for comparison with post-ischemic VO_2 values. After 1, 5 and 10 minutes of ischemia—depending on the measurement—the air-bag was depressurized to 5 mmHg and blood flow restored to initiate the reperfusion phase. Measurements via the VO_2 Sampling Technique were taken at 5, 25, 45, 65, and 85 seconds after the onset of reperfusion as per the 5x15 compression/recovery intermittent sampling cycle. The VO_2 data were divided into groups of hypoxic (<22 mmHg), intermediate (22-40 mmHg), and high (normoxic: >40 mmHg) $P_{ISF}O_2$ values and plotted as shown by plots A, B, and C of Figures 25, 26, and 27.

VO_2 During Early Reperfusion Following 1 Minute of Ischemia

Baseline values taken from the initial, linear component of the ODC at the onset of ischemia were averaged for all ischemia/reperfusion (I/R) experiments regardless of the subsequent duration since they were reflective of the tissue's resting state. The mean values for baseline (BL) VO_2 were determined to be 1.97 (SE: 0.10; n=72) for the normoxic range (mean $P_{ISF}O_2$ = 59.7 ± 1.2 mmHg; n=72), 1.49 (SE: 0.20; n=21) for the intermediate range (mean $P_{ISF}O_2$ = 32.2 ± 2.2 mmHg; n=21), and 0.9 (SE: 0.4; n=6) for the hypoxic range (mean $P_{ISF}O_2$ = 16.4 ± 4.1 mmHg; n=6). Following 1 minute of ischemia and 5 seconds of reperfusion, VO_2 had

significantly increased to 149% (mean=2.93 ± 0.27 ml O_2/100 cm^3min; n=11) over baseline (p=0.046) for normoxic measurements (mean $P_{ISF}O_2$ = 54.8 ± 3.0 mmHg; n=11) and 197% (mean = 2.93 ± 0.2 ml O_2/100 cm^3min; n=14) over baseline (p=0.0002) for the intermediate range of tissue oxygenation (mean $P_{ISF}O_2$ = 33.2 ± 2.7 mmHg; n=14). By 25 seconds after the onset of reperfusion, VO_2 had been reduced to 116 and 157% over baseline for the normoxic and intermediate ranges of $P_{ISF}O_2$. While this demonstrated a slight trend in continued elevation of tissue respiration at this time point, the data were not statistically significant over baseline (p= 0.997 for normoxic; p=0.83 for intermediate). By the R45 measurement point, VO_2 had approximately returned to baseline values. As illustrated in Figure 25, plot A, the hypoxic measurements showed no apparent change in VO_2 over the timecourse of reperfusion compared with baseline.

VO_2 During Early Reperfusion Following 5 Minutes of Ischemia

Baseline values, as indicated above, were assessed from all ODCs at the onset of ischemia regardless of the ischemic duration. Following 5 minutes of complete flow arrest of the measurement area, reperfusion was initiated and VO_2 sampling was begun 5 seconds later. Since the recovery of $P_{ISF}O_2$ is a function of oxygen demand, as well as supply, the R5 measurement point did not yield values above 40 mmHg due to a high degree of oxygen utilization. The intermediate $P_{ISF}O_2$ range, however, did contain some data for the R5 measurement and revealed a significant increase in VO_2 by 262% of baseline (mean= 3.91 ± 0.45 mlO_2/100 cm^3min; p< 0.0001; n=4). Twenty-five seconds of reperfusion showed significantly elevated VO_2 values for both normoxic (mean= 4.31 ± 0.36 mlO_2/100 cm^3min; $P_{ISF}O_2$= 62.7± 4.1 mmHg; n=6) and intermediate (mean= 3.35 ± 0.30 mlO_2/100 cm^3min; $P_{ISF}O_2$=27.5 ± 3.4 mmHg; n=9)

measurements of 218% and 225% over baseline, respectively ($p<0.0001$ for both). By a reperfusion time of 45 seconds, VO_2 for the normoxic (mean= 3.23 ± 0.3 $mlO_2/100\ cm^3min$; $P_{ISF}O_2$ = 66.4± 3.4 mmHg; n=9) and intermediate (mean= 2.92± 0.30 $mlO_2/100\ cm^3min$; $P_{ISF}O_2$ = 30.76 ± 3.4 mmHg; n=9) ranges had fallen slightly, but remained significantly elevated at 163% ($p=0.0038$) and 196% ($p=0.0032$) over baseline values, respectively. As illustrated by Figure 26, plots C and B, there is a continued trend in reduction of the oxygen consumption rates back to resting values for both the normoxic and intermediate measurements over the subsequent R65 and R85 time points. VO_2 showed no statistical difference from baseline for these last two measurements. Measurements taken during hypoxic conditions (Figure 26, plot C) show a lack of change in VO_2 over the time course of reperfusion as compared to baseline.

VO_2 during Early Reperfusion Following 10 Minutes of Ischemia

Baseline values, as indicated above, were assessed from all ODCs at the onset of ischemia for each ischemic duration. Following 10 minutes of complete flow arrest of the measurement area, reperfusion was initiated and VO_2 sampling was begun 5 seconds later. Since the recovery of $P_{ISF}O_2$ is a function of oxygen demand, as well as supply, the R5 measurement point did not yield values above 40 mmHg due to a high degree of oxygen utilization. The intermediate range, however, did contain data points for the R5 measurement and revealed an increase in VO_2 by 254% of baseline (mean= 3.79±0.80 $mlO_2/100\ cm^3min$; n=2). Due to the low sample size, statistical analysis was not performed. Twenty-five seconds of reperfusion showed significantly elevated VO_2 values for both normoxic (mean= 5.75 ± 0.40 $mlO_2/100\ cm^3min$; $P_{ISF}O_2$ = 56.0 ± 5.1 mmHg; n=4) and intermediate (mean = 3.18 ± 0.30 $mlO_2/100\ cm^3min$; $P_{ISF}O_2$ = 27.1± 3.8 mmHg; n=7) measurements of 292% and 213% over baseline, respectively (p

< 0.0001 and p = 0.0009). By a reperfusion time of 45 seconds, VO_2 for the normoxic (mean= 3.45 ± 0.36 ml O_2/100 cm^3min; $P_{ISF}O_2$ = 64.38 ± 4.1 mmHg; n=6) and intermediate (mean = 2.75± 0.30 mlO_2/100 cm^3min; $P_{ISF}O_2$ = 32.0 ± 3.4 mmHg; n=9) ranges had fallen slightly, but remained significantly elevated at 175% (p = 0.0057) and 185% (p = 0.02) over baseline values, respectively. As illustrated by Figure 27, plots C and B, there is a continued trend reduction of the oxygen consumption rates back to resting values for both the normoxic and intermediate $P_{ISF}O_2$ measurements over the subsequent R65 and R85 time points. The normoxic R65 time point showed a reduced VO_2 (as compared to R45), but still significantly elevated VO_2 over baseline (mean = 3.19± 0.27 mlO_2/100 cm^3min; $P_{ISF}O_2$ = 60.7 ± 3.0 mmHg; p= 0.0014; n=11). The remaining values showed no statistical difference from baseline for these last two measurements. Measurements taken during hypoxic conditions (Figure 27 plot C) show a lack of change in VO_2 over the time course of reperfusion as compared to baseline.

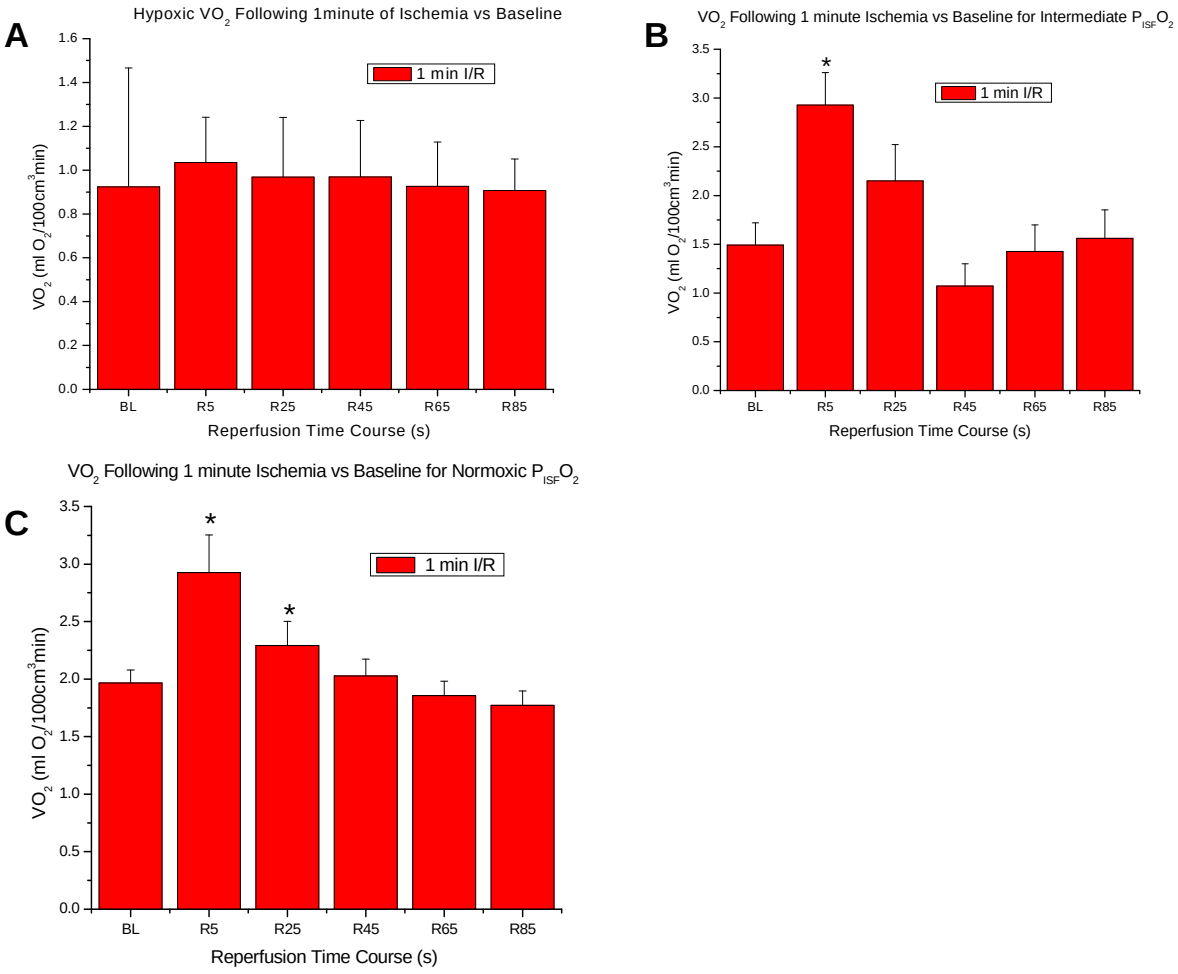

Figure 25: Comparison of VO_2 during early reperfusion following 1 minute of total ischemia. BL indicates the pooled and averaged measurements from the initial ODC at the onset of ischemia and acts as a control for resting skeletal muscle VO_2. R5-R85 indicate the time points of measurement using the VO_2 Sampling Technique during reperfusion. **A:** Hypoxic measurements of VO_2 during reperfusion showed no change compared with BL. **B:** The intermediate range of $P_{ISF}O_2$ measurements show an elevated VO_2 at R5 with a progressive decline back to baseline by ~R45. **C:** Normoxic measurements also show an elevated R5 VO_2 with a decline back to baseline by ~R45.

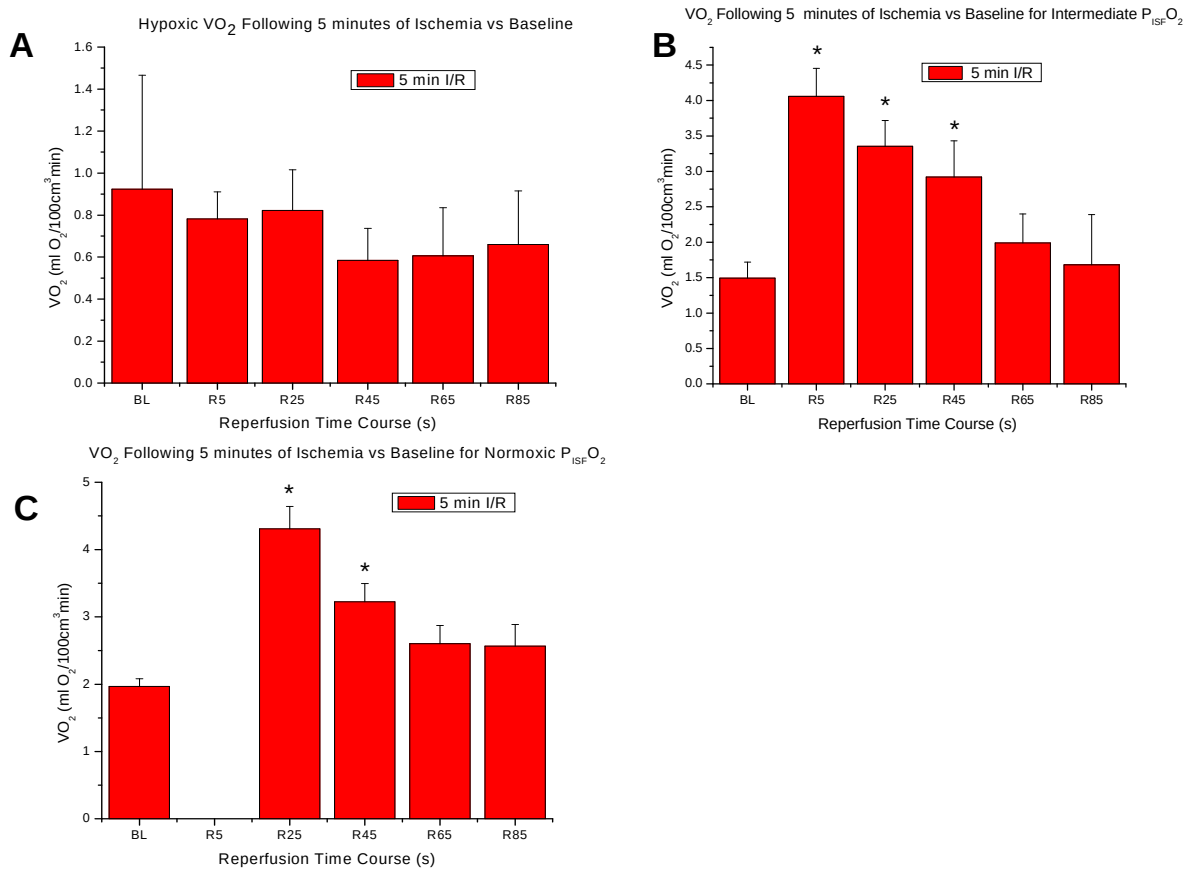

Figure 26: Comparison of VO_2 during early reperfusion following 5 minutes of total ischemia. BL indicates the pooled and averaged measurements from the initial ODC at the onset of ischemia and acts as a control for resting skeletal muscle VO_2. R5-85 indicate the time points of measurement using the VO_2 Sampling Technique during reperfusion. **A:** Hypoxic measurements of VO_2 during reperfusion showed no change compared with BL. **B:** The intermediate range of $P_{ISF}O_2$ measurements show elevated VO_2 readings at R5, R25, and R45 that progressively fall back towards BL with R65 and R85 showing no difference from BL. **C:** Normoxic measurements show elevated VO_2 readings at R25 and R45 that trend toward a decline back to baseline with R65 and R85 not significantly different from BL. Normoxic R5 measurements could not be made due to a slow recovery of $P_{ISF}O_2$.

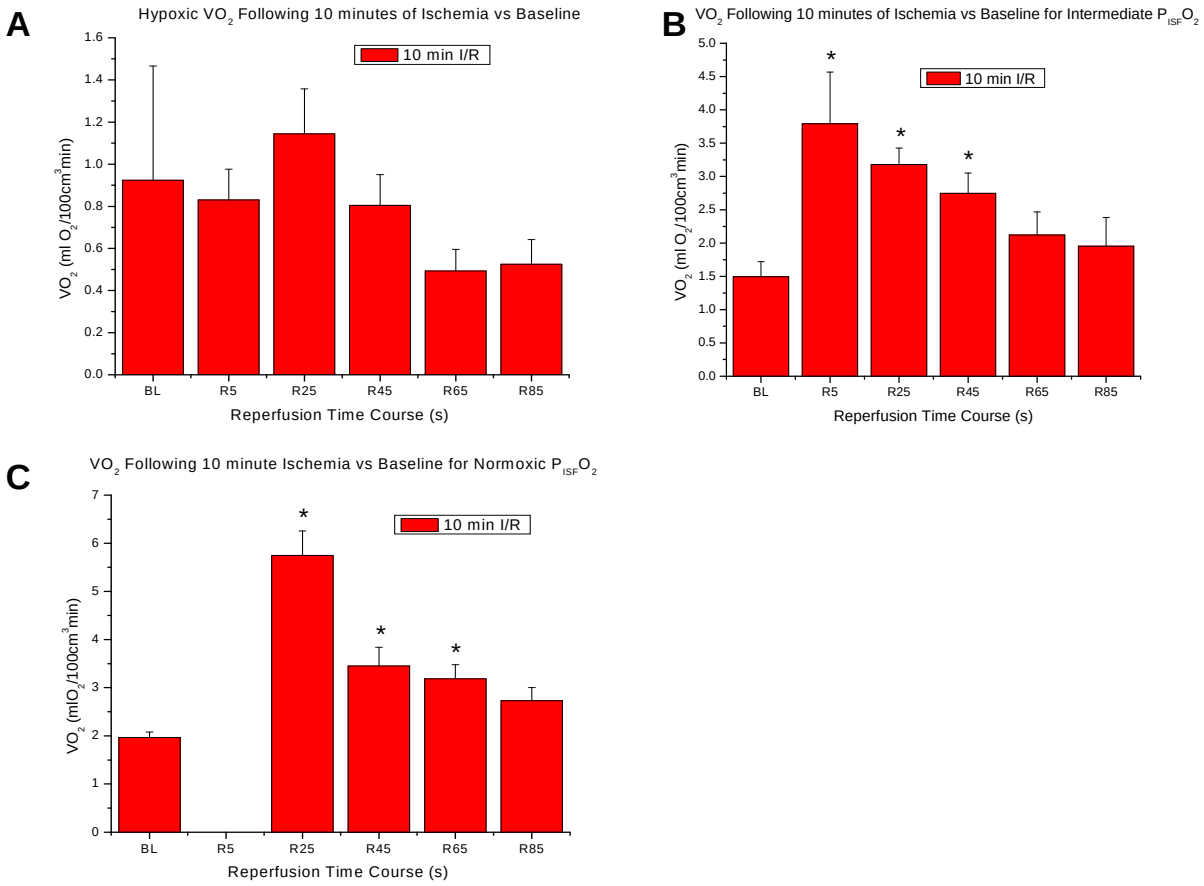

Figure 27: Comparison of VO_2 during early reperfusion following 10 minutes of total ischemia. BL indicates the pooled and averaged measurements from the initial ODC at the onset of ischemia and acts as a control for resting skeletal muscle VO_2. R5-85 indicate the time points of measurement using the VO_2 Sampling Technique during reperfusion. **A:** Hypoxic measurements of VO_2 during reperfusion showed no change compared with BL. **B:** The intermediate range of $P_{ISF}O_2$ measurements show elevated VO_2 readings at R5 (not significant), R25, and R45 that progressively fall back towards BL with R65 and R85 showing no difference from BL. **C:** Normoxic measurements show elevated VO_2 readings at R25, R45, and R65 that trend towards a decline back to baseline with R85 not significantly different from BL. Normoxic R5 measurements could not be made due to a slow recovery of $P_{ISF}O_2$.

Results: Influence of Cyanide on I/R

Cyanide Dose-Response

As a confirmation that the changes in VO_2 for the I/R protocols were linked to cytochrome c oxidase oxygen utilization, the mitochondrial respiratory inhibitor cyanide (CN) was used for comparison against control. Given that systemic administration of CN would be inappropriate, a topical application to the skeletal muscle was carried out. A range of three doses from 0.01 mM to 1 mM was chosen for a dose-response assessment (see Figure 28) in one pilot experiment to determine the minimum effective concentration for comparison against control I/R measurements.

Control measurements using the I/R protocol preceded the applications of increasing CN concentrations. Resting VO_2 (BL) in the spinotrapezius muscle changed progressively from 1.95 (control) to 1.63 $mlO_2/100\ cm^3min$ (CN 0.01), to 1.65 $mlO_2/100\ cm^3min$ (CN 0.1) to 0.72 $mlO_2/100\ cm^3min$ (CN 1mM). A 1-minute ischemic duration was chosen to precede the measurements of reperfusion in order to keep measurements in the normoxic range for ease of comparison. At 5 seconds of reperfusion, the same inverse relationship between CN concentration and VO_2 existed (control: 4.29; CN 0.01mM: 4.04; CN 0.1 mM: 3.08; and CN 1 mM: 1.15 $mlO_2/100cm^3min$) with 1 mM having only a slight elevation compared to resting conditions. Measurements of VO_2 beyond the R5 time point steadily declined back to their baselines for control and CN concentrations of 0.01 and 0.1 mM. CN 1 mM, however, did not appear to show any trend in VO_2 over its entire timecourse, indicating that any elevation or depression was due to noise. This profile of VO_2 for the 1 mM dose of CN was similar to that of the hypoxic controls for the 1-minute I/R protocol.

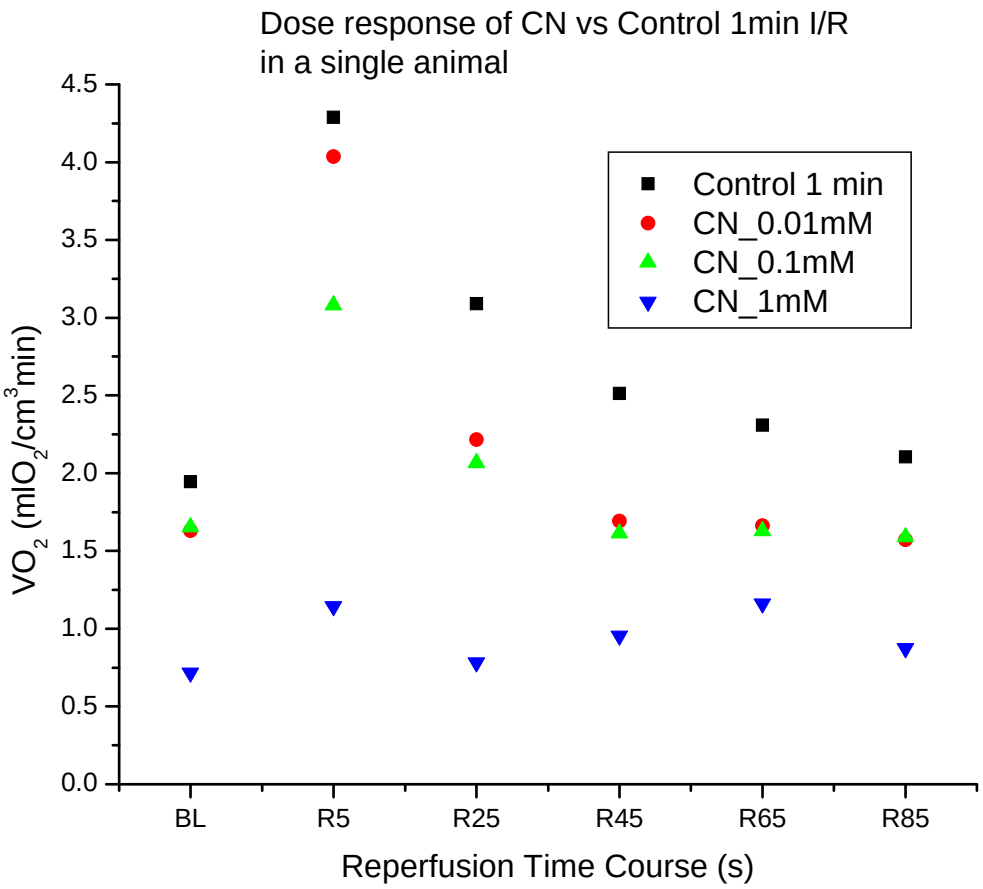

Figure 28: Dose response pilot to 0.01, 0.1, and 1 mM Cyanide (CN) during 1 minute I/R. The data plotted for control are specific to this study and preceded the application of CN. Following control measurements, each dose of CN was topically applied to the tissue in the order of increasing concentration. All plotted measurements satisfied the condition of normoxia. There is a progressive decline in VO_2 with increasing concentrations of CN. The 1 mM concentration produced an apparent insensitivity to the 1 minute ischemic intervention.

Influence of 1 mM Cyanide on Resting VO_2

The influence of 1 mM Cyanide (CN) on the resting state VO_2 of the rat spinotrapezius muscle was measured and compared to control conditions to assess whether mitochondrial respiration is responsible for the increased oxygen consumption rates measured during reperfusion following blood flow arrest. Cyanide was chosen due to its function as a mitochondrial respiratory chain inhibitor that acts at the level of cytochrome c oxidase. At a sufficient concentration, it was expected to reduce or eliminate the consumption of oxygen for the purpose of ATP generation. It was not predicted to quench all sources of VO_2, as processes like ROS generation would still occur at normal or possibly accelerated rates.

Figure 29 shows a comparison of VO_2 between control and tissue topically treated with 1 mM cyanide during resting conditions. CN-treated tissue showed a 36% reduction in VO_2 (mean= 1.26±0.15 $mlO_2/100\ cm^3min$; $P_{ISF}O_2$= 83.0±2.6 mmHg; n= 30) as compared to control (mean= 1.97±0.1 $mlO_2/100\ cm^3min$; $P_{ISF}O_2$= 59.8±1.6; n= 72) that was statistically significant ($p = 0.0023$). The CN measurements also demonstrated a profound increase in $P_{ISF}O_2$ by 139% of control ($p < 0.0001$), which was consistent with a widespread reduction in the oxygen demand of the spinotrapezius muscle.

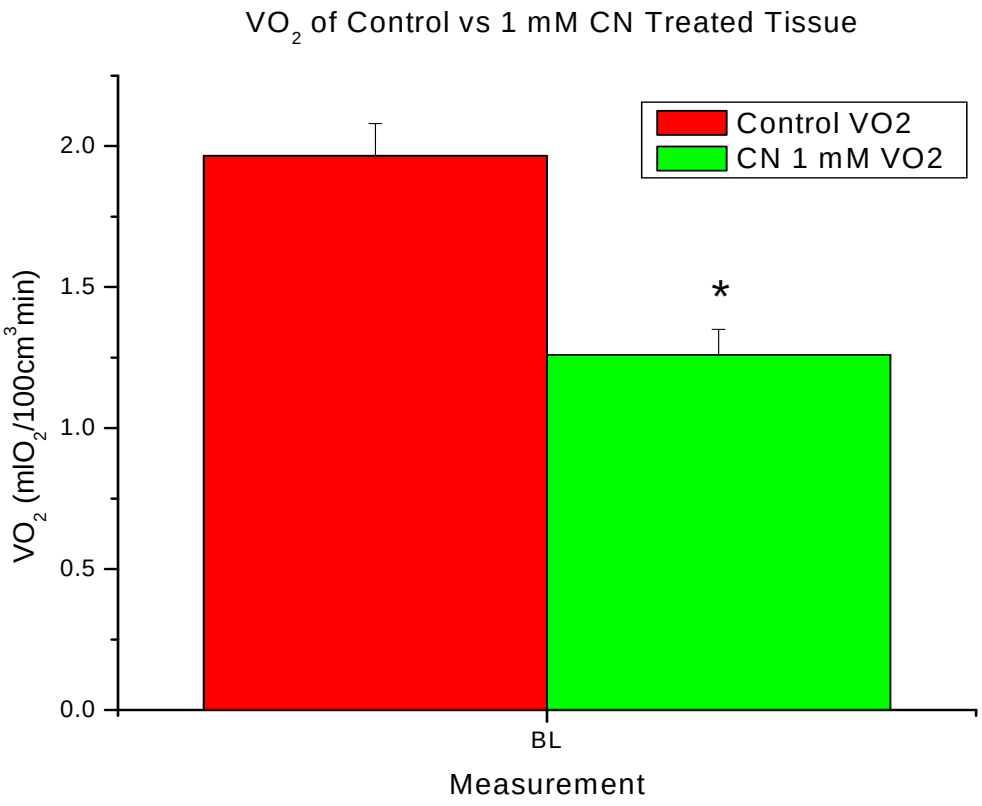

Figure 29: Resting VO_2 of Control vs 1 mM cyanide (CN)-treated skeletal muscle. The topical application of 1 mM CN resulted in a reduction of resting state VO_2 in skeletal muscle of 36% ($p = 0.0023$). These measurements were derived from initial compression of ischemic induction for the 1-, 5- and 10-minute I/R protocols and used as baselines for comparison against the reperfusion time course. Due to the $P_{ISF}O_2$-enhancing effect of CN, these values are representative of the normoxic situation only.

Influence of 1 mM Cyanide during Hypoxia and Intermediate $P_{ISF}O_2$

Measurements of resting state VO_2 under hypoxic conditions were difficult to obtain following treatment with 1 mM CN due to the elevated $P_{ISF}O_2$ in response to a reduction in oxygen demand. Thus, the hypoxic comparisons for CN vs control were made following 5 and 10 minute periods of ischemia at the R5 time point. These data were plotted alongside the intermediate $P_{ISF}O_2$ range as a reference of higher oxygen availability.

As shown in Figure 30, the two ischemic durations sufficient to produce hypoxic data were 5 (top) and 10 (bottom) minutes. First, following 5 minutes of ischemia conducted under the standard I/R protocol, measurements of the R5 time point during hypoxia revealed a 186% increase in VO_2 for tissue treated with 1 mM CN (mean = 1.45 ± 0.30 $mlO_2/100\ cm^3min$; $P_{ISF}O_2$ = 15.3 ± 5.1 mmHg; n=6) over control (mean = 0.78 ± 0.15 $mlO_2/100\ cm^3min$; $P_{ISF}O_2$ = 10.58±2.42 mmHg; n= 27) that was statistically significant (p= 0.037). The average $P_{ISF}O_2$ was statistically different between CN and Control measurements by about 5 mmHg (p=0.007), but as all measurements had P_0 values below the 22 mmHg threshold for inclusion in the category of hypoxia, this difference should not have affected VO_2. For the hypoxic R5 measurement following 10 minutes of ischemia, there was a similar increase in VO_2 (164%) found in 1 mM CN-treated muscles (mean: 1.36 ± 0.33 $mlO_2/100\ cm^3min$; $P_{ISF}O_2$ = 16.3 ± 5.1 mmHg; n= 6) over control (mean: 0.83 ± 0.15 $mlO_2/100\ cm^3min$; $P_{ISF}O_2$ = 10.2±2.3 mmHg; n=30), but there appeared to be insufficient data to establish significance (p= 0.14). In this case, the $P_{ISF}O_2$ values were also significantly higher for the CN group (p= 0.0001), but all measurements still fell within the range of hypoxia (<22 mmHg).

For the intermediate range of $P_{ISF}O_2$ for the R5 measurement point following 5 minutes of ischemia, there appeared to be no difference in VO_2 between 1 mM CN-treated tissue (mean=

4.03±0.40 mlO_2/100 cm^3min; $P_{ISF}O_2$ = 29.8±6.3 mmHg; n= 4) and control (mean= 3.91±0.40 ml O_2/100 cm^3min; $P_{ISF}O_2$ = 28.1 ± 6.3 mmHg; n=4). Following 10 minutes of ischemia, there were insufficient control data to make a statistical comparison, but 1 mM CN-treated tissue had a VO_2 of 2.64 ml O_2/100 cm^3min (SE: 0.46; $P_{ISF}O_2$ = 23.6 ± 7.2 mmHg).

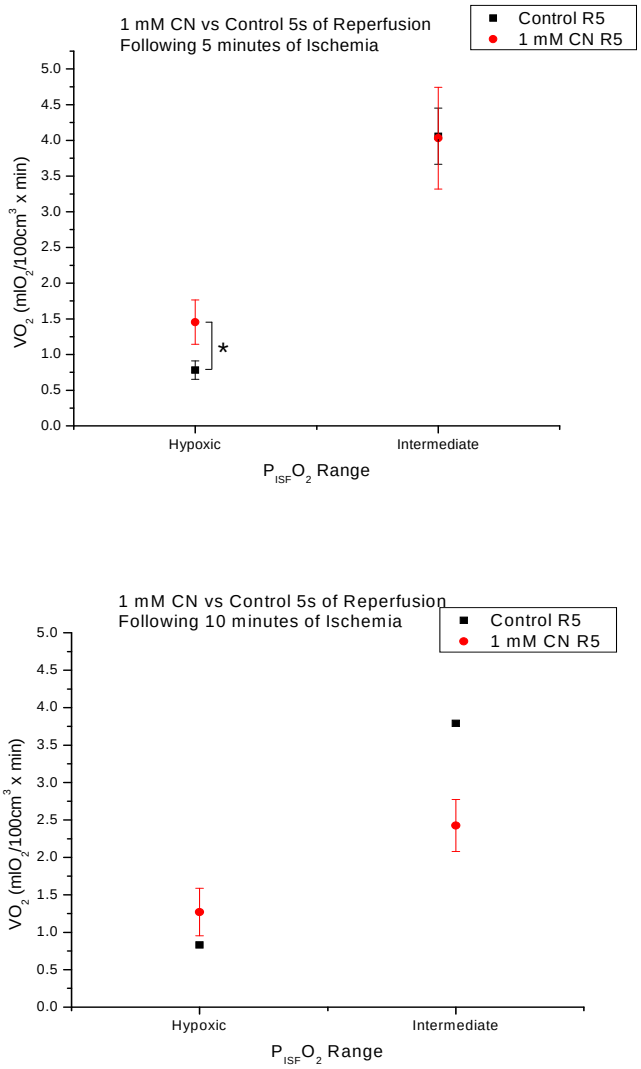

Figure 30: Influence of 1 mM CN on R5 VO_2 for the hypoxic and intermediate $P_{ISF}O_2$ range. The R5 measurement following the 5 and 10 minute durations of ischemia were the only reliable source of hypoxic VO_2 measurements for 1 mM CN-treated tissue. **Top:** The hypoxic R5 VO_2 in the CN group following 5 minutes of ischemia showed a significant elevation over control. VO_2 for the intermediate $P_{ISF}O_2$ group was not significantly different from that of the control situation. **Bottom:** The hypoxic R5 VO_2 in the CN group following 10 minutes of ischemia trended towards an elevation over control, but the difference was not significant. The intermediate group lacked sufficient measurements for statistical analysis.

Influence of Cyanide on VO_2 Profile during Reperfusion

Tissues to which 1 mM CN had been topically applied were observed over the reperfusion timecourse of 1-, 5- and 10-minute durations of ischemia in terms of VO_2 and compared against control. Since CN causes an overall rise in $P_{ISF}O_2$ by decreasing the tissue's demand for oxygen, there were few measurements made beyond reperfusion time point R5 that fell within either the intermediate or hypoxic range. Therefore, only measurements made under normoxic conditions were analyzed for the entire reperfusion timecourse.

The reperfusion profile of 1 mM CN-treated tissue following 1 minute of ischemia showed an overall reduction in VO_2 that was significantly different from control at time point R25 (1 mM CN, mean = 1.40 ± 0.22 ml O_2/100 cm^3min; n=11; Control, mean = 2.29 ± 0.21 ml O_2/100 cm^3min; n= 24; p= 0.015). All other values, although not statistically different from their control counterparts, did show a trend towards attenuation of VO_2 for tissue treated with 1 mM CN. Comparison amongst the CN measurement time points during reperfusion with Tukey's HSD revealed no significant difference in measured VO_2 rates. There was, however, a positive trend in measurements for the R5 time point compared to baseline.

The time course of VO_2 during reperfusion for tissue treated with 1 mM CN following 5 minutes of ischemia showed an overall reduction in VO_2 that was significantly different from control at time points R45 (1 mM CN, mean=2.08 ± 0.21 ml O_2/100 cm^3min; n= 8; Control, mean= 3.23 ± 0.3 ml O_2/100 cm^3min; n=9; p= 0.005) , R65 (1 mM CN, mean= 1.48 ± 0.15 ml O_2/100 cm^3min; n= 10; Control, mean= 2.60 ± 0.27 ml O_2/100 cm^3min; n= 13; p= 0.003) , and R85 (1 mM CN, mean= 1.35 ± 0.45 ml O_2/100 cm^3min; n= 10; Control, mean= 2.57 ± 0.32 ml O_2/100 cm^3min; n= 7; p= 0.006). Measurements at time points R5 and R25, although not found to be significantly different between control and CN groups, did show a trend towards the

attenuation of VO_2 in CN treated tissue as compared with control. The reperfusion time course of the CN groups showed a clear elevation in VO_2 at R25, as compared to baseline, which then returned to baseline by R65.

The reperfusion profile of 1 mM CN-treated tissue following 10 minutes of ischemia showed an overall reduction in VO_2 that was significantly lower than control at time points R65 (1 mM CN, mean= 2.27 ± 0.22 ml O_2/100 cm^3min; n= 8; Control, mean = 3.19 ± 0.29 ml O_2/100 cm^3min; n= 11; p= 0.033) , and R85 (1 mM CN, mean= 1.95 ± 0.18 ml O_2/100 cm^3min; n= 8; Control, mean= 2.73 ± 0.27 ml O_2/100 cm^3min; n= 12; p= 0.047). The measurements at time point R25, although not found to be significantly different between control and CN groups, did show a trend towards the attenuation of VO_2 in CN-treated tissue as compared with control. The R45 measurement was not different from control. The reperfusion time course of the CN groups showed a clear elevation in VO_2 at R25, as compared to baseline, which then returned towards baseline (see Figure 31).

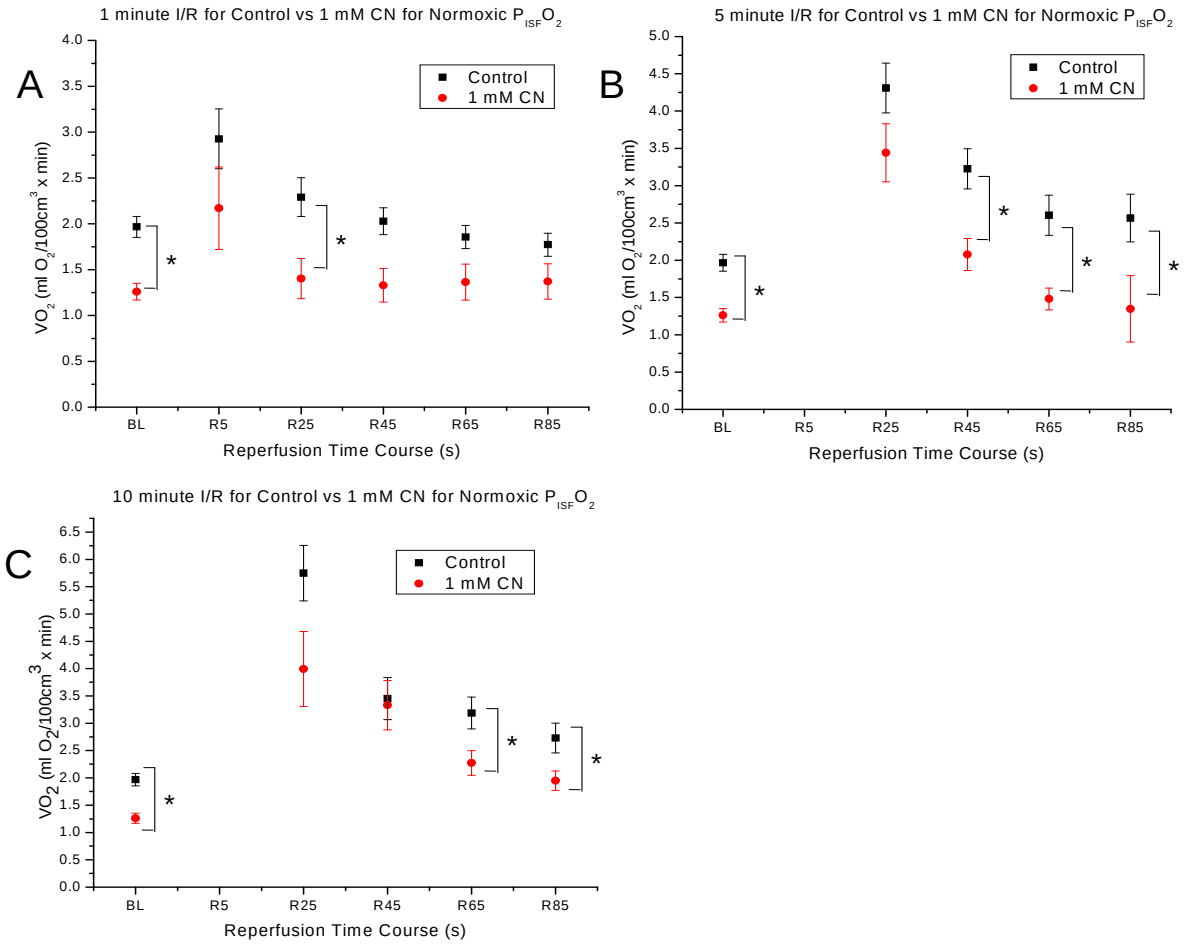

Figure 31: Influence of 1 mM CN on VO_2 for 1-, 5- and 10-minute I/R protocols. 1 mM CN was topically applied to the spinotrapezius muscle and measurements were made with the standard I/R protocol with varying ischemic durations of 1, 5, and 10 min. **A:** There was a brief elevation in VO_2 for the CN-treated group at R5 compared to BL, but this was not significant. The R25 time point was the only measurement to show a significant difference from control. **B:** Following 5 minutes of ischemia, the CN group had a VO_2 profile similar to that of the control group, but with reduced magnitude. **C:** Following 10 minutes of ischemia, the CN group showed a VO_2 time course similar to that of the control group, but with a reduced magnitude. Incomplete inhibition of VO_2 by CN likely explains some of the continued oxygen consumption by the treated tissue.

Influence of Nitroglycerin on I/R

The mechanism of preconditioning that confers protection against long term ischemic durations is activated during brief periods of ischemia with reperfusion similar to those conducted in this study and has been associated with changes in the tissue distribution of nitric oxide. Therefore, to better understand the mechanisms responsible for the observed reperfusion time course of VO_2 following ischemia, nitric oxide (NO) levels were pharmacologically elevated by the topical application of nitroglycerin (NTG) during the I/R protocols. Arteriolar diameter was measured as an indicator of changing NO concentrations in the tissue.

Time course of NTG Activity on Arteriolar Diameter

The effect of altered nitric oxide (NO) concentration on the responses observed during the I/R protocol was tested by topically applying the NO donor nitroglycerin (NTG) to the spinotrapezius muscle. A dose-response curve was generated over the range of 0.01 to 1 mM NTG. To assess whether NO was being delivered to the tissue in appropriate concentrations, changes in arteriolar diameter were related to the applied NTG concentration and time of dosing.

In one pilot animal, 5 arterioles of 50-90 μm in diameter were selected and their diameters were measured to establish a baseline. Next, 100 μl of PBS was dripped onto the tissue. A 2-minute incubation period was allowed to pass before another 100 μl of PBS was applied and the tissue was recovered with the Krehalon film. The diameters of the 5 arterioles were then measured every minute for 15 minutes to establish a baseline to which the diameters following NTG applications would be compared. This procedure was then repeated for each dose of NTG starting with 0.01 mM and increasing to 1 mM for the same 5 arterioles. The data

were assessed semi-quantitatively for the time required to achieve the maximum response and the duration of the effect, but were not otherwise subjected to statistical analysis.

As plotted in Figure 32, plot A, following the topical application of 0.01 mM NTG, the arterioles reached a maximum dilation (mean diameter = 93 ± 4 μm) 3 minutes after the application procedure was completed. This level of dilation lasted another 2 minutes when a rapid return to baseline occurred (mean diameter at 6 minutes post application = 86 ± 3 μm; minute 6 control mean diameter = 84 ± 4 μm). Baseline values persisted for both control and 0.01 mM NTG-treated groups beyond this point.

As plotted in Figure 32, plot B, following the topical application of 0.1 mM NTG, arteriolar dilation reached a maximum (mean diameter = 93 ± 4 μm) by the 3 minute time point. This level of dilation persisted for another 3 minutes (mean diameter = 92 ± 4 μm) and then declined back to baseline by minute 11 (mean diameter at 11 minutes post application = 87 ± 5 μm; minute 11 control mean diameter = 86 ± 4 μm). Baseline values persisted for both control and 0.1 mM NTG-treated groups beyond this point.

As plotted in Figure 32, plot C, the topical application of 1 mM NTG resulted in a maximum arteriolar dilation (mean diameter = 94 ± 4 μm) by minute 5 of measurement. This level of dilation persisted for 2 minutes (7-min mean diameter = 90 ± 3 μm) and then declined to baseline by minute 11 (11-min mean diameter = 85 ± 4 μm; 11-min control mean diameter = 86 ± 4 μm). Approximate baseline values persisted beyond this time point, but 1 mM NTG-treated arterioles appeared to be slightly dilated when compared to the lower doses for the 12- to 15-minute measurements.

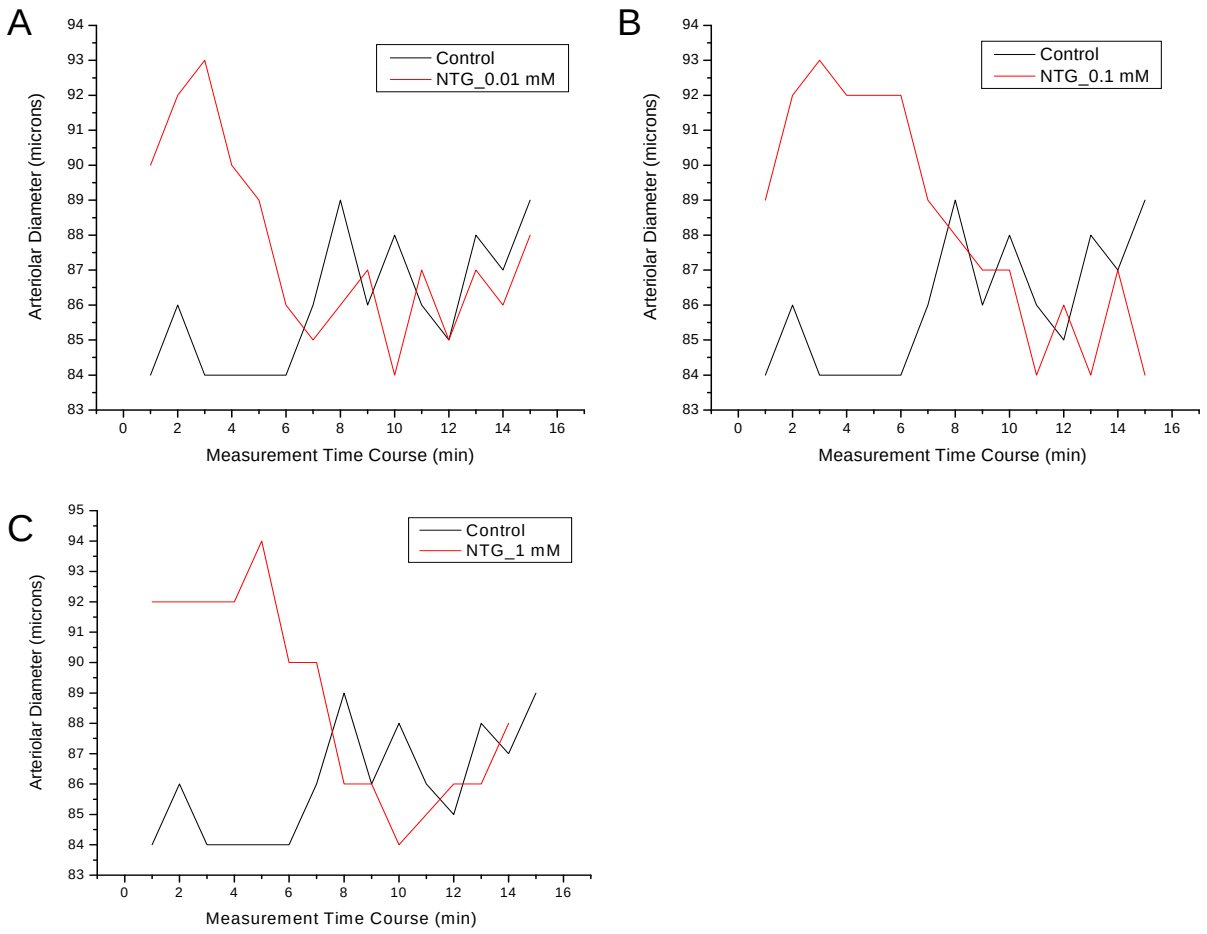

Figure 32: Time course of arteriolar diameter response to 0.01-1 mM NTG. In a single pilot experiment, phosphate buffered saline (control) was topically applied to the spinotrapezius muscle and arteriolar diameters were measured for 15 minutes. This process was then repeated with 0.01, 0.1, and 1 mM doses of NTG applied in the same fashion. Each plotted line represents the mean values of 5 arterioles, which were observed over the different doses. Error bars were not included in the interest of visual clarity.

Dose-Response of Arteriolar Diameter to NTG

Each assessment of NTG's influence on VO_2 for both resting and reperfusion conditions was coupled with observations of arteriolar diameter (see Figure 33). This was done to ensure that measurements were conducted on tissue where NO levels had observably changed. Baseline values were measured prior to and following the untreated control VO_2 measurements to ensure that the VO_2 Sampling Technique did not appreciably alter the vasculature. With a mean initial BL value of 73 ± 3 μm and a subsequent mean value of 73 ± 4 μm following measurements of VO_2 over resting and various I/R protocols, there was no significant change in arteriolar diameter. Application of the 0.01 mM dose of NTG resulted in an average dilation to 106% of baseline (mean diameter = 77 ± 4 μm), which was not significant. After all VO_2 measurements were completed, arteriolar diameter returned approximately to baseline (mean diameter = 73 ± 3 μm before the next dose. It should be noted that an extra dose of the same concentration was applied before the 10 minute ischemic duration based on the time course of NTG effectiveness as determined by results of the pilot experiment presented in Figure 32.

The topical application of 0.1 mM NTG resulted in a 117% arteriolar dilation (mean diameter = 85 ± 5 μm) from baseline (mean diameter = 73 ± 3 μm), which did not quite achieve significance ($p=0.0525$), but showed a strong trend. Following all subsequent VO_2 measurements during rest and various I/R protocols and a brief pause, the arteriolar diameters had returned approximately to baseline (mean diameter = 74 ± 4 μm). As with the previous concentration, an extra dose of this concentration was applied immediately prior to the 10-minute ischemic duration. Finally, 1 mM NTG was applied topically to the tissue and elicited a 120% dilation (mean diameter = 87 ± 6 μm) from the initial average baseline value (mean diameter = 73 ± 3 μm), which was found to be significant ($p= 0.034$). Arteriolar diameter was not measured

at the conclusion of this round of resting and I/R VO_2 measurements, but an assessment was made prior to the application of the second 1 mM dose of NTG that preceded the 10-minute ischemic duration. Average arteriolar diameter (mean diameter = 75 ± 4 μm) had returned close to the baseline value.

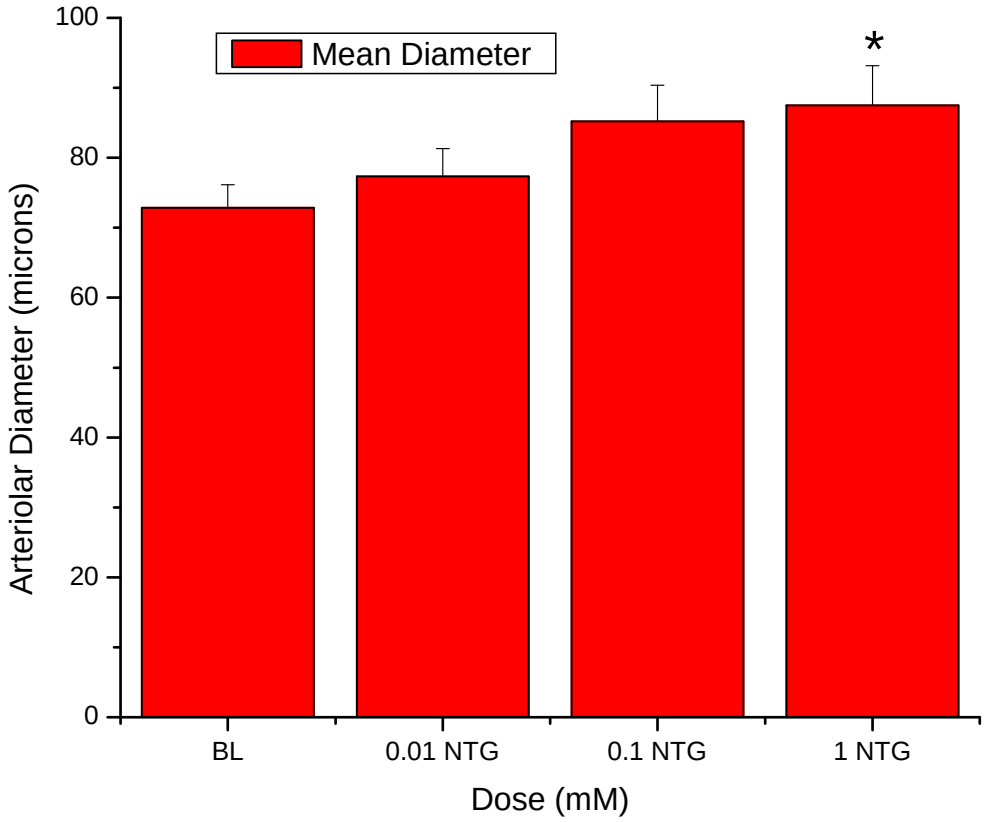

Figure 33: Arteriolar diameter dose-response to topical application of NTG. These data represent 16 different arterioles over 4 animals. The same sites for the same 4 arterioles were measured in each animal over the range of NTG concentrations. Baseline measurements were made prior to the topical application of NTG and used as a comparison for the magnitude of dilation. * indicates significance at the p = 0.05 level.

Dose-Response of Resting VO_2 to NTG

Three doses of NTG—0.01, 0.1, and 1 mM—were topically applied to the spinotrapezius muscle and their influence on VO_2 was determined (see Figure 34). The 0.01 mM dose caused a 25% (mean VO_2 = 1.48±0.10 ml O_2/100 cm^3min; $P_{ISF}O_2$ = 58 ±3 mmHg; n= 13) reduction in VO_2 compared to control (mean VO_2 = 1.97±0.10 ml O_2/100 cm^3min; $P_{ISF}O_2$ = 59.8 ± 1.5 mmHg; n= 72), which showed a strong trend (p= 0.079). The control vs 0.01 NTG $P_{ISF}O_2$ values did not show any statistically significant difference. The next stepwise dose of 0.1 mM NTG caused a similar reduction in VO_2 by ~27% (mean VO_2 = 1.43 ± 0.30 ml O_2/100 cm^3min; $P_{ISF}O_2$ = 70.8±3.9 mmHg; n=11) of control (mean VO_2 = 1.97 ± 0.10 ml O_2/100 cm^3min; $P_{ISF}O_2$ = 59.8 ± 1.5 mmHg; n= 72), which showed a strong trend (p= 0.095). The average $P_{ISF}O_2$ for the 0.1 mM dose was significantly elevated to 122% of control (p= 0.013), which was consistent with a reduced tissue respiration rate. The final dose of 1 mM NTG produced a substantial 43% reduction in VO_2 (mean VO_2 = 1.13 ± 0.20 ml O_2/100 cm^3min; $P_{ISF}O_2$ = 64.7±5.1 mmHg; n=9) from control (mean VO_2 = 1.97 ± 0.1 ml O_2/100 cm^3min; $P_{ISF}O_2$ = 59.8±1.5 mmHg; n= 72), which was significant (p= 0.013). $P_{ISF}O_2$ for measurements made during the 1 mM application of NTG were slightly elevated at 108% of baseline, but this difference was not found to be significant.

According to the mean arteriolar diameter vs. time data (see Figure 32), the observable effects of each NTG dose lasted only 6 to 11 minutes before baseline conditions returned. Therefore, following each series of measurements, the measured reductions in VO_2 were unlikely to be additive when stepping upwards to the next dose.

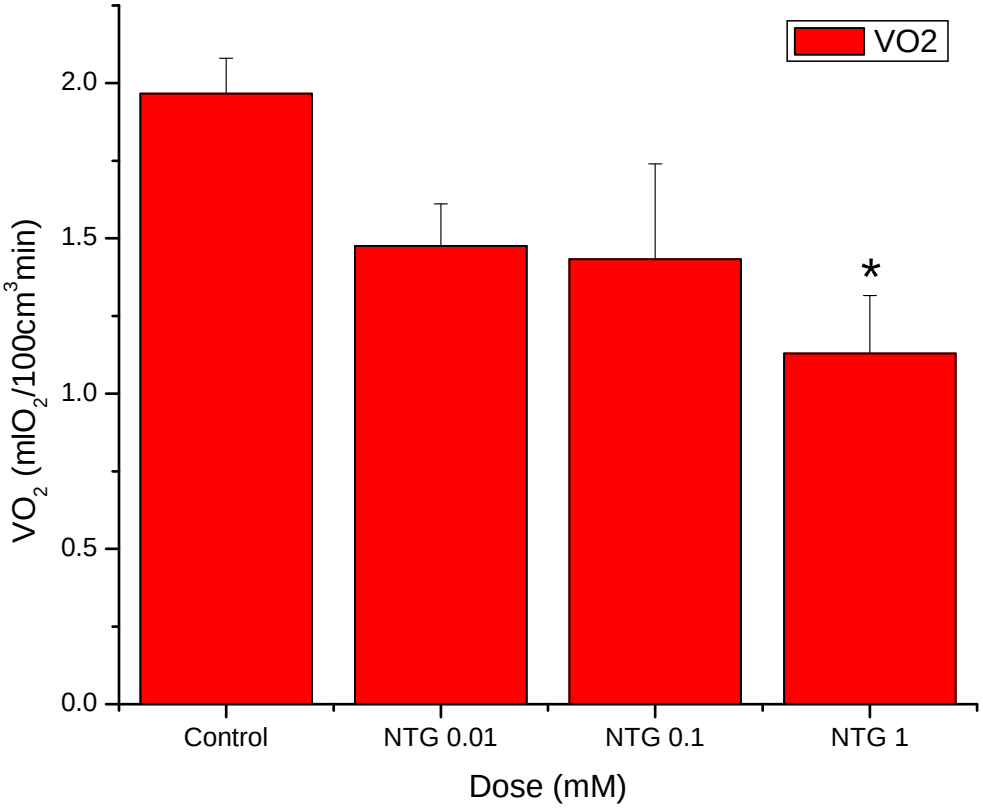

Figure 34: VO_2 of Control vs NTG-treated skeletal muscle tissue. 4 spinotrapezius muscles were subjected to increasing doses of 0.01, 0.1 and 1 mM NTG and assessed for their resting state VO_2 rates. Measurements here are representative of normoxic conditions only. * indicates a significant difference as compared to control at p= 0.05.

Influence of NTG on I/R

The effect of 0.01, 0.1, and 1 mM doses NTG on VO_2 was measured during reperfusion following 1-, 5- and 10-minute durations of ischemia. These doses were administered topically to the rat spinotrapezius muscle as 2 rounds of 100 µl applications spaced 2 minutes apart. The resulting data were then divided into groups of hypoxic, intermediate and normoxic oxygen tensions by their P_0 ($P_{ISF}O_2$ immediately prior to air-bag pressurization. NTG resulted in an across the board reduction in VO_2, but, as shown by Figure 35, consistent statistical differences over the reperfusion time course could only be demonstrated between control VO_2 and that for the 0.1 mM dose in the intermediate range of P_0 ($22 < P_0 < 40$ mmHg).

Baseline (BL) measurements of VO_2 over the intermediate range of P_0 for control (1.49 ± 0.23 ml O_2/100 cm^3min; P_0 = 32.2±0.9 mmHg; n= 21) and 0.1 mM NTG-treated muscles (mean VO_2 = 0.39 ± 0.06 ml O_2/100 cm^3min; P_0 = 28.6 ± 6.5 mmHg; n= 2) were not significantly different from each other (p= 0.16), but did appear to show a trend in the reduction of VO_2 by 0.1 mM NTG. Values for P_0 were not found to be significantly different between control and NTG-treated tissue. Attainment of a more accurate VO_2 for resting skeletal muscle in the intermediate range of P_0 would likely occur with a larger number of observations.

Figure 35, plot A, shows the VO_2 time course during reperfusion following 1 minute of ischemia for control vs 0.1 mM NTG-treated tissue. At 5 seconds after the onset of reperfusion (R5) the NTG group exhibited a 66% reduction in VO_2 (mean VO_2 = 0.98 ± 0.29 ml O_2/100 cm^3min; P_0 = 28.6 ± 6.5 mmHg; n= 3) compared to the R5 control measurements (mean VO_2 = 2.93 ± 0.33 ml O_2/100 cm^3min; P_0 = 33.2 ± 1.4 mmHg; n= 14), which was found to be significant (p= 0.019). P_0 for the NTG group was also found to be significantly lower than control (p= 0.048), but all measurements remained within the intermediate range of P_0. At 25 seconds after

the onset of reperfusion (R25) the NTG group showed an 82% reduction in VO_2 (mean VO_2 = 0.38 ± 0.29 ml O_2/100 cm^3min; P_0 = 28.0 ± 2.5 mmHg; n= 3) compared to the R25 control measurements (mean VO_2 = 2.15 ± 0.37 ml O_2/100 cm^3min; P_0 = 31.3 ±2.8 mmHg; n= 5), which was found to be significant (p= 0.012). There was no statistically significant difference for P_0 between control and NTG groups. At 45 seconds after the onset of reperfusion (R45) the NTG group demonstrated an 87% reduction in VO_2 (mean VO_2 = 0.14 ± 0.09 ml O_2/100 cm^3min; P_0 = 30.3 ± 5.8 mmHg; n= 3) compared to the R45 control measurements (mean VO_2 = 1.07 ± 0.23 ml O_2/100 cm^3min; P_0 = 32.6 ± 3.1 mmHg; n= 4), which was found to be significant (p= 0.008). There was no statistically significant difference for P_0 between control and NTG groups. At 65 seconds after the onset of reperfusion (R65) the NTG group demonstrated an 96% reduction in VO_2 (mean VO_2 = 0.06 ± 0.06 ml O_2/100 cm^3min; P_0 = 29.4 ± 4.7 mmHg; n= 2) compared to the R65 control measurements (mean VO_2 = 1.43 ± 0.27 ml O_2/100 cm^3min; P_0 = 32.4 ± 2.3 mmHg; n= 6), which was found to be significantly different (p= 0.004). There was no statistically significant difference for P_0 between control and NTG groups. At 85 seconds after the onset of reperfusion (R85) the NTG group showed a 94% reduction in VO_2 (mean VO_2 = 0.09 ± 0.08 ml O_2/100 cm^3min; P_0 = 30.2 ± 5.0 mmHg; n= 2) compared to the R85 control measurements (mean VO_2 = 1.56 ± 0.29 ml O_2/100 cm^3min; P_0 = 33.9 ± 2.5 mmHg; n= 6), which was found to be significantly different (p= 0.033). There was no statistically significant difference for P_0 between control and NTG groups.

Figure 35, plot B, shows the VO_2 timecourse during reperfusion following 5 minutes of ischemia for control vs 0.1 mM NTG-treated tissue. There were insufficient NTG measurements at the R5 time point for a comparison against control due to hypoxic P_0's. At 25 seconds after the onset of reperfusion (R25) the NTG group showed a 46% reduction in VO_2 (mean VO_2 =

1.80 ± 0.32 ml O_2/100 cm^3min; P_0 = 29.3 ± 5.2 mmHg; n= 3) compared to the R25 control measurements (mean VO_2 = 3.35 ± 0.36 ml O_2/100 cm^3min; P_0 = 27.5±1.3 mmHg; n= 9), which was found to be significant (p= 0.043). There was no statistically significant difference for R25 P_0 between control and NTG groups. Measurements of VO_2 for NTG-treated tissue at the R45 and R65 time points were lower than control on average, but these differences were not significant (p= 0.39 and 0.71 respectively). There were also no significant differences in P_0 found between NTG and control groups for either R45 or R65 time points. At 85 seconds after the onset of reperfusion (R85) the NTG group showed a 70% reduction in VO_2 (mean VO_2 = 0.51 ± 0.09 ml O_2/100 cm^3min; P_0 = 29.6 ± 2.2 mmHg; n= 2) compared to the R85 control measurements (mean VO_2 = 1.68 ± 0.71 ml O_2/100 cm^3min; P_0 = 33.4 ± 2.9 mmHg; n= 5), which was found to be significant (p= 0.0098). There was no statistically significant difference for P_0 at R25 between control and NTG groups.

Figure 35, plot C, shows the VO_2 time course during reperfusion following 10 minutes of ischemia for control vs 0.1 mM NTG-treated tissue. There were insufficient measurements of the NTG group at both the R5 and R25 time points for a comparison against control due to hypoxic P_0's. At 45 seconds after the onset of reperfusion (R45) the NTG group showed a 55% reduction in VO_2 (mean VO_2 = 1.23 ± 0.22 ml O_2/100 cm^3min; P_0 = 25.6 ± 4.5 mmHg; n= 3) compared to the R45 control measurements (mean VO_2 = 2.75 ± 0.31 ml O_2/100 cm^3min; P_0 = 32.0±1.3 mmHg; n= 9), which was found to be significant (p= 0.022). There was no statistically significant difference for P_0 at R25 between control and NTG groups. Measurements of VO_2 for NTG-treated tissue at R65 and R85 were lower than control on average, but these strong trends were not significant (p= 0.09 and 0.23, respectively). There were also no significant differences in P_0 found between NTG and control groups for either R65 or R85 time points.

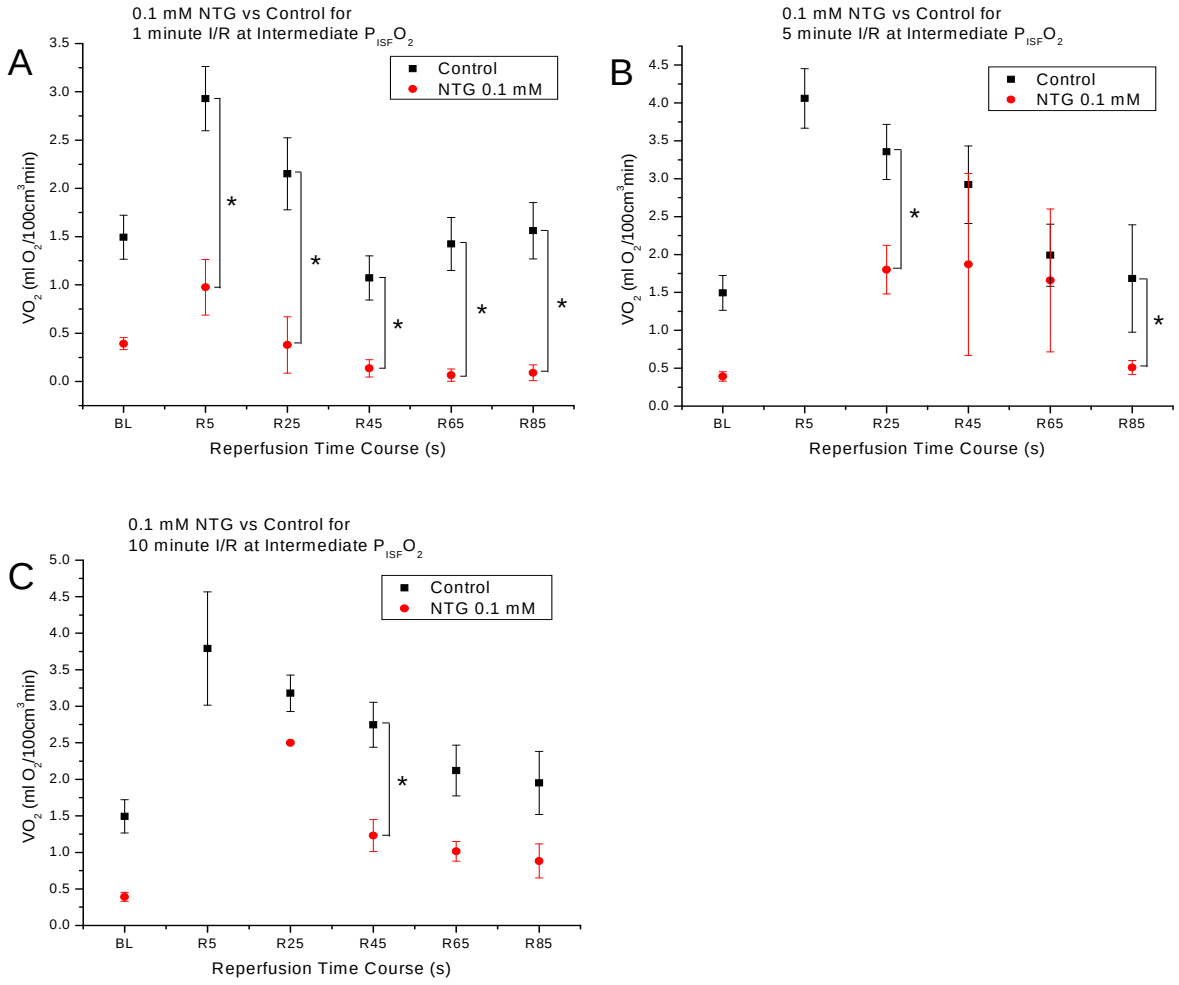

Figure 35: Control vs 0.1 NTG-treated tissue for 1-, 5- and 10-minute I/R protocols. The reperfusion time course of VO_2 was plotted against control following 1-, 5- and 10-minute ischemic durations for the intermediate $P_{ISF}O_2$ range. BL measurements were derived from the initial drop in $P_{ISF}O_2$ from the ODC at the onset of ischemia. NTG showed a tendency to reduce VO_2 across the board, but the 0.1 mM dose with measurements in the intermediate range of $P_{ISF}O_2$ contained the most complete data for statistical comparisons against control. * indicates a statistically significant difference between control and experimental measurements for that measurement time point (p= 0.05).

Influence of L-NAME on I/R

Following the assessment of VO_2 dynamics during rest and various durations of ischemia with reperfusion with pharmacologically elevated levels of NO from topically applied NTG, similar measurements were made for the condition of reduced NO concentration. L-NAME, a non-specific inhibitor of NOS, was topically applied to the exteriorized spinotrapezius muscle preparation and the changes in arteriolar diameter were observed as an indicator of the effective action of L-NAME to alter microvascular NO concentration. A pilot study was conducted to determine the best dosage of L-NAME that clearly influenced arteriolar diameter and VO_2, but did not cause such a degree of vasoconstriction that the reduced oxygen supply would severely depress $P_{ISF}O_2$. Following the selection of the appropriate dosage, L-NAME's influence on VO_2 during conditions of rest and reperfusion following 1-, 5- and 10-minute durations of ischemia was measured using the VO_2 Sampling Technique.

L-NAME Pilot

A single animal was used as a pilot to study the effects of L-NAME on arteriolar diameter and VO_2 over a range of doses. The intact, exteriorized spinotrapezius muscle was treated with 200 μl over two topically applied doses (PBS or L-NAME) of 100 μl each spaced two minutes apart. Following observation of selected arterioles for changes in diameter (see Figure 36), measurements of resting (see Figure 37) and reperfusion VO_2 dynamics were made via the 1-minute I/R protocol (see Figure 38). All measurements falling below the normoxic range were excluded from comparison for this pilot, since any oxygen-dependence of VO_2 would obscure the effects of L-NAME in this limited study.

Arterioles with diameters in the range of 40-100 μm showed a baseline average of 94 ± 4 μm (n=2). Following the application of 0.0015 mM L-NAME, the same arteriolar sites showed an immediate (<1min) reduction in diameter by ~10% (86 ± 4 μm). This level of vasoconstriction was maintained through the next dose (86 ± 4 μm) as 0.015 mM showed no further reduction in diameter. Application of 0.15 mM L-NAME further reduced arteriolar diameters by an additional 11% (76 ± 4 μm; 21% total reduction from BL). The final dose of 1.5 mM L-NAME did not result in a further decrease in vessel diameter at the measured sites. Additional measurements were made for both larger (>100 μm) and smaller (<40 μm) arterioles (data not shown) and they demonstrated similar profiles of constriction compared to the 40 to 100 μm range.

Resting skeletal muscle VO_2 was assessed over Control and L-NAME treatments for normoxic conditions. Three measurements were taken per dose as plotted in Figure 37. Control measurements were specific to this experiment. Application of 0.0015 mM L-NAME resulted in an elevation of VO_2 to 114% of baseline (Control, mean VO_2 = 1.91 ± 0.18 ml O_2/100 cm^3min; n=3; 0.0015 mM dose, mean VO_2 = 2.18 ± 0.16 ml O_2/100 cm^3min; n=3). The 0.015 mM dose of L-NAME reduced VO_2 by 35% (0.015 mM dose, mean VO_2 = 1.24 ± 0.08 ml O_2/100 cm^3min; n=3) compared to baseline. The 0.15 mM dose of L-NAME reduced VO_2 by 38% (0.15 mM dose, mean VO_2 = 1.17 ± 0.08 ml O_2/100 cm^3min; n=3) compared to baseline. The final and most potent dose of 1.5 mM L-NAME reduced VO_2 by 42% (mean VO_2 = 1.11 ± 0.12 ml O_2/100 cm^3min; n=3) compared to baseline. No statistical analyses were performed as this dose response study was not repeated in additional animals.

The VO_2 profile during reperfusion following 1 minute of ischemia was assessed for increasing doses of L-NAME from 0.0015 to 1.5 mM. VO_2 values that did not meet the

requirement of having a corresponding P_0 in the normoxic $P_{ISF}O_2$ range were excluded from comparisons (see Figure 38). The lack of control measurements for the reperfusion timecourse made for a difficult comparison to resting conditions, but over the range of L-NAME doses there was a trend towards a reduction in VO_2 for the various measured time points. The largest difference appeared to follow the application of the 0.015 mM dose with marginal reductions following the 0.15 and 1.5 mM concentrations. This trend was consistent and sustained with the result being a dose-dependent reduction in VO_2 by the topical application of L-NAME.

The arteriolar diameter, resting VO_2, and I/R response to the range of topically applied doses of L-NAME were compared in terms of measured effectiveness and a single dose was selected for more rigorous study with the I/R protocols. Arteriolar diameters appeared to show a maximum dilation at 0.15 mM L-NAME and, although 1.5 mM showed a slightly higher effect on VO_2, the 0.15 mM dose was deemed most practical in terms of effectiveness at the lowest concentration.

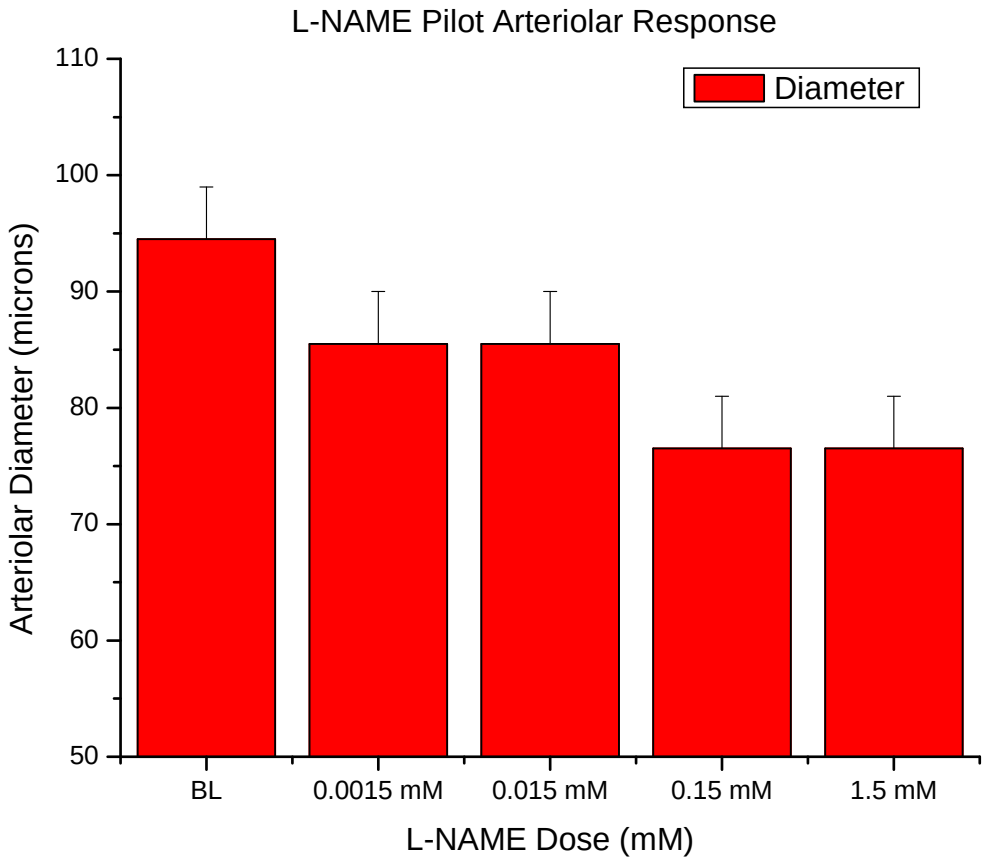

Figure 36: Arteriolar diameter dose-response to topically applied L-NAME. Arteriolar diameters were measured in response to increasing doses of L-NAME and are plotted here for the size range of 40-100 μm (n=2). This pilot study was performed in one animal.

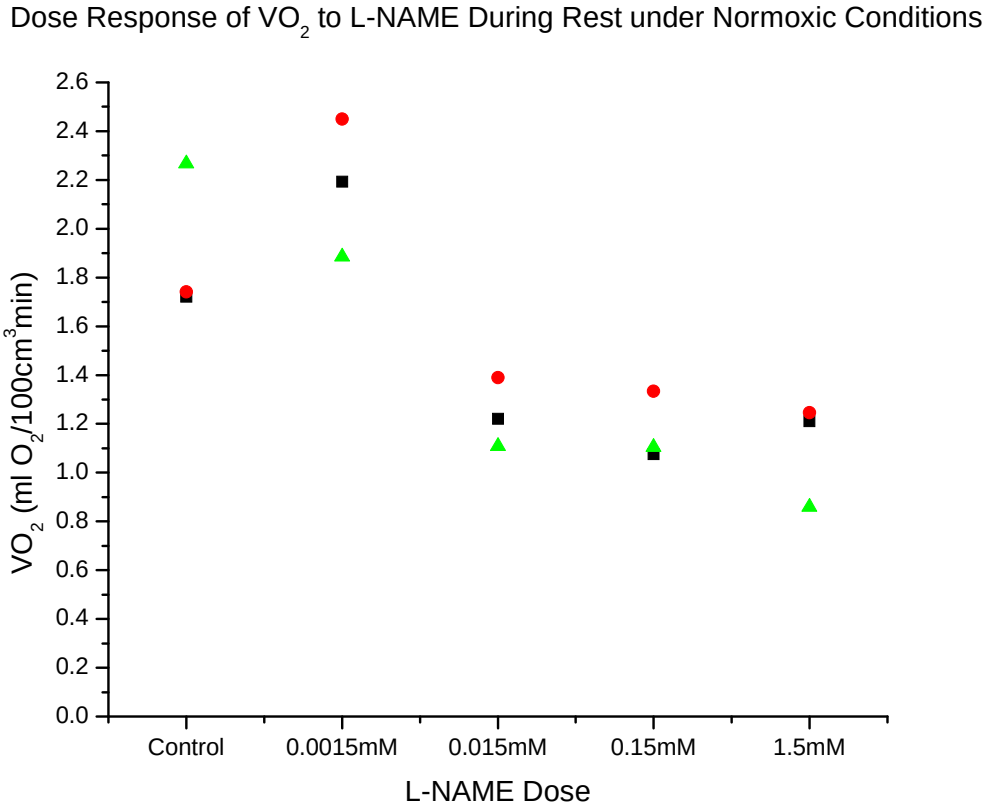

Figure 37: Dose-response of resting VO_2 to L-NAME. Measurements of resting VO_2 are reported here for control and L-NAME-treated tissue. The symbols each represent a single measurement in the order they were made with **Black** being first, **Red** being second, and **Green** being third for each dose of L-NAME. All measurements of resting VO_2 had corresponding P_0 values in the range of normoxia (>40 mmHg).

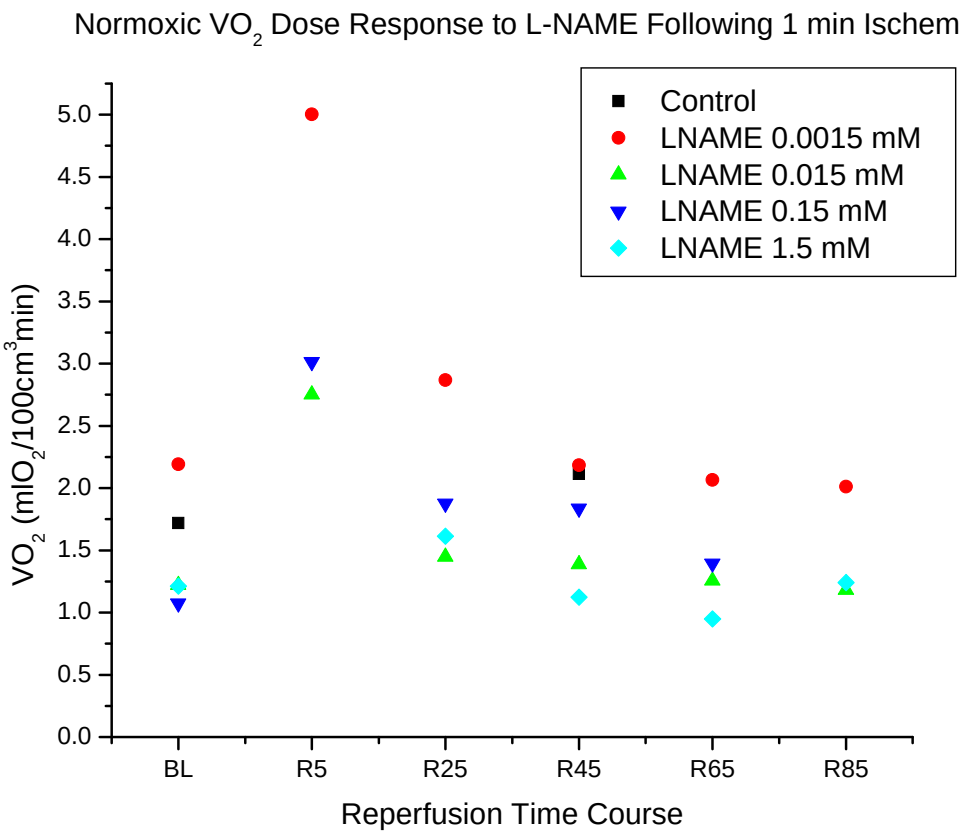

Figure 38: L-NAME pilot study for VO_2 dose response following 1 minute of ischemia. For each measurement, the relevant dose (PBS for Control) was applied and the tissue subjected to the 1-minute I/R protocol. During reperfusion, the VO_2 Sampling Technique was used to assess changes in tissue respiration. This pilot experiment was conducted in 1 animal and some control values that fell below the 40 mmHg criteria for inclusion in the normoxic range were excluded. The R85 value for the highest dose of L-NAME also failed to meet this P_0 requirement.

Nitric Oxide Synthase Inhibition by L-NAME

L-NAME's Influence on Arteriolar Diameter

L-NAME's inhibition of NO production by NOS was confirmed by the vascular consequences of reducing overall [NO]. 11 arterioles with an initial mean diameter of 66 ± 4 μm were measured over 6 animals for their responsiveness to 0.15 mM L-NAME. Following the topical application of L-NAME to the spinotrapezius muscle, vessel diameters for the same sites were measured within 2 minutes of the dosing procedure completion and revealed a 30% reduction in size (treated mean= 46 ± 7 μm). This vasoconstrictor response was significant from baseline values ($p=0.017$) and indicative of a reduction in NO production by NOS (see Figure 39).

L-NAME's Influence on Resting VO_2

Resting VO_2 following treatment with 0.15 mM L-NAME was measured and compared to Control measurements in the range of $P_{ISF}O_2$ for which VO_2 is PO_2-independent. Resting VO_2 data were calculated from the initial drop in $P_{ISF}O_2$ recorded during the onset of ischemia for the 1-, 5- and 10-minute I/R protocols. A total of 35 normoxic measurements conducted on 6 animals revealed that 0.15 mM L-NAME-treated tissue showed a 14% reduction in resting VO_2 (1.69 ± 0.14 ml O_2/100 cm^3min; P_0 = 71.2 ± 2.6 mmHg; n=35) from Control (1.97 ± 0.1 ml O_2/100 cm^3min; P_0 = 59.8 ± 1.5 mmHg), but this trend was not found to be significant ($p= 0.15$; see Figure 40). P_0 was significantly higher for L-NAME-treated tissue ($p<0.0001$) for the assessment of resting VO_2, but all measurements remained within the normoxic range.

L-NAME's Influence on Hypoxic Reperfusion

For an assessment of the suppression of NO production during hypoxia, the R5 measurements following 5 and 10 minutes of ischemia were chosen (see Figure 41). These time points contained a sufficiently large number of values in the hypoxic range, by the nature of the slow recovery of $P_{ISF}O_2$ following 5 and 10 minutes of ischemia, for both Control and L-NAME-treated tissues for statistical comparison. The R5 measurement of L-NAME-treated tissue for the 5-minute I/R protocol revealed an increase in VO_2 to 155% (mean VO_2 = 1.13 ± 0.25 ml O_2/100 cm^3min; P_0 = 13.4±1.0 mmHg, n=10) of Control (mean VO_2 = 0.73 ± 0.10 ml O_2/100 cm^3min; P_0 = 10.2 ± 0.6 mmHg, n= 26), but this strong trend was not found to be significant (p= 0.11). P_0 was slightly, but significantly, higher than the Control value for L-NAME-treated tissue (p= 0.011) and all measurements were confined to the hypoxic range. The R5 measurement of L-NAME-treated tissue for the 10-minute I/R protocol demonstrated an increase in VO_2 to 182% (mean VO_2 = 1.59 ± 0.30 ml O_2/100 cm^3min; P_0 = 15.5±1.0 mmHg, n=12) of Control (mean VO_2 = 0.83 ± 0.10 mlO_2/100 cm^3min; P_0 = 10.2 ± 0.5 mmHg, n= 30), which was significant (p= 0.015). P_0 was slightly, but significantly, higher than Control for L-NAME-treated tissue (p<0.0001) and all measurements were confined to the hypoxic range.

L-NAME's Influence during Normoxic Reperfusion

The suppression of NO during the reperfusion phases following 1, 5, and 10 minute ischemic durations was evaluated for changes in VO_2 from Control for the R5-R85 time points. Measurements were exclusive for normoxic P_0's.

Following 1 minute of ischemia (see Figure 42, plot A), measurements of 0.15 mM L-NAME-treated tissues at R5 showed a strong trend towards a reduction in VO_2 (1.93 ± 0.40 ml O_2/100 cm^3min; P_0 = 49.2 ± 1.9; n= 7) compared to Control R5 (2.93 ± 0.30 ml O_2/100 cm^3min;

P_0 = 54.8 ± 2.3 mmHg; n= 11), which was not statistically significant (p= 0.07). P_0 values did not show a statistically significant difference either (p= 0.10). Mean VO_2 values for measurements at R25 through R85 continued to appear depressed, but none were found to be statistically different from their Control counterparts. P_0 values were likewise statistically the same for both Control and L-NAME-treated tissue.

Following 5 minutes of ischemia (see Figure 42, plot B), measurements of 0.15 mM L-NAME-treated tissues at R5 were not possible for the normoxic range due to a slower timecourse of $P_{ISF}O_2$ recovery. R25 measurements for Control and L-NAME-treated tissues were not significantly different from each other in terms of both VO_2 and P_0. R45 for L-NAME showed a trend towards a reduction in VO_2 (2.39 ± 0.30 ml O_2/100 cm^3min; P_0 = 58.3 ± 4.8 mmHg; n= 13) compared to Control R45 (3.23 ± 0.30 ml O_2/100 cm^3min; P_0 = 66.4±25.7 mmHg; n= 9), which was not statistically significant (p= 0.083). P_0 values were also statistically the same (p= 0.29). Mean VO_2 values for measurements at R65 and R85 continued to appear depressed, but none were found to be statistically different from their Control counterparts. P_0 values were likewise statistically the same for both Control and L-NAME-treated tissue.

Following 10 minutes of ischemia (see Figure 42, plot C), measurements of 0.15 mM L-NAME-treated tissues at R5 were not possible for the normoxic range due to a slower timecourse of $P_{ISF}O_2$ recovery. Mean VO_2 values for measurements at R25 through R85 consistently appeared depressed, but none were found to be statistically different from their Control counterparts or to show any strong trends. P_0 values were likewise statistically the same for both Control and L-NAME-treated tissue.

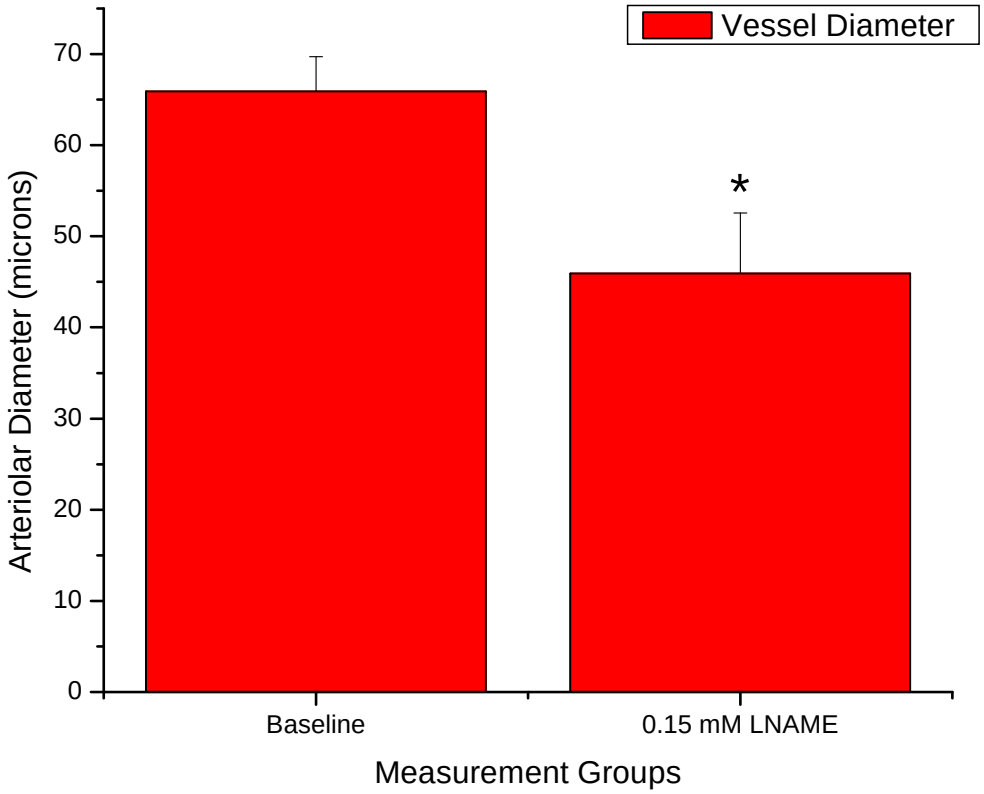

Figure 39: Influence of L-NAME on arteriolar diameter. 0.15 mM L-NAME was topically applied to the tissue and the resultant change in arteriolar diameter was measured during transillumination observation of the microvasculature. The application of L-NAME produced a significant vasoconstriction that was presumably associated with a decrease in NO production by NOS. * indicates a significant difference from baseline ($p<0.05$).

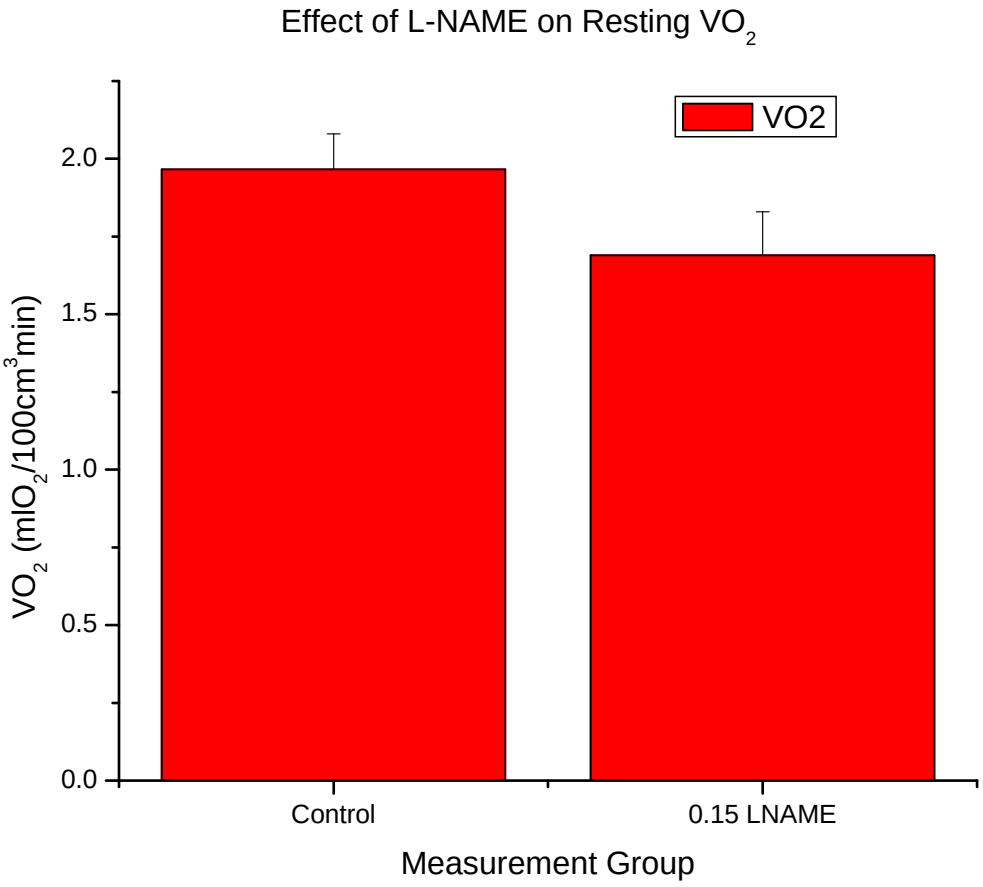

Figure 40: L-NAME vs. Control for resting skeletal muscle VO_2. Resting VO_2 measurements for L-NAME-treated muscles were taken from the initial fall in $P_{ISF}O_2$ during the onset of ischemia over the three I/R protocols and compared to Control. VO_2 showed a slightly negative trend when exposed to L-NAME, but this difference was not significantly different ($p=0.15$). Average P_0 was significantly higher for measurements in L-NAME-treated tissue ($p<0.0001$) over Control, but measurements from both groups remained confined to the normoxic range which exhibits a $P_{ISF}O_2$-independent VO_2.

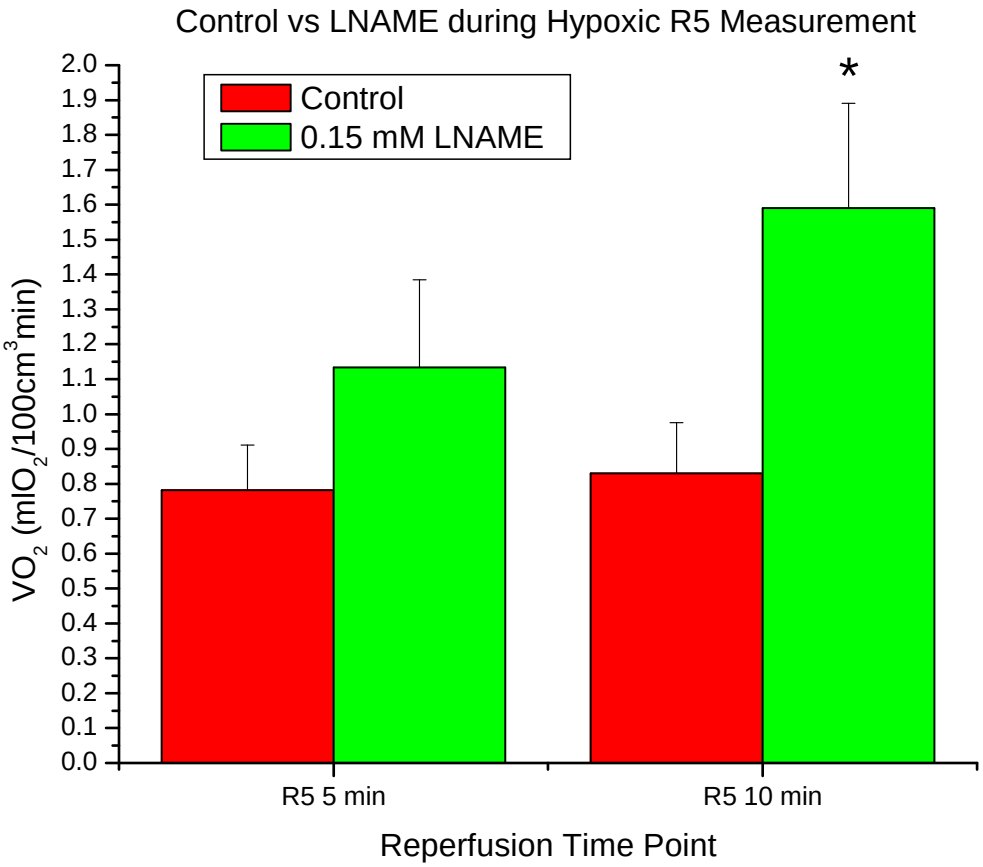

Figure 41: VO_2 for L-NAME vs Control during hypoxia. The R5 time point following 5-and 10-minute durations of ischemia provided evidence of how L-NAME alters VO_2 in comparison with control. For both L-NAME treated groups, there was an observable rise in VO_2 over control with the 10 minute duration showing significance (p= 0.015). * indicates a significant difference from the associated control measurement.

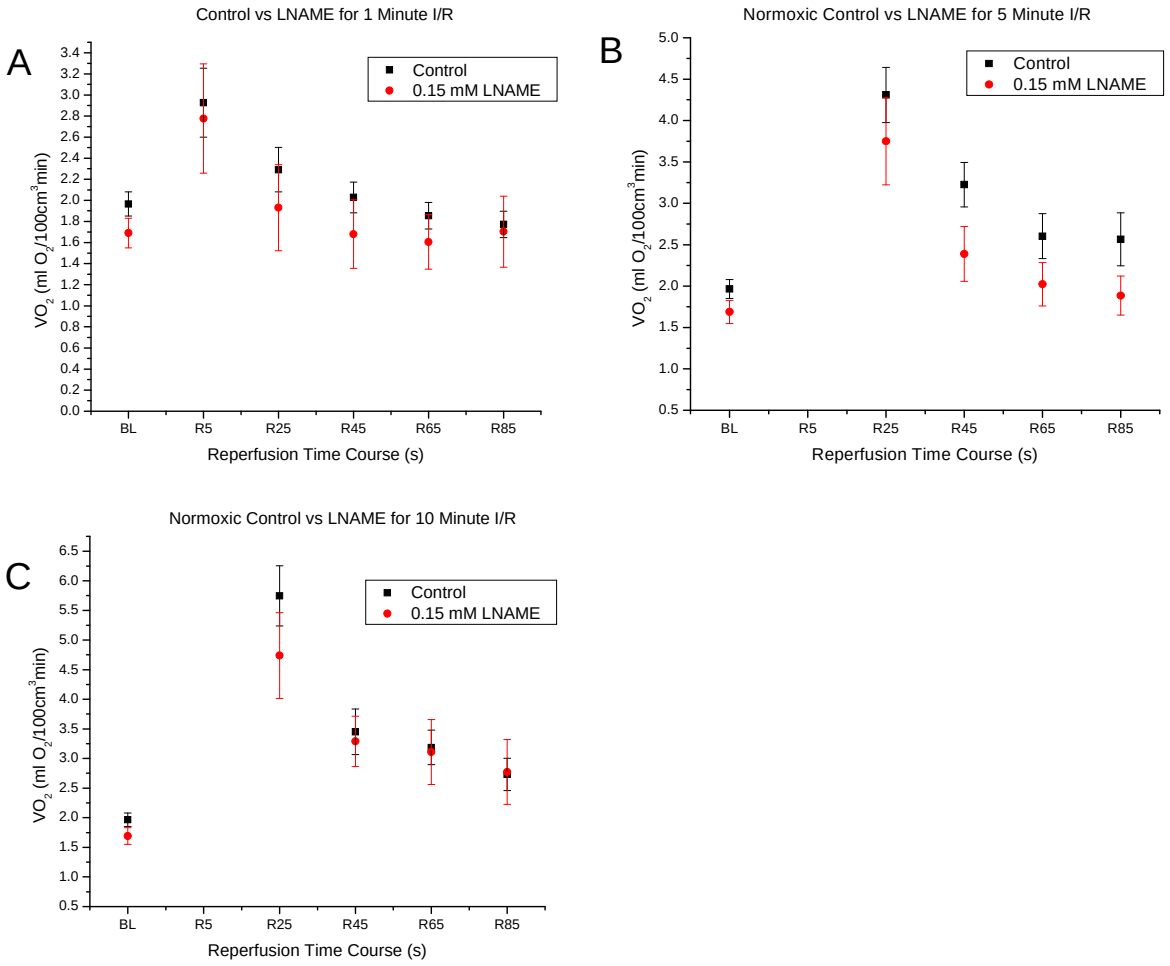

Figure 42: VO_2 for Control vs. LNAME during reperfusion. The reperfusion time course of VO_2 was assessed with the VO_2 Sampling Technique following 1-, 5- and 10-minute durations of ischemia in 0.15 mM L-NAME-treated tissue compared to Control. No significant differences were observed for any of the measured time points among the various reperfusion periods shown above, however strong trends showing a depression in VO_2 for L-NAME-treated tissue vs. control exist where a clear separation occurs between the means. P_0 values were not found to be significantly different between Control and L-NAME groups at similar time points and were all within the normoxic range.

DISCUSSION

Summary of Study

A novel technique for multiple and quasi-continuous measurements of VO_2 dynamics in thin tissues was developed and employed in the rat spinotrapezius muscle under various metabolic conditions. The VO_2 measurement technique was adapted from a previously described method that utilized externally transduced pressure to rapidly arrest blood flow while concurrently observing the resultant drop in interstitial fluid oxygen tension ($P_{ISF}O_2$) with Phosphorescence Quenching Microscopy (PQM) (Golub et al, in revision). Originally designed to measure the entire oxygen disappearance curve (ODC) during flow-arrest produced by rapid compression of a transparent, pressurized air-bag, this system was upgraded by the addition of an Automatic Dual Pressure System providing it with the capabilities necessary for the continuous VO_2 Sampling Technique. This control circuit rapidly (<1 s) and repeatedly toggled the air-bag's pressurization between high and low pressures, enabling brief periods of compression to assess VO_2, followed by a recovery period to restore $P_{ISF}O_2$ to near its baseline value. In its current configuration, the cycling profile for the VO_2 Sampling Technique was determined to be ideal at 5 seconds of high pressure followed by 15 seconds of recovery in terms of a sufficient recovery of $P_{ISF}O_2$ to baseline, no cumulative effect on serial VO_2 measurements, and a maximal number of VO_2 measurements per minute (3/min). This technique was further assessed following 1 minute durations of complete flow arrest (ischemia)—produced by a sustained air-bag pressurization—for its influence on the recovery of $P_{ISF}O_2$ during reperfusion. There was a slight indication of hyperemia for recovery profiles exposed to the VO_2 Sampling Technique, but this was neither significant nor should have altered VO_2. The upper compression pressure was

also found to be optimal from 120-140 mmHg, with minimal perturbation of the tissue for the 5 s x 15 s compression/recovery cycle.

Assessment of the linear fall in $P_{ISF}O_2$ was found to have 3 components: tissue VO_2, consumption by PQM (characterized by the constant K; see Eq. 9), and refill by passive O_2 diffusion into the excitation region (characterized by the constant R; see Eq. 9). Using an in vitro analysis, both K and R values were determined and a correction factor was developed to directly relate the initial part of the ODC to VO_2 with minimal noise. This correction was universally applicable to PQM measurements made with the R2 probe under the conditions of topical application described in the Materials and Methods section of this dissertation.

Resting skeletal muscle VO_2 was assessed and plotted against $P_{ISF}O_2$ to determine over what range cytochrome c oxidase became a limiting factor for respiration as measured through PQM's assessment of $P_{ISF}O_2$. VO_2 data were then separated into three categories: Hypoxic, Intermediate, and Normoxic, according to the $P_{ISF}O_2$ immediately prior to bag compression and flow arrest (P_0). This allowed data within those groups to be compared on equal terms. The resting state VO_2 of the rat spinotrapezius muscle was then pharmacologically altered with cyanide, nitroglycerin, and L-NAME and compared to baseline values in the same preparations.

The VO_2 time course for 5 through 85 seconds of reperfusion following ischemic durations of 1, 5 and 10 minutes was assessed with the VO_2 Sampling Technique and measurements were similarly compared within the categories of Hypoxia, Intermediate, and Normoxia. Ischemia clearly produced a rise in VO_2 over baseline during early reperfusion that was related to the duration of the ischemic period. This effect was attenuated, but not abolished, with the treatment of cyanide, which helped attribute at least some of the ischemia-induced elevation to cytochrome c oxidase activity. Treatment with the nitric oxide donor nitroglycerin

produced a similar reduction in VO_2 and a corresponding enhancement in $P_{ISF}O_2$. L-NAME, an inhibitor of nitric oxide synthase (NOS), functioned to slightly reduce tissue PO_2 through a reduction in vascular oxygen delivery by vasoconstriction of arterioles, but lower [NO] did not appear to stimulate tissue respiration in the normoxic $P_{ISF}O_2$ range as might be expected. It did, however, produce a significant rise in VO_2 during hypoxia, which may indicate that NO has a greater influence on respiration during hypoxia.

Determination of Compression Duration

The development of rapid blood flow arrest, along with the extrusion of red blood cells (RBCs), to minimize the confounding influence of the oxygen carrier hemoglobin on the ODC, required an externally applied force to be directed onto the measurement area. A transparent Krehalon bag was designed and fitted to the 20X microscope objective of the PQM setup (see Figure 10) and regulated by an Automatic Dual Pressure System for rapid switching between high and low pressures (see Figure 11). The necessary pressure was initially set by the need to overcome the rat systemic pressure pressure (based on existing measurements of MAP, which indicated that the air-bag's upper pressure setting should be 140 mmHg. Once applied to the tissue, the immediate effects of compression (i.e., rapid flow-arrest in <1 s and RBC extrusion) were evidenced by direct observation of the microcirculation through transillumination and by use of PQM (see Figure 16 for development of ODC upon compression). The result of flow-arrest and RBC extrusion on interstitial fluid PO_2 was recorded with PQM as a linear fall in $P_{ISF}O_2$ until reaching the level of hypoxia, where the ODC began to curve towards the "zero" $P_{ISF}O_2$ asymptote. At a 10 Hz excitation frequency, 5 seconds of compression covered most of

the linear range of the ODC (P_0= ~60 mmHg) and provided 50 data points, which were more than sufficient to produce an accurate linear fit of $-dPO_2/dt$ for eventual conversion to VO_2.

The 5-second duration of compression for this new technique was a conservative choice to allow for an adequate amount of time to obtain an accurate estimate of VO_2 from the initial decline in PO_2. Shorter durations of compression down to ~2 seconds are likely possible in future studies as 20 points would be sufficient to obtain an accurate estimate of the linear trend of the early ODC with good signal-to-noise ratio.

Determination of Compression Interval for the Rate of VO_2 Sampling

Any measurement by its very nature is invasive and, as such, one measurement can often influence the results of a subsequent one. As the VO_2 Sampling Technique requires repeated measurements that necessitate brief reductions in tissue oxygenation at the same site, an assessment of the amount of time between each compression needed for the recovery of $P_{ISF}O_2$ back to baseline was needed to determine the optimal sampling rate that did not bring about appreciable and cumulative changes in both $P_{ISF}O_2$ and VO_2.

The compression/recovery cycle of 5 seconds high pressure (120-140 mmHg) and 15 seconds of low pressure (5 mmHg) was determined for the resting state of the exteriorized spinotrapezius muscle to allow for the complete recovery of $P_{ISF}O_2$ back to baseline. No cumulative impact on VO_2 over repeated measurements with an excellent sampling rate of 3 per minute (see Figure 16) was also demonstrated. A reduction of this time course, in future studies, may allow for an even better temporal resolution when coupled with lower compression duration. Based on overall experience with the technique, with a 2-second compression, it may be possible to reduce the recovery period to 8 seconds, thereby achieving twice as many samples

of VO_2 per minute in the normoxic range of P_0's. Additionally, a shorter recovery time, as shown by the 5 s x 5 s measurements (Figure 16, plot A), would allow for quasi-continuous VO_2 measurements in the hypoxic or intermediate PO_2 ranges without additional interventions to artificially lower $P_{ISF}O_2$.

Influence of the 5x15 VO_2 Sampling Profile on Reperfusion

The 5 s x 15 s compression/recovery cycle appeared sufficiently suited to quasi-continuous measurements of VO_2 during resting conditions of the exteriorized rat spinotrapezius muscle, but whether its utility extended to situations of reperfusion following ischemia was not clear. Measurements of $P_{ISF}O_2$ were thus taken during the early reperfusion phase following 1-minute durations of ischemia with and without (Control) VO_2 sampling. The results were averaged and normalized to their initial baseline measurements. The $P_{ISF}O_2$ recovery during reperfusion was then compared between Control and VO_2 Sampling Technique groups (see Figure 22).

Following reperfusion, the Control group (no VO_2 sampling) showed a rapid rise in $P_{ISF}O_2$ that reached a plateau by 40 seconds post reperfusion onset. This plateau was higher than the initial baseline $P_{ISF}O_2$ and likely a demonstration of the reactive hyperemic response to the prolonged arrest in blood flow. The group with intermittent VO_2 sampling showed a similar profile to Control with a slightly higher (5%) hyperemic response over Control. This overshoot gradually relaxed back to Control levels by 85 seconds post-reperfusion onset. It was likely the case that multiple 5-second compressions induced a slightly higher magnitude of reactive hyperemia, but this difference had no bearing on normoxic measurements of VO_2 since VO_2 was insensitive to PO_2 in the range of the overshoot.

Air Bag Pressurization on $P_{ISF}O_2$ Recovery and $-dPO_2/dt$

Early measurements with the air bag used an upper compression pressure of 140 mmHg to arrest blood flow for the assessment of the ODC under various conditions with the understanding that this pressure would be sufficient to overcome the arterial systolic pressure. To minimize the impact of each compression, and thereby maximize the VO_2 Sampling Technique's relevance over time, a range of pressures from 40 to 140 mmHg was tested using the 5x15 sampling profile for the recovery of $P_{ISF}O_2$ (see Figure 22) and the rate of oxygen disappearance during compression ($-dPO_2/dt$; see Figure 23).

No significant difference was found for the recovery of $P_{ISF}O_2$ over the range of compression pressures from 40 to 140 mmHg. It was expected that, at some point, recovery would either show a pronounced hyperemic response or begin to show protracted recovery times if compression pressure brought about vascular damage. Neither situation occurred, though there did appear to be a statistically insignificant elevation in $P_{ISF}O_2$ during recovery from about 70 mmHg of pressure. Likely, the detrimental effects of compression would have occurred at higher pressures, but they were not tested as anything over 140 mmHg greatly increased the probability of air bag rupture.

Stepwise increases in compression pressure of 10 mmHg, starting with 40 mmHg and ending with 140 mmHg (5 mmHg was considered low pressure for the purpose of extrusion of any surface fluid layer that might confound PQM measurements), showed the corresponding rise in $-dPO_2/dt$ that one might expect as flow-arrest became more and more complete until reaching a plateau. Compressions from 80 mmHg to 140 mmHg did not yield a significant change in $-dPO_2/dt$ as shown in Figure 23, which indicated that complete flow arrest had been achieved.

Measurements at 90 and 100 mmHg appeared to be slightly elevated over measurements made from 110 to 140 mmHg, but this difference was not statistically significant (see Figure 22).

Since higher pressures did not appear to have any adverse consequences on either VO_2 or the recovery of $P_{ISF}O_2$, and the VO_2 sampling interval was determined using 140 mmHg, the decision to use a range of compression pressures from 120 to 140 was deemed appropriate. This allowed for a justifiable adjustment in compression pressure to accommodate a range of tissue sizes and sensitivities. The effectiveness of flow arrest was always visualized prior to measurement and 120 to 140 mmHg had a consistently high success rate over the course of experimentation.

Another point of interest was the relevance of the $-dPO_2/dt$ vs pressure profile on the microvasculature below complete flow arrest. As pressure rose, perfusion declined approximately linearly. If these pressures had been continued beyond 5 seconds, an eventual point where the reduction in perfusion could no longer keep up with oxygen demand would be reached—inevitably resulting in hypoxia. This sort of situation has been found to occur in Compartment Syndrome and a study looking into the pressure needed to exceed this "tipping point" in the development of hypoxia using the present approach would appear to be warranted.

Oxygen Consumption by the Method

PQM's determination of the oxygen tension of a particular measurement region relies on the ability of oxygen to quench the phosphorescence of an excited phosphorescent probe (R2 in this case). In doing so, there is a certain probability that oxygen will quench this phosphorescence signal by its own conversion to singlet oxygen resulting in a PQM-induced consumption of oxygen. This effect has been previously reported (Golub and Pittman, 2008),

but quantification is instrument-specific. To observe the rate of oxygen consumption exclusively by PQM, an in vitro alginate gel (0.5 mm thick) was loaded with the R2 probe bound to 5% human serum albumin and treated similarly to an intact, perfused spinotrapezius muscle preparation. It was thermo-equilibrated to ~38 ^{o}C on the thermostatic animal platform's heated pedestal and wrapped in a Krehalon sheet to isolate it from contamination by atmospheric oxygen. Measurements were then conducted with PQM for the same excitation intensity and region diameter as performed in the in vivo setting with an exteriorized, perfused spinotrapezius muscle. In this case, however, there were no sources of oxygen consumption in addition to that of the triplet state interaction and conversion of oxygen to singlet oxygen by PQM. Furthermore, similar to the situation of flow-arrest, the only oxygen inflow came from that of refill at the periphery of the excitation area by passive oxygen diffusion as an oxygen gradient was developed over successive flashes. These two conditions provided data that could be analyzed to yield the coefficient of PQM's oxygen consumption (K) and the coefficient of oxygen refill (R), respectively.

K was found to be $7.16x10^{-4}\pm1.87x10^{-4}$ per flash (n=10), which can be converted to approximately 5.1% of resting skeletal muscle oxygen consumption. This value corresponds to the measured tissue concentration of the R2 albumin-bound probe of 19.5±2.3 μg/ml (prepared and measured at 20 μg/ml) for a 300 μm diameter octagon with an excitation energy of 5.366±0.0078 μW per flash. This 5% consumption by the method was considered tolerable in terms of the invasiveness of the technique and used to correct all VO_2 values derived from the $-dPO_2/dt$ data. Further studies using physical quenchers reactive oxygen species (ROS) formation to reduce the probability of singlet oxygen formation have resulted in an appreciable decrease in oxygen consumption by PQM (data not shown). These studies were conducted for much higher

concentrations of the phosphorescent probe (approximately 5-fold), indicating a utility for the simple assessment of the effectiveness of anti-oxidants using PQM. Additionally, no difference in the reported K value was seen when this experiment was repeated in 100 μm thick sealed microslides (see Table 1), which lends credence to the relevance of the gel measurements and demonstrates the consistency of R2's behavior in different media and settings.

The coefficient of refill (R) was measured by the magnitude of the offset from zero where the ODC approached its asymptote. This offset was attributed to a balance between oxygen consumption by the method and diffusive refill. As indicated in Table 1, R was found to be small in the cases of gel and microslide measurements. Additionally, as shown by Figure 15, the difference in $P_{ISF}O_2$ between inside the excitation area and outside—the driving force for refill—is slow to progress and only reaches about 1.5 mmHg after 50 flashes under resting conditions. This calculation was based on existing $-dPO_2/dt$ measurements and extrapolated to outside the excitation area (which could not be measured directly) by factoring out PQM's oxygen consumption. As both the difference in $P_{ISF}O_2$ between inside and outside the excitation area and the measured R were both small (<0.01% of total VO_2), even after 50 flashes, it was determined that Equation 5 could be simplified, by removal of the refill component, to Equation 8 for the conversion of $-dPO_2/dt$ to VO_2. Smaller excitation areas would have a greater surface to volume ratio and thus have larger refill components. Eventually a tipping point would be reached with smaller excitation regions where refill became relevant and would need to be accounted for in future studies.

In Vivo VO_2 of the Rat Spinotrapezius Muscle at Rest

Application of the quasi-continuous VO_2 Sampling Technique during resting conditions in the intact, exteriorized rat spinotrapezius muscle produced an average VO_2 of 1.97 ± 0.1 ml O_2/100 cm^3min for measurements in the high or "normoxic" range of $P_{ISF}O_2$. As a comparison, measurements using Fick's Principle have produced mean values for VO_2 ranging from 0.054 to 0.92 ml O_2/100 g min (Edmunds et al, 2001; Hoy et al, 2009), which are somewhat lower than those values produced by the VO_2 Sampling Technique. A possible explanation for this discrepancy involves the range of $P_{ISF}O_2$ in which the measurements were made. Employing the VO_2 Sampling Technique, it soon became apparent that not all measurements of P_0 were equal as sites varied in terms of perfusion and functional capillary density. It was realized that as P_0 dropped below 40 mmHg, VO_2 concomitantly decreased as well, indicating an approximate region of oxygen dependence for VO_2 using this technique. Measurements of VO_2 were plotted against P_0 and then divided into three categories for comparison: Normoxic (P_0>40 mmHg), Intermediate (22<P_0<40 mmHg), and Hypoxic (P_0<22 mmHg) as shown in Figure 24. VO_2 was clearly depressed for situations where $P_{ISF}O_2$ dropped below 22 mmHg. Since the VO_2 Sampling Technique makes direct assessments of the interstitial PO_2 that bathes the muscle fibers, it is more localized and tissue-specific than measurements made with the Fick Principle. This means that physiologically hypoxic regions can be separated from normoxic regions and are not subject to mixing, which would tend to reduce overall VO_2 values. Since these regions are considered physiological in terms of the acknowledgement that oxygen gradients exist in tissue (Popel et al, 1989, Bertuglia and Guisti, 2005), an assessment of VO_2 using Fick's Principle is accurate in determining the physiological oxygen consumption of a whole organ at rest. But the VO_2 Sampling Technique goes a step further to break down those respiratory rates into tissue conditions of normoxia through hypoxia.

Measurements of resting skeletal muscle VO_2 have also been made under conditions of hyperoxia in an attempt to eliminate the confounding influence of hypoxic regions on the measurement. Values consistent with the high-end values found with Fick's Principle have been reported (Honig et al. 1971), and while this may invalidate the idea of hypoxic regions driving down whole organ VO_2 measurements, it is possible that hyperoxia also depresses VO_2. As shown by Figure 2, ROS production is enhanced under hypoxic and hyperoxic conditions (Clanton 2007). As ROS is destructive to the mitochondrial electron transport chain, there is a possibility that hyperoxic conditions could result in a significant reduction in VO_2. Further study would be needed to confirm this by exposing skeletal muscle tissue to conditions of high oxygenation prior to usage of the VO_2 Sampling Technique. In the meantime, the measured normoxic value of 1.97 ml O_2/100 cm^3min was found to be reasonable and highly reproducible over many different animals and experiments and thus provided an excellent comparison to VO_2 values in altered metabolic states.

As a note to the observed drop in VO_2 from the normoxic to the hypoxic range of $P_{ISF}O_2$, a "critical point", or oxygen tension at which VO_2 becomes diffusion-limited at the mitochondrial level, has been previously reported. For isolated mitochondria, critical PO_2 was determined to be <1 mmHg (Wilson et al. 1979) and for measurements of the resting rat spinotrapezius preparation, a critical $P_{ISF}O_2$ of 2.4 – 2.9 mmHg was quantified (Richmond KN, et al. 1999). Observations of VO_2 with the VO_2 Sampling Technique confirmed that there was a dependence of VO_2 on $P_{ISF}O_2$, but the point of dependence appeared to occur somewhere between 22 and 40 mmHg. This order of magnitude difference may be realistic in terms of the drop in PO_2 over the extra- to intracellular oxygen gradient and down to the level of cytochrome c oxidase, but these mitochondrial PO_2 values have yet to be confidently assessed in vivo for rat

skeletal muscle. However, the measurement of an interstitial critical PO_2 of 2.4 to 2.9 mmHg did appear different from the results using the VO_2 Sampling Technique. It is possible that part of this discrepancy is due to the methodology used to arrest flow, which does not allow for RBC extrusion from the measurement site, and limited sampling points along the ODC, which was due to a sampling rate of 0.5 Hz. Another factor may be that they observed single muscle fibers, whereas the measurement region in this study was 300 μm in diameter and thus covered multiple fibers. Thus, over the course of many measurements, small pockets of hypoxia may have been obscured by an otherwise high $P_{ISF}O_2$ leading to a depressed reading of VO_2. Additionally, our study does not define a "critical $P_{ISF}O_2$" but rather a range where an observed transition from $P_{ISF}O_2$-independence to dependence of VO_2 comes into play. Further analysis of the full VO_2 vs $P_{ISF}O_2$ curve would be required for a more precise comparison to what has been defined in the literature as the "critical PO_2." For the purposes of this study, VO_2 was related to $P_{ISF}O_2$ and separated into the categories of Normoxia, Intermediate, and Hypoxia to allow for the relevant comparison of measurements.

VO_2 Dynamics of Early Reperfusion Following 1-, 5- and 10-Minute Durations of Ischemia

Presented here are the first in vivo measurements of VO_2 dynamics during early reperfusion following brief periods of ischemia. Durations of 1, 5, and 10 minutes were used to help assess the consumption of oxygen during periods of ischemia reported to be associated with preconditioning in skeletal muscle as an indicator of mitochondrial function. VO_2 was assessed at 5, 25, 45, 65 and 85 seconds after onset of reperfusion for all durations of ischemia, and VO_2 comparisons were made against baseline (pre-ischemic) measurements made during resting conditions within the relevant ranges of P_0.

After 1 minute of ischemia, VO_2 had risen to 149% of baseline at the 5-second (R5) time point after reperfusion had begun for normoxic conditions. This initial elevation in VO_2 returned to baseline by the R45 time point and remained there. VO_2 measurements taken in the intermediate range of P_0 values showed a similar elevation of 197% of baseline at the R5 time point that returned to baseline by R45 and persisted there for the remaining measurements. The hypoxic range of P_0 values showed no influence of 1-minute ischemia on VO_2 during reperfusion as compared to baseline (see Figure 25).

Following 5 minutes of ischemia, VO_2 measurements first met the conditions of normoxia at time point R25 and showed an elevation of 218% of baseline. By R45, VO_2 remained high, but was now 163% of baseline and then returned to near baseline by R65. Measurement at the R5 time point was possible in the intermediate range and showed a substantial elevation in VO_2 by 262% of baseline. Then, similar to the normoxic measurements, VO_2 fell progressively over the next few measurements (225% at R25, 196% at R45) until approximately returning to baseline by R65. As with the 1-minute I/R, the hypoxic range of VO_2 measurements showed no change over the reperfusion time course when compared to baseline (see Figure 26).

Following 10 minutes of ischemia, VO_2 measurements first met the conditions of normoxia at time point R25—similar to the 5-minute duration—and were profoundly elevated to 295% of baseline. Subsequent measurement points showed a progressive reduction to 175% for R45 and 162% for R65 with no statistical difference from baseline at R85. For the intermediate range of P_0 values, VO_2 was found to be 254% of baseline at R5 and showed a progressive return to baseline by R65 (213% at R25 and 185% at R45). Hypoxic P_0 measurements continued to

show no change during reperfusion as a result of the 10-minute ischemic duration when compared to baseline (see Figure 27).

Measurements of VO_2 made with P_0 values < 22 mmHg were grouped together under the category of Hypoxia. Over the reperfusion timecourses following 1-, 5- and 10-minute durations of ischemia, there was no apparent change in these VO_2 values. This was consistent with the observation that VO_2 is diffusion-limited by the $P_{ISF}O_2$ within this range. Realistically, P_0 values had a lower limit of ~7-9 mmHg due to limitations of the R2 probe to accurately report $P_{ISF}O_2$ values below 5 mmHg, so these measurements did not include extreme lows in VO_2. It is thus safe to say that for the P_0 range of 9 to 22 mmHg, a value of 0.59 ± 0.1 ml O_2/100 cm^3min (P_0 = 13.5 ± 0.4 mmHg) is a physiological V_{max} (VO_2 cannot increase regardless of demand)for these conditions measured with the VO_2 Sampling Technique.

The intermediate range of P_0 values produced similar increases to the normoxic range in VO_2 during reperfusion following 1-and 5-minute durations of ischemia, but exhibited no further elevation following 10 minutes of ischemia. This could be related to the overlap of PO_2-dependent and independent VO_2 regions within the $P_{ISF}O_2$ range of 22 to 40 mmHg. The benefit of this range appeared in measurements of the R5 time point following 5 minutes of ischemia. The recovery of $P_{ISF}O_2$ was protracted following the longer periods of ischemia due to a substantial elevation in VO_2, and thus failed to rise above 40 mmHg by 5 seconds after the onset of reperfusion. P_0 values did fall within the intermediate range, however, and showed an increase in VO_2 following 5 minutes of ischemia over 1 minute of ischemia for the R5 time point. There was no apparent rise in VO_2 for time point R5 following 10 minutes of ischemia when compared to 5 minutes of ischemia, but this could be due to a small number of observations.

The normoxic range of P_0 values allowed for observations of VO_2 without limitation by diffusion. As a result, 1-,5- and 10-minute durations of ischemia resulted in ever increasing rises in reperfusion VO_2 with progressively longer time courses of recovery back to baseline. These measurements were limited in proximity to reperfusion onset by the amount of time it took for the recovery of $P_{ISF}O_2$ to rise above 40 mmHg due to heightened oxygen demand following the two longer durations of ischemia.

Quantification of individual contributors to this VO_2 enhancement following increasing durations of ischemia was not possible with this method, but likely has several components. During ischemic conditions where mitochondrial respiration becomes limited by cytochrome c oxidase activity, associated rises in NADH have been recorded and linked to a cellular energetic deficit (Richmond et al. 1999; Clanton 2007). There is also a functional reserve of electron transport chain activity during normoxic resting conditions that is utilized during conditions of increased energy demand such as muscle contraction. Measurements of the products of ATP hydrolysis such as ADP show a 10-fold increase with only a small change in ATP levels during high intensity exercise compared to rest, indicating that ATP synthesis is able to match this 10-fold increase in energy utilization for at least a brief period of time (Sahlin et al. 1998). Based on this evidence, it appears reasonable to suggest that the majority of the observed rise in VO_2 following ischemia is due to enhanced metabolic activity to recover cellular ATP stores. There may also be some minor component associated with the ROS burst that has been observed following brief periods of ischemia that is necessary for the induction of protection by pre-conditioning (Santos et al, 2002; Dost et al, 2008), but to what magnitude this factors into overall VO_2 could not be discerned by the VO_2 Sampling Technique in its current form.

Influence of Cyanide on Resting and Reperfusion VO_2

Cyanide was used to demonstrate an association between VO_2 as measured by the VO_2 Sampling Technique and cytochrome c oxidase activity—the site of inhibition by cyanide. A pilot dose-response experiment in one animal revealed that a 1 mM topically applied dose was sufficient to produce a suppression in VO_2 during normoxic conditions that was similar to control VO_2 measurements during hypoxic conditions (see Figure 28). This indicated a substantial, but not total, inhibition of mitochondrial respiration by cyanide. Additional spinotrapezius muscle preparations were exposed to this 1 mM topically applied dose and measured in accordance with the defined 1-, 5- and 10-minute I/R protocols.

Resting skeletal muscle VO_2 in the normoxic range was found to be reduced by 36% in cyanide-treated muscles compared to Control. Mean $P_{ISF}O_2$ was also considerably higher for cyanide-treated muscles, which is consistent with an overall decrease in tissue oxygen demand. The incomplete inhibition of respiration by cyanide is likely due to an incomplete saturation of the muscle preparation's mitochondrial volume. Higher doses (10-100 mM) were undesirable due to potential systemic toxicity, but did show more dramatic reductions in VO_2 during a single pilot experiment (data not shown).

Cyanide-treated tissue was subjected to the 1-, 5- and 10-minute I/R protocols and VO_2 was assessed during reperfusion. The R5 time point following 5 and 10 minutes of ischemia were the only measurements to include hypoxic VO_2 values for cyanide. Following 5 minutes of ischemia, VO_2 was found to be significantly higher than the value under control conditions. Average P_0 values were also higher for cyanide by 5 mmHg and, although they still fell within the hypoxic range, there is a possibility that this difference contributed to the measured elevation in VO_2. Another thought is that prolonged exposure to cyanide resulted in sufficient

mitochondrial dysfunction to induce a substantial increase in ROS that may have lower kinetic constraints than cytochrome c oxidase for oxygen utilization, but this hypothesis remains unsupported by this work.

Treatment with 1 mM cyanide resulted in an overall depression of VO_2 during the time courses of reperfusion for each of the ischemic durations as compared to Control. Over the course of these measurements, however, it was clear that cyanide's inhibition of VO_2 was incomplete and thus failed to suppress some of the elevation in VO_2 found during reperfusion following ischemia. The progressive fall in VO_2 back to baseline was also similar over the reperfusion time course. This is likely the result of some cellular populations retaining a mostly functional mitochondrial capacity for ATP production, which enabled them to pursue a normal restorative time course following prolonged energy depletion, while other cellular populations with suppressed respiratory function could not restore the energetic balance—hence the overall observed reduction in VO_2. Additionally, cyanide was observed to have a reduced inhibitory effect on VO_2 as time elapsed following topical application (data not shown). Thus, the conclusions of this section of the study are simply that mitochondrial respiration is a component of the observed VO_2 and that the concentration of cyanide used in the topical application is insufficient to produce a maximal inhibition of mitochondrial respiration.

Effect of Nitroglycerin on I/R

Nitric oxide administration has been reported to mimic the ischemic pre-conditioning effect in skeletal muscle (Ozaki et al, 2002) and, as such, this study sought to measure its effect on resting and reperfusion VO_2 dynamics with the employment of the VO_2 Sampling Technique. NO has proven itself resistant to direct measurement in vivo by both its elusive nature and the

occurrence of other molecules that can interfere in the chemical and physical detection of NO. Therefore, instead of attempting to measure the concentration of NO in the microvasculature, the NO donor nitroglycerin was added to the spinotrapezius muscle, Dose-response changes in VO_2 and arteriolar diameter to the topical application of 0.01, 0.1, and 1 mM concentrations of the NO-donor nitroglycerin (NTG) were measured during resting and I/R conditions in skeletal muscle. Since we did not possess a reliable method for the detection of NO *in vivo*, the vasodilatory response by microvascular arterioles was used to confirm the effective release of NO into the tissue.

Measurements on four animals showed that 0.1 mM and 1 mM concentrations of NTG produced similar arteriolar vasodilations to 117% and 120% of baseline, respectively. The 0.01 mM dose caused an apparent elevation in vessel diameter which was not statistically significant. Considering the low concentrations of NO (~5 nM) that have recently been predicted to be physiologically relevant (Hall and Garthwaite, 2009), and corresponding findings of NO-dependent arteriolar dilations of the same magnitude (Shibata et al. 2006) at both 0.1 and 1 mM doses of NTG, 0.1 mM was considered sufficient to produce a clear effect on the microvasculature without delivering needlessly high concentrations of NO to the tissue. The effectiveness of this dose was confirmed when NTG's time course of effective influence on arteriolar diameter when topically applied to the spinotrapezius muscle was recorded. The 0.1 and 1 mM doses both resulted in sustained vasodilatory responses lasting 6 and 7 minutes, respectively, with a progressive return to baseline by minute 11. This indicated a relatively short half-life, but still sufficient for measurements of resting VO_2 and the ischemic durations of 1 and 5 minutes. Ten-minute I/R measurements were also conducted, but a sustained elevation in NO could not be confirmed with corresponding measurements of arteriolar diameter. Considering

the duration of NTG activity as observed by the arteriolar diameter response time course to topical administration (Figure 32), the 1 minute I/R data most likely contained the highest level of NO throughout the measurement period.

The dose-response of resting VO_2 to 0.01, 0.1 and 1 mM NTG showed a progressive reduction in normoxic VO_2 from baseline with increasing dose. Although the 0.01 and 0.1 mM doses showed strong trends in reducing VO_2, only 1 mM NTG-treated tissue showed a significant decline of 43% compared to baseline. This suppression of VO_2 is consistent with the description of NO as a reversible, competitive inhibitor of cytochrome c oxidase activity (Brown 2001). The more dramatic decrease in skeletal muscle VO_2 by the 1 mM dose than the 0.1 mM dose indicates that the maximum response of the microvascular arterioles does not necessarily translate to the maximum response of tissue respiration to NO, but since a measurement of delivered local NO concentrations was not possible in this study, a minimally effective dose remains desirable and likely 0.1 mM NTG's suppression of resting VO_2 would have achieved significance with an increase in sample size.

The dose-response of VO_2 during reperfusion for the I/R protocols was measured and determined to show a uniform reduction at each time point as compared to Control values. However, only the 0.1 mM dose in the intermediate $P_{ISF}O_2$ range had consistently sufficient number of observations for statistical analysis. Reperfusion following 1 minute of ischemia showed dramatic reductions in VO_2 for all measurement points as compared to Control. P_0 values for NTG were significantly lower at the R5 measurement point, but otherwise statistically the same for other measurements. Following 5 minutes of ischemia, the reperfusion time course showed a continued depression in VO_2 for NTG-treated tissue compared to Control, but significance was only observed for measurements at R25 and R85. There were no significant

differences in P_0 between NTG-treated tissue and Control. Following 10 minutes of ischemia, the trend in reduced VO_2 readings for NTG-treated tissues continued, but significance was found only at the R45 measurement point. As indicated by the time course of effective arteriolar dilation by NTG, it is uncertain by what magnitude the reperfusion time course following 10 minutes of ischemia was influenced by NO compared to the reperfusion periods following 1 and 5 minutes of ischemia (see Figure 35). What is clear is that NO appreciably reduces VO_2 during reperfusion and that this mechanism functions by the competitive inhibition of cytochrome c oxidase.

Reduction of NO by L-NAME

To reduce the overall levels of NO, enzymatic production was targeted for inhibition with L-NAME—a non-specific inhibitor of nitric oxide synthase (NOS). To judge the effective reduction in [NO], arteriolar diameters were measured following treatment with L-NAME and compared to baseline. Finally, the VO_2 Sampling Technique assessed changes in VO_2 dynamics during these periods of reduced [NO] for resting and I/R conditions.

A single animal was used to demonstrate the dose-response of arteriolar diameter and VO_2 to 0.0015, 0.015, 0.15, and 1.5 mM topical applications of L-NAME (see Figures 36 and 37). The 0.15 mM dose appeared to show the greatest amount of vasoconstriction and was not much different from the 0.015 and 1.5 mM doses for VO_2's measured for resting conditions and reperfusion following the 1-minute I/R protocol. Contrary to predictions, however, increasing doses of L-NAME produced a progressive reduction in VO_2.

Based on the pilot, a dose of 0.15 mM L-NAME was chosen for topical application to the spinotrapezius muscle followed by assessment of changes in arteriolar diameter and VO_2.

Arteriolar diameter decreased by 30% following treatment with L-NAME which was consistent with another finding of a 25% constriction of arterioles in the rat spinotrapezius muscle following treatment with 0.1 mM L-NAME (Xiang et al. 2008). This level of vasoconstriction produced significant drops in measured $P_{ISF}O_2$, but far from the point where data could no longer be collected from the normoxic range for measurements of resting and reperfusion VO_2.

Treatment with L-NAME produced an apparent decrease in resting VO_2 compared to Control measurements in the range of normoxia, but this difference was not significant (see Figure 40). $P_{ISF}O_2$ values for L-NAME-treated tissues were significantly higher by about 11 mmHg over Control, but whether this would cause a negative trend in VO_2 is unclear and counterintuitive.

To assess the effects of L-NAME on hypoxic respiration where NO has been proposed to have a greater role in respiratory regulation (Schweizer and Richter, 1994), the R5 measurements following 5 and 10 minutes of ischemia were chosen, since these time points primarily consisted of P_0 values in the range of hypoxia (see Figure 41). Following 5 minutes of ischemia, VO_2 was elevated for L-NAME-treated tissues at hypoxic time point R5, but this trend was not found to be significant. Following 10 minutes of ischemia, however, there was a similar, but more pronounced elevation in VO_2 for L-NAME-treated tissues that was found to be significant vs. Control. These hypoxic measurements at time point R5 following 5 and 10 minutes of ischemia were the occasions where VO_2 was enhanced over baseline while NO production was suppressed by L-NAME. It is possible, though in need of further study of VO_2 during hypoxic conditions, that suppression of endogenous NO is better visualized under low oxygen conditions due to a greater involvement of NO in regulating cytochrome c oxidase activity. Thus, VO_2 would be more sensitive to changes in [NO] at lower PO_2. $P_{ISF}O_2$ values were also slightly, but

significantly, higher in L-NAME-treated tissues compared to Control and if the "critical PO_2" of cytochrome c oxidase activity had been left-shifted by a reduction in inhibition, then this difference may be relevant when discussing the observed elevations in hypoxic VO_2 for L-NAME-treated tissues.

For the reperfusion time courses in 0.15 mM L-NAME-treated spinotrapezius muscle preparations, VO_2 was consistently, but not significantly, lower than under control conditions (see Figure 42). P_0 values were also reduced on average, but did not reach the point of being significantly lower than Control. It is possible this slight depression in $P_{ISF}O_2$ resulted in an overall reduction in VO_2, but the current data suggest there was no significant difference between Control and L-NAME-treated tissues in terms of VO_2 during reperfusion. Additionally, the VO_2 points of elevation and time course of return to baseline were similar to those of the Control situation. This trend in NOS suppression resulting in a reduction in VO_2 has been reported elsewhere and described as a possible increase in ATP production efficiency due to reduced cytochrome c oxidase inhibition (Baker et al. 2006), but whether the results from the VO_2 Sampling Technique reflect mitochondrial efficiency or some compensatory mechanism that regulates oxygen demand when oxygen supply is reduced is unclear and beyond the scope of this study.

Conclusions

The employment of a new technique to continuously measure the *in vivo* oxygen consumption rate of the rat spinotrapezius muscle has yielded results that are consistent with, more precise than, and unique to similar publications on this subject. Validation of the VO_2 Sampling Technique indicated that a sampling rate of 3 measurements per minute was minimally

invasive and provided a long timecourse of measurements over which muscle metabolism could be monitored through continuous inspection of changing $P_{ISF}O_2$ levels. The robust applicability of this technique was demonstrated as VO_2 was measured during both resting conditions and following ischemia with minimal effect on the recovery of $P_{ISF}O_2$ to baseline and subsequent measurements of VO_2. A correction factor to eliminate the intrinsic methodological contribution of PQM to VO_2 was also established and employed with success to prevent overestimates of these values. This correction factor and the protocol for calibration of any PQM setup are presented here and should afford future measurements of $P_{ISF}O_2$, with and without the VO_2 Sampling Technique, a higher degree of accuracy and an overall strong confidence in the method itself.

The VO_2 Sampling Technique was used experimentally to resolve the VO_2 dynamics of the rat spinotrapezius muscle during the conditions of rest and reperfusion following varying durations of ischemia. Measurements at rest confirmed PO_2 ranges where VO_2 is independent of and dependent on $P_{ISF}O_2$. These measurements were grouped into Hypoxic, Intermediate, and Normoxic categories according to the average $P_{ISF}O_2$ immediately prior to tissue compression for better inter-comparison. Resting skeletal muscle VO_2 values were slightly higher than published values using other methods. This is likely due to the VO_2 Sampling Technique's superior spatial resolution and direct observation of $P_{ISF}O_2$'s that allowed for better selection of regions where VO_2 was independent of oxygen tension over the physiological range. The first direct measurements of VO_2 dynamics during the initial parts of reperfusion following 1-, 5- and 10-minute durations of ischemia were made and found to be highly reproducible. These data confirmed that hypoxic VO_2 values were indeed limited by oxygen availability, that the intermediate PO_2 range contained both oxygen-dependent and independent components of VO_2,

and how tissue respiration progressively reacts to compensate for increasing durations of severe hypoxia. When VO_2 was independent of $P_{ISF}O_2$, a 3-fold increase was observed at 25 seconds of reperfusion following 10 minutes of ischemia. This value was presumably higher at earlier time points, but the current implementation of the VO_2 Sampling Technique was unable to consistently make measurements earlier in reperfusion. The majority of this response was reasonably associated with an increase in mitochondrial respiration to restore the ATP/ADP ratio. It was also considered possible that a minor component of this increased VO_2 seen during the reperfusion phases of increasing durations of ischemia was an increase in ROS production as reported by others in the study of brief ischemic durations in skeletal muscle. A direct assessment of ROS could not be made with this technique and would require additional methods to observe the magnitude of change in ROS production and relate it to VO_2 values over the same timecourse.

Cyanide, nitroglycerin, and L-NAME were topically applied to the rat spinotrapezius muscle and assessed for their influences on VO_2 dynamics during rest and conditions of reperfusion following 1-, 5- and 10-minute durations of ischemia. Cyanide was chosen for its similar site of action as NO in inhibiting electron transport activity at the level of cytochrome c oxidase. It attenuated VO_2 measurements for all conditions, but was ineffective overall in completely suppressing mitochondrial function. This was likely due to a combination of insufficient concentration of cyanide in the topical application to suppress mitochondrial respiration and a seemingly short duration of functionality (CN at physiological pH exists as a volatile gas and may have diffused away from the muscle). Its usage did confirm that the measured VO_2 dynamics were the result of mitochondrial activity, but due to a lack of complete mitochondrial inhibition, it was not possible to use these data to calculate the contributions to

VO_2 of other oxygen consumers. Nitroglycerin (NTG) behaved as expected showing a dose-dependent vasodilatory response in microvascular arterioles and in suppressing VO_2 during both resting and reperfusion conditions. Normoxic resting rates of VO_2 were suppressed in a dose-dependent manner, with the highest dose showing the greatest effect. The influence of NTG on arteriolar diameter appeared to be maximal for the medium dose, thus indicating that physiological levels of constitutive NO production were likely surpassed by the highest dose used. Inhibition of mitochondrial respiration is consistent with the reported action of NO as a competitive inhibitor of cytochrome c oxidase. How pharmacological application of an NO-donor prior to a brief period of ischemia affects VO_2 during early reperfusion had not been previously reported to our knowledge. For the 0.1 mM dose of NTG in the intermediate range of $P_{ISF}O_2$, there was a clear depression in VO_2 following the 1-minute duration ischemic period. The reperfusion time course following 5 minutes of ischemia also showed a decrease in VO_2, but time points R25 and R45 did not show statistical significance. There was also a graphically clear depression following 10 minutes of ischemia, but only 1 time point showed significance and therefore generalization to the entire time course is not warranted. It is also unclear whether NTG was able to maintain a high level of NO release over the measurement duration of 10 minutes of ischemia with reperfusion. The reduction of NO production by inhibition of NOS with L-NAME resulted in a clear vasoconstrictive response, but showed no statistically significant effect on VO_2 over the range of normoxic measurements for resting and reperfusion conditions. There was, however, a trend in hypoxic VO_2 elevation over control values for the R5 time point following 5 minutes of ischemia. Following 10 minutes of ischemia, this elevation persisted and was found to be significant. This may be an indication and confirmation of other reports that physiological levels of NO have increasing regulatory control over respiration as

development of hypoxia progresses. Further study over the influence of NO donation and depletion is necessary for the condition of hypoxia to confirm the role of NO in this process.

NO has been found to mimic the ischemic pre-conditioning effect that confers protection against subsequent ischemic events. We show here that NO causes a suppression in mitochondrial respiratory activity during reperfusion following brief periods of ischemia, which is consistent with findings that a necessary step in the development of protection through ischemic pre-conditioning is a reduction in the kinetics of the mitochondrial electron transport chain. If this connection is valid, the VO_2 Sampling Technique may be useful in demonstrating the utility of other drugs in achieving similar profiles of reperfusion as potential mimics of ischemic pre-conditioning. A reduction in physiological NO levels did not appear to alter normoxic respiratory rates during conditions of rest and reperfusion, but there was a visible elevation in VO_2 following 10 minutes of ischemia during hypoxia for tissues with suppressed [NO]. As L-NAME has been found to reverse the effects of pre-conditioning in rabbit hearts (Horimoto et al. 2000), this finding of enhanced VO_2 by a reduction in NO supports the concept that mitochondrial electron transport chain kinetics are key to the development of ischemic pre-conditioning protection in skeletal muscle. It is thus that the treatment of oxygen withdrawal, as occurs during ischemia, may be best performed by tempering the kinetics of VO_2 during the early period of reoxygenation associated with reperfusion.

Future Studies

In principle, the applications of this technique to a wide range of metabolic states and interventions in different combinations with various thin tissues are abundant. For the near future, however, improvement of sampling time resolution using shorter tissue compression

intervals and recovery times should lead to a better delineation of VO_2 dynamics during reperfusion following ischemia and during muscle contraction. Development of a "critical PO_2" value for VO_2 with further experimentation and analysis would also greatly support data on the influence of $P_{ISF}O_2$ on respiration so that future studies could be designed to specifically target certain magnitudes of hypoxia, normoxia, and hyperoxia. Finally, the study of ischemia with reperfusion requires data on ROS production that correspond to the time points of reperfusion described by this study. Additional studies that manipulate and measure [NO] during hypoxia may be able to take advantage of cytochrome c oxidase as a rough quantifier of physiologically relevant levels of NO that regulate electron transport chain function during rest and conditions of reperfusion and muscle contraction. Such information would be invaluable to the development and testing of new therapies for the pharmacological induction of the ischemic pre-conditioning effect.

LITTERATURE CITED

Addison PD, Neligan PC, Ashrafpour H, Khan A, Zhong A, Forrest CR, and Pang CY. Noninvasive remote ischemic preconditioning for global protection of skeletal muscle against infarction. *Am J Physiol Heart Circ Physiol.* **285**: H1435-H1445, 2003.

Bachetti T, Conini L, Curello S, Bastionon D, Palmieri M, Bresciani G, Callea F, Ferrari R. Coexpression and modulation of neuronal and endothelial nitric oxide synthase in human endothelial cells. *J Molecular and Cellular Cardiology*. **37**: 939-945, 2004.

Baker DJ, Krause DJ, Howlett RA, Hepple RT. Nitric oxide synthase inhibition reduces O2 cost of force development and spares high-energy phosphates following contractions in pump-perfused rat hindlimb muscles. *Exp Physiol*. (**3**):581-9, 2006.

Bayliss WM. On the local reactions of the arterial wall to chances of internal pressure. *J Physiol* **28**: 220-231, 1902.

Bertuglia S, and Giusti A. Role of nitric oxide in capillary perfusion and oxygen delivery regulation during systemic hypoxia. *Am J Physiol Heart Circ Physiol* **288**: H525-H531, 2005.

Boegehold MA. Effect of salt-induced hypertension on microvascular pressures in skeletal muscle of Dahl rats. *Am J Physiol* **260**(6 Pt 2): H1819-H1825, 1991.

Boveris A. Mitochondrial production of superoxide radical and hydrogen peroxide. In: *Tissue Hypoxia and Ischemia*. Edited by Reivich M, Coburn R, Lahiri S, and Chance B. New York: Plenum. 1977, p. 67-82.

Brandao ML, Roselino JE, Piccinato CE, and Cherri J. Mitochondrial alterations in skeletal muscle submitted to total ischemia. *J Surg Res*. **110**: 235-240, 2003.

Brookes PS, Kraus DW, Shiva S, Doeller JE, Barone M-C, Patel RP, Lancaster JR jr, and Darley-Usmar V. Control of mitochondrial respiration by NO, effects of low oxygen and respiratory state. *J of Biological Chemistry*. **278**: 34; 31603-31609, 2003.

Brown GC. Regulation of mitochondrial respiration by nitric oxide inhibition of cytochrome c oxidase. *Biochimica et Biochysica Acta*. **1504**: 46-57, 2001.

Brown GC and Borutaite V. Nitric Oxide, mitochondria, and cell death. *IUBMB Life*. **52**: 3-5; 189-195, 2001.

Brown GC and Cooper CE. Nanomolar concentrations of nitric oxide reversibly inhibit synaptosomal respiration by competing with oxygen at cytochorome oxidase. *FEBS* Lett. **356**: 295-298, 1994.

Buehler PW and Alayash AI. Oxygen Sensing in the Circulation: "Cross Talk" Between Red Blood Cells and the Vasculature. *Antioxidants and Redox Signaling* **6**: 6, 1000-1010, 2004.

Buerk DG. Nitric Oxide Regulation of Microvascular Oxygen. *Antioxidants & Redoc Signaling*. **9**: 7; 829-843, 2007.

Cabrales P, Tsai AG, Frangos JA, and Intaglietta M. Role of endothelial nitric oxide in microvascular oxygen delivery and consumption. *Free Radic Biol Med* **39**: 1229-1237, 2005.

Carlson BE, Arviero JC, and Secomb TW. Theoretical model of blood flow autoregulation: roles of myogenic, shear-dependent, and metabolic responses. *Am J Physiol Heart Circ Physiol* **295**: H1572-H1579, 2008.

Cheatle TR, Potter LA, Coper M, Delpy DT, et al. Near-infrared spectroscopy in peripheral vascular disease. *Br J Surg* **78**(4): 405-408, 1991.

Chen K, and Popel AS. Vascular and Perivascular nitric oxide release and transport: Biochemical pathways of neuronal nitric oxide synthase (NOS1) and endothelial nitric oxide synthase (NOS3). *Free Radical Biology & Medicine*. **42**: 811-822, 2007.

Chen Q, Vazquez EJ, Moghaddas S, Hoppel CL, Lesnefsky EJ. Production of ROS by mitochondria: central role of complex III. *J Biol Chem* **278**: 36027-31, 2003.

Chen X, Jaron D, Barbee KA, Buerk DG. The influence of radial RBC distribution, blood velocity profiles, and glycocalyx on coupled NO/O_2 transport. *J Appl Physiol*. **100**: 482-492, 2006.

Chi C, Ozawa T, Anzai K. In vivo nitric oxide production and iNOS expression in x-ray irradiated mouse skin. *Biol Pharm Bull*. **29**: 2; 348-353, 2006.

Clanton TL. Yet another paradox. *J Appl Physiol* **99**: 1245-1246, 2005.

Cosby K, Partovi KS, Crawford JH, et al. Nitrite reduction to nitric oxide by deoxyhemoglobin vasodilates the human circulation. *Nature Medicine*. **9**: 12; 1498-1505, 2003.

Costanzo, Linda S. Physiology 3rd Ed. Baltimore: Lippincott Williams & Wilkins, 2003.

Cuperus R, Leen R, Tytgat GAM, Caron HN, and Van Kuilenburg ABP. Fenretinide induces mitochondrial ROS and inhibits the mitochondrial respiratory chain in neuroblastoma. *Cell Mol Life Sci*. **67**(5): 807–816, 2010.

De Blasi, RA, Luciani R, Punzo G, Arcion R, et al. Microcirculatory changes and skeletal muscle oxygenation measured at rest by near-infrared spectroscopy in patients with and without diabetes undergoing haemodialysis. *Crit Care*. **13**(suppl5): S9, 2009.

De Clerck I, Boussery K, Pannier JL, and Van De Voorde J. Potassium potently relaxes small rat skeletal muscle arteries. *Med Sci Sports Exerc* **35**(12): 2005-12, 2003.

Dost T, Cohen MV, and Downey JM. Redox signaling triggers protection during the reperfusion rather than the ischemic phase of preconditioning. *Basic Res Cardiol*. **103**: 378-384, 2008.

Dunphy I, Vinogradov SA, and Wilson DF. Oxyphor R2 and G2: phosphors for measuring oxygen by oxygen-dependent quenching of phosphorescence. *Anal Biochem* **310**: 191-198, 2002.

Eberlin KR, et al. Ischemic Preconditioning of Skeletal Muscle Mitigates Remote Injury and Mortality. *J of Surgical Research*. **148**: 24-30, 2008.

Edmunds NJ and Marshall JM. Vasodilation, oxygen delivery and oxygen consumption in rat hindlimb during systemic hypoxia: roles of nitric oxide. *Journal of Physiology* **532**(1): 251-259, 2001.

Ellsworth ML, Forrester T, Ellis CG, and Dietrich HH. The erythrocyte as a regulator of vascular tone. *Am J Physiol* **269**: H2155-H2161, 1995.

Ellsworth ML. Red blood cell-derived ATP as a regulator of skeletal muscle perfusion. *Med Sci Sports Exerc* **36**: 35-41, 2004.

Faber JE. In situ analysis of alpha-adrenoreceptors on arteriolar and venular smooth muscle in rat skeletal muscle microcirculation. *Circ Res* **62**: 37-50, 1988.

Feron O. Nitric Oxide Synthases: Which, Where, How, and Why? Ed. Thomas Michel. *J. Clin. Invest*. **100**: 9; 2146-2152, 1997.

Ferreira LF, Poole DC, & Barstow TJ. Muscle blood flow – O_2 uptake interaction and their relation to on-exercise dynamic of O_2 exchange. *Respir Physiol Neurobiol* **147**: 91-103, 2005.

Folkow B, Sonnenschein RR, Wright DL. Loci of neurogenic and metabolic effects on precapillary vessels of skeletal muscle. *Acta Physiol Scand* **81**: 459-471, 1971.

Furchgott RF and Zawadzki JV. The obligatory role of endothelial cells in the relaxation of arterial smooth muscle by acetylcholine. *Nature* **288**: 373-376, 1980.

Garhofer G, Zawinka C, Resch H, Menke M, Schmetterer L, and Dorner GT. Effect of Intravenous Administration of Sodium-Lactate on Retinal Blood Flow in Healthy Subjects. *Investigative Ophthalmology and Visual Science* **44**: 3972-3976, 2003.

Golub AS, Barker MC, and Pittman RN. PO_2 Profiles Near Arterioles and Tissue Oxygen Consumption in Rat Mesentery. *Am J Physiol Heart Circ Physiol* **293**: H1097-H1106, 2007

Golub AS and Pittman RN. PO2 measurements in the microcirculation using phosphorescence quenching microscopy at high magnification. *Am J Physiol Heart Circ Physiol*. **294**(6):H2905-16, 2008.

Golub AS, Tevald MA, and Pittman RN. Phosphorescence quenching micro-respirometry of skeletal muscle *in situ*. Submitted for publication.

Green DJ, O'Driscoll G, Blanksby BA, and Taylor RR. Control of skeletal muscle blood flow during dynamic exercise: contribution of endothelium-derived nitric oxide. *Sports Med* **21**(2): 119-46, 1996.

Griffiths EJ and Halestrap AP. Mitochondrial non-specific pores remain closed during the cardiac ischemia, but open upon reperfusion. *Biochem J*. **307**: 93-98, 1995.

Halestrap AP. Calcium, mitochondria and reperfusion injury: a pore way to die. *Biochem Soc Trans*. **34**: 232-237, 2006.

Halestrap AP, Clarke SJ, and Khaliulin I. The role of mitochondria in protection of the heart by preconditioning. *Biochimica et Biophysica Acta*. **1767**: 1007-1031, 2007.

Hall CN and Garthwaite J. What is the real physiological NO concentration in vivo? *Nitric Oxide* **21**: 92-103, 2009.

Han Z, Chen Y-R, Jones CI 3rd, Meenakshisundaram G, Zweier JL, Alevriadou BR. Shear-induced reactive nitrogen species inhibit mitochondrial respiratory complex activities in cultured vascular endothelial cells. *Am J Physiol Cell Physiol*. **292**: C1103-C1112, 2007.

Hausenloy DJ, Mocanu MA, and Yellon DM. Cross-talk between the survival kinases during early reperfusion: its contribution to ischemic preconditioning. *Cardiovasc Res*. **63**: 305-312, 2004.

Hellsten Y, Frandsen U, Orthenblad N, Sjodin B, Richter EA. Xanthine oxidase in human skeletal muscle following eccentric exercise: a role in inflammation. *J Physiol* **498**: 239–248, 1997

Herrera M, Hong NJ, and Garvin JL. Aquaporin-1 Transports NO Across Cell Membranes. *Hypertension*. **48**: 1-8, 2006.

Honig CR, Frierson JL, and Nelson CN. Oxygen transport and VO_2 in resting muscle: significance for tissue-capillary exchange. *Am J Physiol*. **220**: 357-363, 1971.

Horimoto H, Gaudette GR, Saltman AE, Krukenkamp IB. The role of nitric oxide, K(+)(ATP) channels, and cGMP in the preconditioning response of the rabbit. *J Surg Res*. **92**(1): 56-63, 2000.

Hoy AJ, Peoples GE, and McLennan PL. The effect of vascoconstrictors on oxygen consumption in resting and contracting skeletal muscle of the autologous pump-perfused rat hindlimb. *J. Physiol and Pharmo* **60**(3): 155-160, 2009.

Hudlicka O. Regulation of muscle blood flow. *Clin Physiol* **5**(3): 210-29, 1985.

Ignarro LJ, Buga GM, Wood KS, Byrns RE, and Chaudhuri G. Endothelium-derived relaxing factor produced and released from artery and vein is nitric oxide. *Proc Natl Acad Sci USA* **84**: 9265-9269, 1987

Jensen FB. The dual roles of red blood cells in tissue oxygen delivery: oxygen carriers and regulators of local blood flow. *J Exp Bio* **212**: 3387-3393, 2009.

Jia L, Bonaventura C, Bonaventura J, and Stamler JS. S-nitrosohaemoglobin: a dynamic activity of blood involved in vascular control. *Nature*. **380**: 221-226, 1996.

Kaley G, Rodenburg JM, Messina EJ, Wolin MS. Endothelium-associated vasodilators in rat skeletal muscle microcirculation. *Am J Physiol* **256**: H720-H725.

Kashiwagi S, Kajimura M, Yoshimura Y, Suemastsu M. Nonendothelial Source of Nitric Oxide in Arterioles But not in Venules: Alternative Source Recealed In Vivo by Diaminofluorescein Microfluorography. *Circ Res*. **91**: e55-e64, 2002.

Kerr PM, Suleiman MS, and Halestrap AP. Reversal of permeability transition during recovery of hearts from ischemia and its enhancement by pyruvate. *Am J Physiol*. **276**: H496-H502, 1999.

Kevin LG, Camara AK, Riess ML, Novalija E, and Stowe DF. Ischemic preconditioning alters real-time measure of O_2 radicals in intact hearts with ischemia and reperfusion. *Am J Physiol Heart Circ Physiol*. **284**(2): H566-74, 2003.

Kim JS, Jin YG, Lemasters JJ. Reactive oxygen species, but not Ca^{2+} overloading, trigger pH and mitochondrial permeability transition-dependent death of adult rat myocytes after ischemia-reperfusion. *Am J Physiol* **290**: H2024-H2034, 2006.

Kleinbongard P, et al. Red blood cells express a functional endothelial nitric oxide synthase. *Blood*. **107**:7; 2943-2951, 2006.

Klitzman B, Damon DN, Gorczynski RJ, Duling BR. Augmented tissue oxygen supply during striated muscle contraction in the hamster. Telative contributions of capillary recruitment, functional dilation, and reduced tissue PO_2. *Circ Res* **51**: 711-721, 1982.

Korge P, Ping P, Weiss JN. Reactive Oxygen Species Production in Energized Cardiac Mitochondria during hypoxia/ Reoxygenation: Modulation by Nitric Oxide. *Circ Res*. **103**(8): 873-880, 2003.

Korthuis RJ, Granger N. Ischemia-reperfusion injury: Role of oxygen-derived free radicals. In Taylor AE, Matalon S, Ward PA (eds): Physiology of Oxygen Radicals. Bethesda, ME: *Am Physiol Soc*, 217-249, 1986.

Kuo L, Davis MJ, Chilian WM. Endothelium-dependent, flow-induced dilation of isolated coronary arterioles. *Am J Physiol* **259**: H1063-H1070, 1990.

Kuo L, Chilian WM, Davis MJ. Interaction of pressure- and flow-induced responses in porcine coronary resistance vessels. *Am J Physiol*. **261**: H1706-H1715, 1991.

Lane P and Gross SS. Nitric Oxide: Promiscuous and Duplicitous. *Science and Medicine*. March/April, 96-107, 2002.

Larsen FJ, Weitzberg E, Lundberg JO, and Ekblom B. Effects of dietary nitrate on oxygen cost during exercise. *Acta Physiol*. **191**: 59-66, 2007.

Laskowski I, Pratschke J, Wilhelm MJ, et al. Molecular and cellular events associated with ischemia-reperfusion injury. *Ann Transplant* **5**: 29, 2000.

Li H and Poulos TL. Structure-function studies on nitric oxide synthases. *J of Inorganic Biochem*. **99**: 293-305, 2005.

Liu X, Miller MJS, Joshi MS, Thomas DD, and Lancaster JR jr. Accelerated reaction of nitric oxide with O_2 within the hydrophobic interior of biological membranes. *Proc. Natl. Acad. Sci. USA*. **95**: 2175-2179, 1998.

Lodish H, et al. Molecular cell biology. 4th ed. New York: W.H. Freeman and Co. 2000

Lodish H, et al. Molecular cell biology. 5th ed. New York: W.H. Freeman and Co. 2004

Lopez-Figueroa MO, Day HEW, Lee S, River C, Akil H, Watson SJ. Temporal and anatomical distribution of NOS mRNA expression and NO production during central nervous system inflammation. *Brain Research*. **852**: 235-246, 2000.

Lynn EG, Zhongping Lu, Diane Minerbi, Michael N. Sack. The regulation, control, and consequences of mitochondrial oxygen utilization and disposition in the heart and skeletal muscle during hypoxia. *Antioxidants & Redox Signaling*. September 2007, **9**(9): 1353-1362. doi:10.1089/ars.2007.1700.

Martou G, O'Blenes CA, Huang N, et al. Development of an in vitro model for study of the efficacy of ischemic preconditioning in human skeletal muscle against ischemia-reperfusion injury. *J Appl Physiol* **101**: 1335-1342, 2006.

Masahide T, Hidemitsu T, Isamu T, Yoshihko K, and Natsuiki S. Non-invasive tissue oxygen monitoring by near-infrared spectroscopy. *Nipon Geka Gakkai Zasshi*. **88**(6): 680-5, 1987.

Mason MG, Nicholls P, Wilson MT, and Cooper CE. Nitric oxide inhibition of respiration involves both competitive (heme) and noncompetitive (copper) binding to cytochrome c oxidase. *PNAS*. **103**: 3; 708-713, 2006.

McCord JM. Oxygen-derived radicals: A link between reperfusion injury and inflammation. *Fed Proc* **46**: 2402-2406, 1987.

McGahren ED, Dora KA, Damon DN, Duling BR. A test of the role of flow-dependent dilation in arteriolar responses to occlusion. *Am J Physiol* **272**: H714-H721, 1997.

McMahon TJ, Moon RE, Luschinger BP, Carraway MS, Stone AE, et al. Nitric oxide in the human respiratory cycle. *Nature Medicine*. **8**: 7; 711-717, 2002

Misra MK, Sarwat M, Bhakuni P, Tuteja R, and Tuteja N. Oxidative Stress and Ischemic Myocardial Syndromes. *Med Sci Monit*. **15**(10): RA209-RA219, 2009.

Moens AL and Kass DA. Tetrahydrobiopterin and cardiovascular disease. *Arterioscler Thromb Vasc Biol*. **26**: 2439-2444, 2006.

Moses MA, Addison PD, Neligan PC, et al. Mitochondrial KATP channels in hindlimb remote ischemic preconditioning of skeletal muscle against infarction. *Am J Physiol Heart Circ Physiol*. **288**: H559-H567, 2005.

Mottram RF. The oxygen consumption of skeletal muscle in vivo. *Physiol* **128**: 268-276, 1955.

Murry CE, Jennings RB, and Keith RA. Preconditioning with ischemia: a delay of lethal cell injury in ischemic myocardium. *Circulation*. **74**(5): 1124-1136, 1986.

Musters RJ, Post JA, and Verkleij AJ. The isolated neonatal rat-cardiomyocyte used in an in vitro model for 'ischemia.' 1. A morphological study. *Biochim Biophys Acta*. **1091**(3): 270-7, 1991.

Narabayashi H, Takeshige K, and Minakami S. Alteration of inner-membrane components and damage to electron-transfer activities of bovine heart submitochondrial particles induced by NADPH-dependent lipid peroxidation. *Biochem. J.* **202**: 97-105, 1982.

Ortenblad N, Macdonald WA, and Sahlin K. Glycolysis in contracting rat skeletal muscle is controlled by factors related to energy state. *Biochem J* **420**: 161-168, 2009.

Pain T, Yang XM, Critz SD, Yue Y, Nakano A, et al. Opening of mitochondrial KATP channels triggers the preconditioning state by generating free radicals. *Circ Res*. **87**: 460-466, 2000.

Palacios-Callender M, Hollis V, Frakich N, Mateo J, and Moncada S. Cytochrome c oxidase maintains mitochondrial respiration during partial inhibition by nitric oxide. *J Cell Sci* **120**: 160-165, 2007.

Pang CY, Forrest CR, and Mounsey R. Pharmocologic intervention in ischemia-induced reperfusion injury in the skeletal muscle. *Microsurgery*. **14**: 176-182, 1993.

Pasupathy S and Homer-Vanniasinkam S. Ischaemic Preconditioning Protects Against Ischaemia/Reperfusion Injury: Emerging Concepts. *Eur J Vasc Endovasc Surg*. **29**: 106-115, 2005.

Pawloski JR, Hess DT, and Stamler JS. Export by red blood cells of nitric oxide bioactivity. *Nature*. **409**: 622-626, 2001.

Pohl U and Busse R. Hypoxia stimulates release of EDRF. *Heart Circ Physiol*. **25**: H1595-H1600, 1989.

Popel AS, Pittman RN, and Ellsworth ML. Rate of oxygen loss from arterioles is an order of magnitude higher than expected. *Am J Physiol Heart Circ Physiol* **256**: H921-H924, 1989.

Qui Y, Rizvi A, Tang XL, Manchikalapudi S, Takano H, Jadoon AK, et al. Nitric oxide triggers late preconditioning against myocardial infarction in conscious rabbits. *Am J Physiol*. **273**: H2931-H2936, 1997.

Rassaf T, Flögel U, Drexhage C, Hendgen-Cotta U, Kelrn M, Schrader J. Nitrite Reductase function of Deoxymyoglobin: O2 sensor and regulator of cardiac energetics and function. *Circ Res*. **100**: 1749-1754, 2007.

Richmond KN, Shonat RD, Lynch RM, and Johnson PC. Critical PO_2 of skeletal muscle in vivo. *Am J Phys Heart Circ*. **46**: H1831- H1840, 1999.

Sahlin K, Tonkonogi M, Söderlund K. Energy supply and muscle fatigue in humans. *Acta Physiol Scand*. **162**(3): 261-6, 1998.

Santos PD, Knowaltowski AJ, Laclau MN, et al. Mechanisms by which opening the mitochondrial ATP sensitive K+ channel protects the ischemic heart. *Am J Physiol Heart Circ Physiol*. **283**: H284-H295, 2002.

Sato H, Sato M, Kanai H, Uchiyama T, et al. Mitochondrial reactive oxygen species and c-Src play a critical role in hypoxic response in vascular smooth muscle cells. *Cardiovascular Research* **67**: 714-722, 2005.

Schoen M, Rotter R, Gierer P, et al. Ischemic Preconditioning Prevents Skeletal Muscle Tissue Injury, But Not Nerve Lesion Upon Tourniquet-Induced Ischemia. *J Trauma*. **63**(4): 788-797, 2006.

Schubert R and Mulvany MJ. The myogenic response: established facts and attractive hypotheses. *Clinical Science* **96**: 313-326, 1999.

Schumacker PT and Samsel RW. Oxygen supply and consumption in the adult respiratory distress syndrome. *Clin Chest Med* **11**(4): 715-22, 1990.

Schweizer M and Richter C. Nitric oxide potently and reversibly deenergizes mitochondria at low oxygen tension. *Biochemical and Biophysical Res Com*. **204**: 1; 169-175, 1994.

Scorrano L, Petronilli V, and Bernardi P. On the voltage dependence of the mitochondrial permeability transition pore—A critical appraisal. *J Biol Chem*. **272**: 12295-12299, 1997.

Segal SS. Regulation of Blood Flow in the Microcirculation. *Microcirculation* **12**: 33-45, 2005.

Shibata M, Qin K, Ichioka S, and Kamiya A. Vascular wall energetics in arterioles during nitric oxide-dependent and –independent vasodilation. *J Appl Physiol* **100**: 1793-1798, 2006.

Singel DJ and Stamler JS. Chemical Physiology of Blood Flow Regulation by Red Blood Cells: The role of nitric oxide and s-nitrosohemoglobin. *Annu Rev Physiol*. **67**: 99-145, 2005

Singal PK, Grepta M. The role of free radicals in drug-induced myocardial effects. In Miquel J, Quintanilha AT, Weber H (eds): CRC Handbook of Free Radicals and Antioxidants in Biomedicine, Vol 1. Boca Raton, FL: CRC Press, Inc., 287-295, 1989.

Smith JK, Carden DL, Korthius RJ. Role of xanthine oxidase in post-ischemic microvascular injury in skeletal muscle. *Am J Physiol* **257**: 1782-1789, 1989.

Solaini G, and Harris DA. Biochemical dysfunction in heart mitochondria exposed to ischemia and reperfusion. *Biochem J* **390**: 377-394, 2005.

Tahara EB, Navarete FDT, Kowaltowski. Tissue-, Substrate-, and Site-specific Characteristics of Mitochondrial Reactive Oxygen Species Generation. *Free Radical Biology and Medicine* **49**(9): 1283-1297, 2009.

Tevald MA. The Effects of Chronic Myocardial Infarction on Microvascular Oxygen Transport in Skeletal Muscle. Diss. Virginia Commonwealth University, 2005. Ann Arbor: ProQuest Information and Learning Company, 2006.

Thaveau F, Zoll J, Rouyer O, Chafke N, Kretz JG, Piquard F, and Geny B. Ischemic preconditioning specifically restores complexes I and II activities of the mitochondrial respiratory chain in ischemic skeletal muscle. *J Vasc Surg*. **43**(3): 541-547, 2007.

Thippeswamy T and Morris R. Evidence that nitric oxide-induced synthesis of cGMP occurs in a paracrine but not an autocrine fashion and that the site of its release can be regulated: studies in dorsal root ganglia in vivo and in vitro. *Nitric Oxide*. **5**: 2; 105-115, 2001.

Thomas DD, Liu X, Kantrow SP, and Lancaster JR jr. The Biological Lifetime of NO: Implications for the Perivascular Dynamics of NO and O_2. *PNAS*. **98**:1; 355-360, 2001.

Tsai AG, Johnson PC, and Intaglietta M. Oxygen gradients in the microcirculation. *Physiol Rev*. **83**(3): 933-63, 2003.

Vanden Hoek TL, Becker LB, Shao Z, Li C, Schumacker PT. Reactive oxygen species released from mitochondria during brief hypoxia induce preconditioning in cardiomyocytes. *Journal of Biological Chemistry* **273**:18092–18098, 1998

Vanderkooi JM, Maniara G, Green TJ, Wilson DF. An optical method for measurement of dioxygen concentration based upon quenching of phosphorescence. *J Biol Chem* **262**: 5476–5482, 1987

Vander Heide RS, Hill MI, Reimer KA, and Jennings RB. Effects of reversible ischemia on the activity of mitochondrial ATPase: relationship to ischemia preconditioning. *J Mol Cell Cardiol*. **28**: 103-112, 1996

Veitch K, Hombroeckx A, Caucheteux D, Pouleur H, and Hue L. Global ischaemia induces a biphasic response of the mitochondrial respiratory chain. *Biochem. J*. **281**: 709-715, 1992.

Vurionen K, Ylitalo K, Peuhkurinen K, Ratikaenin P, Ala-Rami A, and Hassinen IE. Mechanism of ischemic preconditioning in rat myocardium. *Circulation* **91**: 2810-2818, 1995.

Wagner PD. Diffusive resistance to O_2 transport in muscle. *Acta Physiol Scand* **168**(4): 609-614, 2000.

Wallace DC and Fan W. The pathophysiolog of mitochondrial disease as modeled in the mouse. *Genes Dev*. **23**(15): 1714-1736, 2009.

Weibel ER. The Pathway for Oxygen: structure and function in the mammalian respiratory system. Cambridge: Harvard University Press, 1984.

Wilson DF, Erecinska M, Drown C, and Silver IA. The oxygen dependence of cellular energy metabolism. *Arch. Biochem. Biophys*. **195**: 485-493, 1979.

Wilson DF, Vanderkooi JM, Green TJ, Maniara G, DeFeo SP, Bloomgarden DC. A versatile and sensitive method for measuring oxygen. *Adv Exp Med Biol* **215**: 71–77, 1987

Xiang L, Naik JS, Hester RL. Functional vasodilation in the rat spinotrapezius muscle: role of nitric oxide, prostanoids and epoxyeicosatrienoic acids. *Clin Exp Pharmacol Physiol*. 2008 May;*35*(5-6):617-24. Epub 2008 Jan 21.

Yang XM, Proctor JB, Cui L, Krieg T, Downey JM, Cohen MV. Multiple, brief coronary occlusions during early reperfusion protect rabbit hearts by targeting cell signaling pathways. *J Am Coll Cardiol* **44**: 1103-1110, 2004.

Ytrehus K, Liu Y, and Downey JM. Preconditioning protects ischemic rabbit heart by protein kinase C activation. *Am J Physiol*. **266** (Heart Circ. Physiol. 35): H1145-H1152, 1994.

VITA

William H. Nugent was born on December 15th, 1982 in Huntington, New York and as a consequence, was granted the right of American citizenship. At age 13, he and his family relocated to Lynchburg, Va. William received his high school diploma from Jefferson Forest High School in 2001. His interests during this time were deep within the sciences and a health-oriented mindset steered him towards the Biology program at Virginia Commonwealth University. He graduated with a Bachelor of Science in Biology in 2005.

The allure of MCV and the strong cardiovascular component of the Department of Physiology attracted William's interest and he joined Dr. Pittman's lab in the summer of 2006. His first course of investigation was an effort to develop a spatially and temporally sensitive detector of nitric oxide which could be topically applied to the microvasculature. Inconsistent data and a lack of a reliable chemical indicator for NO caused William's project to be redirected to the measurement of oxygen consumption in living tissue. He was an active participant in both the Forbes and Watts graduate symposiums and presented his work frequently for the intradepartmental Data Club. He also submitted three abstracts describing the development of the various techniques and presented posters at three corresponding Experimental Biology Conferences. In 2008, he received the Zweifach Student Award from the Microcirculatory Society.

William and his wife Elizabeth have been married since 2009 and live with their cat Digit.